BONE STROMAL PRODUCTION OF INSULIN-LIKE GROWTH FACTOR BINDING PROTEIN 5 PROMOTES GROWTH AND SURVIVAL OF PROSTATE CANCER

by

Danbin Li

B.Med., Norman Bethune Medical University, China, 1989

A THESIS SUBMITTED IN PARTIAL FULLFILLMENT OF
THE REQUIREMENTS FOR THE DEGREE OF

MASTER OF SCIENCE

in

The Faculty of Graduate Studies

(Experimental Medicine)

THE UNIVERSITY OF BRITISH COLUMBIA

August 2007

ABSTRACT

Prostate cancer (PCa) is the most common cancer among Canadian men and is continuing to be the third-leading cause of male cancer death in Canada. PCa is initially androgen-dependent. Some patients developed metastasis at diagnosis, and are treated by androgen withdrawal therapy. The majority of patients will respond, resulting in tumor growth arrest. However, PCa eventually progresses to androgen-independence and no effective treatment is available. Stromal-epithelial interaction is critical to PCa survival and proliferation. The bone metastasis in PCa indicated compatibility between bone stroma cells and PCa epithelial cells in bone microenvironment. IGF-I and IGF-II are the most abundant growth factors stored in bone. The bioavailability of IGF-I can be modulated by IGFBP-5, the most abundant IGFBP in bone stroma. IGFBP-5 is one of few consistently upregulated genes in mice bone stroma after castration. The functions of IGFs and IGFBP-5 are implicated in PCa growth and survival.

The objective of this thesis was to investigate the role of stroma-derived IGFBP-5 in PCa bone metastasis and progression to androgen-independence. We generated IGFBP-5 expressing bone stroma MG63-BP5 clone, and its vector counterpart MG63-mock clone. We investigated the anti-apoptotic effect of MG63-BP5 conditioned medium on LNCaP PCa cells under androgen-deprived condition through enhancing IGF-I-mediated survival signaling. We observed the ability of MG63 cells to support LNCaP tumor formation in nude mice coinoculated with LNCaP/MG63 cells. We also observed an increase in growth rate and PSA level in LNCaP/MG63-BP5 xenografts compared to LNCaP/MG63-mock xenografts both in intact and castrated mice. Immunohistochemical staining of these xenografts showed no difference in proliferation, however decreased apoptosis was seen in LNCaP/MG63-BP5 xenografts.

Our study is the first to demonstrate that bone stroma-produced paracrine IGFBP-5 played a role in bone microenvironment that favors PCa cell survival as well as androgen-independent progression. We propose that IGFBP-5 can act as a reservoir for IGF-I that allows slowly release of IGF-I for receptor interactions, resulting in amplification of downstream signaling pathways, which promote cell survival. We concluded that this is an adaptive mechanism for PCa to resist undergoing apoptosis and survive under androgen deprivation stress.

TABLE OF CONTENTS

LIST OF FIGURES

LIST OF ABBREVIATIONS

Abbreviation	Description
AD	= Androgen dependent
AI	= Androgen independent
Akt (PKB)	= Protein kinase B
ALS	= Acid labile subunit
AR	= Androgen receptor
ARE	=Androgen response element
ATCC	= American type culture collection
BMP	= Bone morphogenetic protein
BPH	= Benign prostate hyperplasia
CAF	= Carcinoma associated fibroblasts
Cdk	= Cyclin-dependent protein kinases
CM	= Conditioned medium
DHT	= Dihydrotestosterone
ECM	= Extracellular matrix
EGF	= Epithelial growth factor
Erk	= Extracellular signal-regulated protein kinase
FACS	= Fluorescence-activated cell sorting
FBS	= Fetal bovine serum
FGF	= Fibroblast growth factor
GAG	= Glycosaminoglycan
GH	= Growth hormone
GHRH	= Growth hormone releasing hormone
HGF	= Hepatocyte growth factor
hK2	= Human kallikrein 2
hPK	= Human plasma kallikrein
IGF	= Insulin-like growth factor
IGF-IR	= Insulin-like growth factor I receptor
IGF-IIR	= Insulin-like growth factor II receptor
IGFBP	= Insulin-like growth factor binding protein
IGFBPrP	= Insulin-like growth factor binding protein related protein
IHC	= Immunohistochemical
IR	= Insulin receptor
IRS	= Insulin receptor substrate
M6P	= Mannose-6-phophate
MMP	= Matrix metalloproteinase
PAP	= Protatic acid phosphotase
PBS	= Phosphate buffered saline
PCa	= Prostate Cancer
PCR	= Polymerase chain reaction
PDGF	= Platelet derived growth factor
PI3K	= Phosphoinositide 3'-kinase
PSA	= Prostate specific antigen

PTHrP	= Parathyroid hormone related protein
γ-NGF	= Gamma nerve growth factor
RANKL	= Receptor activator of NFκB ligand
RT- PCR	= Reverse transcriptase-polymerase chain reaction
SCID	= Severe combined immunodeficient
Shc	= Src homology 2-containing protein
TGF	= Transforming growth factor
TIF-2	= Transcription intermediary factor-2
TK	= Tyrosine kinase
TMA	= Tissue microarray
uPA	= urokinase plasminogen activator
UGM	= Urogenital sinus mesenchyme
VEGF	= Vascular endothelial growth factor

ACKNOWLEDGEMENTS

I would like to thank my supervisor, Dr. Michael Cox, for his guidance and financial support throughout my Masters degree. I was inspired by your intelligence, scientific attitude and enthusiasm toward work. You are my role model for research. I also like to thank you Mike for taking me into your lab, for teaching me a whole lot about all aspects of research.

I cannot wait to express my gratitude to my parents for their unconditional support throughout my study. To my mother Fangnian Li and father Yunsheng Li, thank for encouraging me to get into this program and keep me going all the way to graduation. You have always supported my goals and my career. To my brother Danjin Li and my sister-in-law Jingtao Liu, thank you for your caring.

Thanks also go to the people at the Prostate Center at Vancouver General Hospital for all their expertise and advice. A special thank you goes to all the members of the Cox lab: Emily Hoag, Elaine Vickers, Gina Rossi, Nikita Ivanov, Kevin Figueiredo and Yubin Guo. You are such nice people to be with and your help has been invaluable.

1 INTRODUCTION

1.1 Introduction

Prostate cancer (PCa) is thet most common cancer among Canadian men and continues to be the third-leading cause of male cancer death in Canada [1]. It is not invariably lethal. However, it is a heterogeneous disease ranging from asymptomatic to a rapidly fatal systemic malignancy. In 2007, it is estimated that 22,300 men in Canada will be diagnosed with PCa and 4,300 will die of it. One in 8 men will develop PCa during his lifetime, mostly after age 60. One in 27 PCa patients will die of it [1]. The goal(s) of the research described in this thesis is to investigate the role of bone stroma-derived IGFBP-5 in PCa metastasis and progression in bone. Through such work, I hope to reveal details of the mechanism by which bone stroma-produced IGFBP-5 performs a growth-promoting and anti-apoptotic function in PCa bone metastasis, that will directly impact therapeutic options for patients with advanced PCa.

1.2 The Prostate

The prostate is a tubuloalveolar exocrine gland of the male reproductive system. It is normally 3 cm long and located between the base of the urinary bladder and urethra. Normal prostate is as big as a large walnut. The main function of the prostate is to produce the seminal fluid, which is part of semen. The prostate also contains some smooth muscles that help expel semen during ejaculation.

The prostate gland is composed of an epithelial compartment and a stromal compartment. The epithelium forms glandular acini, which are separated from a supporting stroma by a basement membrane interface. The epithelium is populated by three cell types: secretory glandular cells,

nonsecretory basal cells, and neuroendocrine cells [2]. The secretory glandular cells represent the major cell type in normal prostate. They are terminally differentiated, express high levels of androgen receptors (AR) and secrete prostate specific antigen (PSA) and prostate acid phosphatase (PAP) into the glandular lumen [3]. The basal cells are located on the basement membrane. They are relatively undifferentiated and are thought to be proliferative precusors to secretory glandular cells. They have low or undectable level of AR and have no secretory activity [4]. The neuroendocrine cells form a small fraction of the cell population in normal prostate gland. They are terminally differentiated and may play a role in regulating the growth and function of the secretory cell [5]. The stroma of the prostate is composed of smooth muscle cells, fibroblasts, lymphoctyes, and neuromuscular tissue embedded in an extracellular matrix. They support the prostatic epithelium and most importantly directly affect differentiation and proliferation of epithelial cells.

1.3 Prostate Cancer

PCa originates from epithelial cells in the glandular acini of the prostate and is called adenocarcinoma. PCa can occur in men as early as 40 years old but the majority takes place in men over 60 years of age [6]. PCa is typically detected through screening based on digital rectal examination and measurement of serum PSA followed by a prostate biopsy. PCa is often initially slow-growing and androgen-dependent (AD). Growth and survival of PCa cells is dependent on the presence of androgen. Androgens enable the tumor to grow by stimulating cell proliferation, while concurrently preventing apoptosis [7]. The treatment of localized cancers typically involves active surveillance, radical prostatectomy and targeted irradiation. However, some patients are diagnosed late and have developed metastasis. Lymph nodes and bone are the major

metastatic sites of PCa. These patients are treated by androgen withdrawal either through medical castration using growth hormone releasing hormone (GHRH) agonists or by orchiectomy. The majority of patients will respond to hormone ablation, resulting in an average remission of about 24 months [8]. During this stage, PCa can progress from an AD to an androgen-independent (AI) phenotype and is typically lethal [7]. Therapeutic alternatives at this stage of disease are very limited, with a median survival between 8 and 12 months [8]. Understanding the adaptive responses of PCa cells that allow them to becomes AI and to metastasize is critical to developing therapeutic stratagies to treat men with advanced and metastatic disease.

1.4 Stromal-Epithelial Interaction in Prostate

1.4.1 Stromal-Epithelial Interaction in Normal Prostate Development

The prostate develops from the urogenital sinus in response to testosterone stimulation. Embryonically the prostate is composed of a multilayer epithelium and surrounding stroma. When ductal budding starts at 10 weeks of gestation, the epithelium bud out to form an elongated and branched duct. Postnatally the prostate grows very slowly until puberty when there is an increase in androgen. At puberty, the multilayer epithelium differentiates into a double layer epithelium of inner-layer cylindrical secretory cells and basal-layer flattened or cubical basal cells.

It is now understood that the stroma is a dynamic environment that directly influences epithelial cell behavior. A significant body of evidence has been accumulated demonstrating that stromal-epithelial interactions play a critical role in the process of normal prostate development [9]. This

interaction is a dynamic network of communications between PCa cells and different kinds of stromal cells, including fibroblasts, smooth muscle cells and vascular endothelium.

Stroma and epithelium interactions are critically involved in prostate development and differentiation. Cunha et al have studied rodent prostate development and differentiation in detail [9, 10]. Using tissue recombination technique and in the presence of androgen, they observed that tissue recombinants composed of wild-type urogenital sinus mesenchyme (UGM) + wild-type epithelium and wild-type + AR-negative epithelium both undergo prostatic development. In contrast, tissue recombinants composed of AR-negative UGM + AR-negative epithelium and AR-negative UGM + wild-type epithelim fail to undergo prostatic development. The common feature of the former is the expression of ARs in the mesenchyma, and is not in the latter [11]. Estrogen also has effects on prostate development which is complex and may involve both indirect and direct action through estrogen receptor [12]. All these implied that mesenchymal AR plays a key role in prostatic development.

Additional experimental results confirmed the role of androgen in prostatic development through stroma-epithelial crosstalk. Association of tissues of embryonic urogenital sinus mesenchyme (UGM) and urogenital sinus epithelium can differentiate into prostatic tissue when implanted under the renal capsule of experimental animals, but not in the absence of androgen [10]. Another investigation showed the necessity for prostatic stroma in the maintenance of adult prostatic secretory epithelium as well. Urinary bladder epithelium went through a redifferentiation into prostate tissue with the ability to express AR and secreting the prostate-specific secretory proteins [13, 14]. This clearly indicated that stroma indeed mediates the AD growth and development of prostate from embryonic epithelium. On the other hand, the

epithelium can in turn effect the behavior and function of stromal cells [15]. The prostate epithelium guide UGM into smooth muscle by differentiation. When UGM was grafted with human prostatic epithelium, it formed thickened smooth muscle layers similar to human prostatic smooth muscle phenotype [15]. All these proved that an epithelial-stromal crosstalk is necessary to mutually direct differentiation and development of prostatic epithelium and stroma.

Though epithelial-stromal interactions play a fundamental role in normal prostate development triggered by androgens, androgen alone is not sufficient to maintain a homeostasis required for normal prostate differentiation and development. In the embryonic and neonatal growth and development of prostate, AR is detectable only in stroma and not in epithelium [16]. This indicates that androgens have an indirect rather than a direct effect on prostate epithelial cells. Furthermore, when combined with wild-type UGM, AR-negative epithelium can undergo AD morphological change and form prostate-like glandular epithelium [11]. This result showed that androgenic effects on epithelium are independent of AR on the epithelium. This has led to the theory that one or more growth factors from stromal cells act in a paracrine fashion to stimulate epithelial development, serving as a mediator of androgen function. These hypothesized androgen-regulated paracrine mediators have been referred to as andromedins [17].

It is now believed that diffused androgens first bind to AR of stromal cells and transactivate stroma-derived growth factors, andromedins. These growth factors then interact with their receptors on the membrane of ARs-negative epithelial cells and mediate differentiation and proliferation of prostate epithelium [18]. An andromedin is defined as a factor that must be sufficient to induce prostatic development and its absence must result in the loss of the prostate formation. It must be regulated directly or indirectly by androgens, and it has to be secreted from the UGM in the same time pattern as prostatic induction. To date, factors including IGF (Insulin-

like Growth Factor), EGF (Epithelial Growth Factor), TGF-α (Transforming Growth Factor-α), TGF-β (Transforming Growth Factor-β), HGF (Hepatocyte Growth Factor), and others has been thought to be andromedins [19]. A good example is IGF-II, which is produced by stromal cells [20], and functions via the IGF-I receptor (IGF-IR). IGF-II is found to be expressed both in epithelial and stromal cells [21, 22]. When added to rodent ventral prostate tissue cultures, it mimics the function of androgen of inducing prostate tissue development [21]. Therefore, network of communication between cells of different types in the microenvironment of prostate is emerging. It is evident that this interaction directing normal prostate development is complicated and multidirectional.

1.4.2 Stromal-Epithelial Interaction in Prostate Carcinogenesis

Stromal-epithelial crosstalk also plays a critical role in prostate carcinogenesis [23]. Tumor stroma is different from the normal stroma. Tumor stroma responds to carcinoma in a similar way to wound healing to create a new stromal microenvironment where cancer cells grow and survive. Through tissue combining approaches [23], BPH-1 cells, an immortalized but nontumorigenic human prostatic epithelial cell line, were combined with rat UGM and transplanted under the renal capsule of an adult male nude mouse. The BPH+UGM recombinants were grown in the host mice. Both ARs and estrogen receptors are only detectable in UGM, but not in BPH-1 cells [12, 24, 25]. BPH-1+UGM grow with relatively normal prostatic glandular phenotype in untreated male mice, however, they undergo malignant transformation in testosterone plus estradiol (T+E2)-treated mice [15, 26]. It is reported that prostate carcinogenesis is induced by paracrine T+E2 mechanism mediated by the stromal microenvironment. Smooth muscle cells normally compose the stroma of benign adult human prostate. Prostatic smooth muscle cells express AR and respond to androgens to maintain a

nonproliferative highly differentiated secretory epithelium via stromal-epithelial interaction [27]. However, reactive stromal cells surrounding prostatic cancer cells are fibroblasts or myofibroblasts [28, 29]. An additional study used BPH-1 cells and carcinoma associated fibroblasts (CAF) isolated from human PCa tissue [30]. Both BPH-1 and CAFs cells were nontumorigenic when grafted by themselves in nude male host mice. Large poorly differentiated carcinoma occurred when BPH-1 and CAFs cells were combined [29], whereas no carcinomas developed when BPH-1 combined with normal prostatic fibroblasts [23]. These suggested that stromal-epithelial interaction is not only necessary but indispensable for carcinogenesis and development of PCa.

1.5 Androgen and AR in Prostate Cancer

Androgen is in no doubt necessary for the growth and survival of cells of normal adult prostate or primary PCa. There are mainly two forms of androgen, testosterone and dihydrotestosterone (DHT), which specifically bind the AR. Testosterone is the principal circulating androgen. Testosterone can be convertd to DHT by 5-reductase within prostate. DHT is 10 times more potent than testosterone because of increased affinity for AR, so it is the most active intracellular androgen in the prostate [31].

The AR is an intracellular steroid receptor of the nuclear receptor super family. After androgen binds to an AR, the dimerized and activated receptor complex enters the nucleus and binds to an androgen response element (ARE) of DNA. In interaction with other cofactor proteins in the nucleus, ARs cause gene transactivation resulting in formation of more messenger RNA to produce specific proteins. The best studied AR target gene is PSA [32] and IGF-IR [33, 34].

Others examples include FGF8 (Fibroblast Growth Factor 8) [35], cyclin-dependent protein kinases (Cdk1, Cdk2) [36, 37], human kallikrein 2 (hK2) and PAP [38].

The mode for androgen and AR regulation of normal prostate development and PCa progression is different. In the developing prostate, only the stroma cells express ARs, suggesting the androgen regulation of prostate development is through the stroma cells [39, 40]. In normal adult prostate, AR expression is found primarily in epithelial cells, but also in the stroma [39, 40]. In PCa specimens, AR staining in epithelial cells is heterogeneous. Variation and sometimes decrease in AR-positive cells can be found in less differentiated tumors, which corresponds with the reported insensitivity to androgen observed in advanced PCa [41, 42].

1.6 IGF axis

Androgen plays a key role in PCa development and progression. Andromedins mediate biological effects of androgen. One such group of androgen regulated growth factors is the IGF axis [43, 44]. The IGF axis consists of two peptide growth factors, IGF-I and IGF-II [45, 46], cell-surface IGF-IR and IGF-II receptors (IGF-IIR) [47, 48], six well-characterized soluble IGF-binding proteins (IGFBP-1–6) [49-54], a family of partially characterized IGFBP proteases and several IGFBP-related proteins (IGFBPrPs) [55].

The IGF axis plays a crucial role in regulating cellular growth, differentiation and apoptosis [56, 57]. These molecules are important in the development and regulation of many tissues. It has also been observed under specific circumstances to play a role in the process of tumorigenesis [45]. It is possible that increased activation of IGF-I signaling may replace

androgen as the primary growth-stimulatory and anti-apoptotic factors in cancer progression independent of androgen.

1.6.1 IGFs and IGF Receptors

IGFI and IGF-II are polypeptides of approximately 7 KDa and share a structural homology with proinsulin [58]. They consist of A and B domains that are homologous to the A and B chains of insulin. They are two major members of growth-promoting factor family. They are potent mitogens and anti-apoptotic factors for many normal and malignant tissues. IGF-I and IGF-II are unique among growth factors because they act both systemically as a hormone in the blood and locally as autocrine/paracrine factors, such as in the bone microenvironment. They have multiple functions including stimulating survival, promoting proliferation and differentiation. The liver is the main source of circulating IGF-I, others being the bone, brain and muscle. IGF-I production by liver is mainly controlled by pituitary growth hormone (GH) [59]. Nutritional status like fasting [60], protein restriction [61], anorexia nervosa [62] as well as estrogen [63] also impact the production of IGF-I. IGF-I and IGF-II are expressed in a wide variety of cells, such as bone, brain and muscle cells, and their expression is regulated in a cell and tissue-type dependent manner. Therefore, the IGFs are normally not viewed as classical endocrine hormones, but rather as paracrine or autocrine growth factors in the local microenvironment, such as bone microenvironment.

There are two types of IGF receptors: IGF-IR and IGF-IIR. Both IGF-I and IGF-II interact with IGF-IR. Like insulin receptor (IR), IGF-IR is also a tetrameric receptor comprising two extra-cellular binding α and two trans-membrane catalytic β subunits ($\alpha_2\beta_2$). The extra-cellular domain of IGF-IR has approximately 50% similarity with IR, and is composed of six structural domains

that form a binding pocket. The cytoplamic tyrosine kinase (TK) domain has 84% sequence homology between IGF-IR and IR. Upon binding IGF-I, the IGF-IR displays intrinsic tyrosine kinase activation and activates intracellular signaling pathways that are similar to those described for the IR. IGF-IR responds to ligand binding by auto-phosphorylation and activation of its tyrosine kinase domain. Initial phosphorylation of the activation site is Y1135 and is followed by phosphorylation of Y1131 and Y1136 [64]. This serial phosphorylation stabilizes this structure and further lead to a major conformational change. A gap is opened and docking sites are provided to allow ATP and the adaptor proteins to bind. These proteins facilitate protein-protein interactions mediating various downstream signaling pathways. Adaptor proteins include Src homology 2-containing protein (Shc) and various isoform proteins of insulin-receptor substrate (IRS) family. Both Shc and the IRS proteins contain SH2 and/or phosphor-tyrosine binding domains that bind phosphorylated tyrosine on the IGF-IR. This leads to activation of two major downstream signaling cascades, the phosphoinositide 3'-kinase (PI3K)/Akt and the Ras/Raf/ErK pathway [65, 66].

IGF-II can also bind to IGF-IIR with high affinity. IGF-IIR is also recognized as mannose-6-phophate (M6P) receptor and perforin receptor, which plays a role in endocytosis and intracellular trafficking of M6P-tagged proteins [67]. Unlike IGF-IR or IR, IGF-IIR is a single transmembrane protein with no intracellular catalytic domain. IGF-IIR is thought to function as a decoy receptor for IGF-II, modulating the extracellular levels of IGF-II [68]. Like IGF-I and IGF-II, IGF-IR and IGF-IIR are also found in various types of cells, including prostate, bone, brain and muscle. Their expression is controlled in a cell- and tissue-specific fashion.

1.6.2 IGF Axis and AR in Prostate Cancer

IGF signaling system plays an important role in PCa [69, 70]. Increased IGF-I serum levels are linked with an increased risk of PCa [69, 71]. A majority of metastatic PCa tissues show an increased IGF-IR expression compared with primary lesions [34, 72, 73]. IGF-I has mitogenic effect to stimulate proliferation of PCa cells in vitro, while downregulation of IGF-IR expression by antisense oligonucleotides against IGF-IR inhibit in vivo tumor growth and prevent PCa cell invasion [74]. In vivo progression of human PCa xenograft to AI is associated with increased expression of both IGF-IR and IGF-I [44]. Increased IGF-IR expression is correlated with AI progression of human PCa [34, 44, 75]. Blockade of IGF-IR signaling using a inhibitory IGF-IR antibody can cause a marked enhancement of the castration effect on prostate tumor growth in a mouse xenograft model [76]. IGF-I-mediated signaling plays a critical role in PCa growth, progression and invasion.

IGF-I can regulate AR activation in PCa cells. IGF-I is able to activate the AR in transfected DU145 human PCa cells [77]. IGF-I enhances androgen-mediated AR transcriptional function in DU145 cell but is unable to activate AR in the absence of androgens [78]. In fact the IGF-I effect on AR transcriptional activity is more complicated and depends on whether it is localized or metastatic PCa [79]. IGF-I enhanced DHT-stimulated, but not basal, AR transcriptional activity under probasin promoter in nonmetastatic AR-transfected PCa cells. However, AR activity in response to DHT is suppressed in these cancer cell-derived metastatic cells. Nevertheless, the activation effect by IGF-IR signaling on the AR transcriptional activity in both localized and metastatic tumors seems to be mediated through the PI3K/Akt pathway [79]. The mechanism by which IGF-IR signaling could directly affect the function of AR is still not well understood. One possible theory is that IGF-IR signaling may change AR phosphorylation status. AR can be

phosphorylated at Ser^{210} and Ser^{790} by IGF-I mediated activation of PI3K/Akt pathway. This AR phosphorylation may inhibit AR-induced apoptosis possibly by disabling the interaction between AR and its co-regulators [80]. Moreover, AR phosphorylation by IGF-I mediated activation of Ras/MAPK pathway may promotes androgen sensitivity of the AR transcriptional function in LNCaP cells [81]. The other assumption is that IGF-IR activation can stimulate AR co-regulators that enhance AR signaling. Mohler and Wilson have demonstrated an increase expression of TIF-2, a AR co-regulator, in most of the recurrent AI PCas that also have a high levels of AR in the nucleus [82]. The mediation of AR activity by IGF-I is in a cell type and location dependent manner.

Conversely, androgen level can also influence IGF-I signaling activation. Our lab demonstrated that androgen is necessary for IGF-I-mediated protection from apoptotic stress and enhanced mitotic activity in LNCaP cells [34]. This protection is through upregulating IGF-IR expression, activation, and signaling to downstream factor IRS-2 and Akt. However, this effect was observed in AI lineage-derived C4-2 cells and tumors. C4-2 cells express higher levels of IGF-IR and greater activation of downstream proteins in the absence of androgen. This indicates that increased IGF-IR expression correlated with AI IGF-IR protection against apoptosis in PCa progression. Later, Pandini et al showed similar results that both DHT and the synthetic androgen R1881 upregulate IGF-IR expression by up to 6-fold and sensitize LNCaP PCa cells to the mitogenic and motogenic biological effects of IGF-I. These effects were inhibited by an IGF-IR blocking antibody [83]. In contrast, DHT and R1881 did not effect IGF-IR expression in PC3 cells. These effects on IGF-IR can be restored in AR-transfected PC3 cells. Androgen-induced IGF-IR upregulation can be inhibited by the Src inhibitor PP2 and the MEK-1 inhibitor PD98059. So it is reasonable to think that a majority of metastatic and AI PCa specimens show

an increase in IGF-IR expression compared to primary lesions [43, 75, 84]. This increase in IGF-IR expression in PCa metastatic cells or tissues implies an adaptive mechanism for PCa cells to survive in a new metastatic enviornment.

It is through stromal-epithelial crosstalk that IGF-I plays a key role in the PCa carcinogenesis and development. The theory was confirmed by Kawada's study. He and his colleagues showed that human normal prostate stromal cell, but not LNCaP and DU145 cells, secreted significant amounts of IGF-I [85]. Coinoculation of normal prostate stromal cell increased the growth of human PCa LNCaP and DU145 SCID mice. Coculture with normal prostate stroma increased the growth of DU145 cells in vitro, but pretreatment of normal prostate stroma with small interfering RNA (siRNA) of IGF-I lost its function to enhance the growth. These indicate that prostate stromal IGF-I mediates tumor-stroma cell interaction of PCa to accelerate PCa growth. IGF-I is indeed involved in the stroma-epithelial interaction of PCa. The local secretion of IGF-I in PCa tissue, in addition to the circulating IGF-I, is thought to play an important role in the prostate carcinogenesis.

1.6.3 IGFBPs

The biological response of cells to IGFs is regulated by various factors in that microenvironment. One important factor is the IGFBPs, which are integral members of the IGF axis [86]. There are six IGFBPs (IGFBP-1 to -6) identified so far. These six binding proteins modulate the biological function of the IGFs through high-affinity binding interactions that influence the ability of IGFs to act as ligands for the IGF-IR (K_d of ~ 10^{-10} M for IGFBPs versus K_d of 10^{-8} ~ 10^{-9} M for IGF-IR) [87]. They share a 50% homologous protein sequence overall. After various post-translational modifications, their molecular size falls in a range of 24 to 44 kDa. They also share

distinct structural and functional characteristics, including an ability to bind IGF with high affinity.

Over 95% of circulating IGFs are bound to IGFBP-3. IGFs are also carried by other IGFBPs. Less than 1% circulate in the unbound, free form [88]. IGFBPs act to regulate the endocrine actions of IGFs by regulating the amount of bioavailable IGF. Similar to IGF-I and IGF-II, IGFBPs are also secreted by many cell types in a cell and tissue-type dependent manner. Because the affinity of IGFBPs for IGFs is higher than that of cell-surface IGF-IR, IGFBP-bound IGFs are restricted in accessing cell-surface IGF-IR. However, some IGFBPs can bind to extracellular matrix (ECM) glycosaminoglycans (GAGs) and other ECM proteins [89]. In addition, the locally produced IGFBPs act as autocrine/paracrine regulators of IGF actions. Furthermore, some of the IGFBPs also act by a mechanism independent of IGFs [90].

1.6.3.1 IGFBP-1

IGFBP-1 is produced in liver and kidney. It binds IGF-I and IGF-II with equal affinity. It is associated with increased ECM production and kidney hypertrophy. It is upregulated by insulin deficiency and downregulated by insulin and steroids [91]. It inhibits metabolic as well as the growth-promoting function of IGF-I [92].

1.6.3.2 IGFBP-4

IGFBP-4 can be identified in all biological fluids. It is produced by various types of cells, such as hepatic cells, prostatic cells and bone cells [93]. It can bind to IGF-I and is regulated by Vitamin D and parathyroid hormone [93].

1.6.3.3 IGFBP-6

IGFBP-6 is produced in ovary and prostate. IGFBP-6 preferentially binds to IGF-II, inhibiting its activity [94]. It is primarily found in serum and cerebrospinal fluid. Its expression is regulated by IGF-II.

1.6.3.4 IGFBP-2, 3, 5

Unlike the above-mentioned three IGFBPs, IGFBP-3, IGFBP-2 and IGFBP-5 are the three IGFBPs that are most extensively investigated in PCa development and progression. Therefore, IGFBP-3, IGFBP-2 and IGFBP-5 are introduced and discussed together.

IGFBP-2 is the second most abundant IGFBP to IGFBP-3 in the circulation. Its concentration level is high in seminal plasma and in cerebrospinal fluid. It is associated with central nervous system development. Reduced insulin level and protein diet increase IGFBP-2 level [95]. Higher serum level of IGFBP-2 has been found in PCa [96]. IGFBP-2 has been shown to have a growth inhibitory effect on normal prostate epithelial cells, while having a potent stimulatory effect on PCa cells [97].

IGFBP-3 has been most extensively studied, compared to other IGFBPs. It has the largest carrying capacity and highest affinity for IGF-I. IGF-I is carried in a trimetric 150 KDa complex composed of IGFBP-3 and a liver derived glycoprotein called acid labile subunit (ALS), which protect the IGFs from proteases and prolong their circulating half-life from about 10 minutes to about 15 hours [98]. The remainder of IGF in the circulation is bound to IGFBP-1, 2 or 4, each of which forms a 50 KDa complex [99]. IGFBP-3 is synthesized in liver, osteoblasts and bone.

IGFBP-5 is found in kidney, placenta and osteosarcoma. Bone matrix contains a considerable amount of IGFBP-5. IGFBP-5 is the most abundant IGFBP stored in bone [100]. In addition, IGFBP-5 is the most consistently increased gene out of 159 genes in DNA microarray of mouse bone marrow after castration and the increase in expression is reversed by testosterone administration [101]. It has a high specific binding affinity for hydroxyapatite and ECM proteins by which IGFBP-5 and its bound IGFs become fixed within bone [100, 102-104]. It is the only IGFBP that has been shown to consistently stimulate osteoblast cell proliferation in vitro [100]. IGFBP-5 is distinct from the other IGFBPs to be a key component of the IGF system in bone.

However, there is not much evidence for a role of IGFBP-5 in normal prostate development. Thomas et al investigated the distribution of staining and found that delayed expression of IGFBP-5 correlated with initiation of apoptosis [105]. However, there is a lack of association between the appearance of apoptotic cells in the prostate and levels of IGFBP-5 expression in the tissue [106]. In addition, IGFBP-5 did not co-stain with apoptotic cell markers in histological sections of developmental prostate. These findings indicated that the role of IGFBP-5 in apoptosis of the normal prostate development is still a controversial issue.

In contrast with the developing prostate, a number of studies with prostate tumor cells have suggested that IGFBP-5 can enhance PCa growth [107-109]. Gleave and his colleagues observed that stable transfection of IGFBP-5 in LNCaP PCa cells resulted in faster growth of cell compared with vector-transfected controls [109]. Apoptosis was induced by androgen withdrawal in both transfected and untransfected cells, but IGF-I prevented only transfected cells from apoptosis [109]. Tumors derived from LNCaP cells stably transfected with IGFBP-5 proceed more rapidly to AI growth following castration of host rats [107]. However, this study

could not definitely demonstrate whether these effects were dependent on IGFs or whether they were the result of IGF-independent activities of autocrinely produced IGFBP-5.

IGFBPs level can be rapidly and significantly altered in the PCa progression from androgen withdrawal to androgen independence [105, 110-113]. An increase in IGFBP-2 and IGFBP-5 and decrease in IGFBP-3 have been observed in human PCa tissues with high Gleason score compared to those with low scores or benign tissues [114]. In rat prostate, apoptosis induced by castration [115], antiandrogen bicalutamide [116] and vitamin D analogue EB1089 [117] results in an increased gene expression of IGFBP-2, 3, 4, 5. Pollak and his group studied IGFBP expression during regression of AD Shionogi carcinoma tumors after castration. They observed a dramatic increase in IGFBP-5 expression, a slight increase in IGFBP-2 and an immediate decrease followed by increase in IGFBP-3 [111]. Moreover, upregulation of IGFBP-5 after castration was significantly reduced by calcium channel blocker treatment, suggesting that IGFBP-5 is more associated with apoptosis than just a simple androgen repressed gene. Miyake et al demonstrated that overexpression of these IGFBP-2 and IGFBP-5 in LNCaP cells significantly enhances cells growth after androgen withdrawal [109]. Antisense oligonucleotides to IGFBP-2 and IGFBP-5 are able to reduce the stimulatory effects of the IGFBPs on LNCaP tumor growth [118]. Treatment of androgen-sensitive Shionogi tumour cells with antisense oligonucleotides to IGFBP-5 inhibited the growth of these cells compared with control vector-transfected cells [107]. All these suggested that not only IGFBP-2 and IGFBP-5 have a stimulatory effect on PCa cells, but they can promote recovery from castration-induced apoptosis and cell cycle arrest. This protective function is thought to be realized by their binding to ECM and maintaining a higher concentration of IGF-I in the neighbourhood of the IGF-IR and

resulting in increased IGF-IR signaling [107]. IGFBP-2, -3 and -5 play an important role in PCa progression from AD to AI.

1.6.4 IGFBP Proteases

In addition to these IGFBPs, it is becoming increasingly appreciated that another important component of the IGF axis is a group of IGFBP proteases, which act to hydrolyse IGFBPs, resulting in a dramatic reduction in affinity between IGFBPs and IGFs, and potentially frees the IGFs to interact with their receptors [119]. The IGFBP proteases fall into three groups: extracellular kallikrein-like serine proteases which cleave IGFBP-3 including PSA [120], gamma nerve growth factor (γ-NGF) [121] and urokinase plasminogen activator (uPA) [122]. PSA also cleaves IGFBP-5 in the seminal plasma [120]. Another serine protease is thrombin which protelyzes IGFBP-5 [123]. Other kallikreins including human plasma kallikrein (hPK) and rennin are relatively poor IGFBP proteases [55]. Matrix metalloproteinases (MMPs) form a family of peptide hydrolases that act in tissue modeling by degrading ECM components such as collagen and proteoglycans. MMP-1 is presented as the primary IGFBP-2 protease [124]. MMP-1 to -3 can proteolyze IGFBP-3 to regulate cellular growth and proliferation [125]. Intracellular cathepsins is another group of proteases which can cleave IGFBP-1 to -5. Cathepsin D is identified as an IGFBP protease in LNCaP and PC3 PCa cell conditioned medium (CM) [126]. These IGFBP proteases play an important role in modulating the bioactivity of IGFBPs, thus indirectly influence the bioavailability of IGFs.

IGFBP proteases have unique structures to perform the function of cleaving the IGFBPs. IGFBPs contain three distinct domains: the conserved N-terminal domain, the highly variable midregion and the conserved C-terminal domain. It is believed that the midregion acts like a hinge between

the N- and C-terminal domains. The high affinity binding of IGFs by IGFBPs is assumed to involve interactions between the N- and C-terminal domains working like a clip. The binding is initiated by IGFs interaction with the N-terminal domain and perhaps part of the midregion. However, participation of the C-terminal domain to hold IGFs tightly is required to complete the high affinity binding. In certain biological environments, IGFBPs can be proteolyzed by these proteases at sites in the midregion, resulting in decreased affinity for IGFs and further breakdown of the IGFs-IGFBPs complex [127, 128]. Increased proteolysis of IGFBP-3 has been shown in PCa by PSA [129], cathepsin D [130], and uPA [131]. A negative correlation between serum IGFBP-3 level and PCa risk suggests a protective role against the effects of systemic IGF-I [132]. All these indicated that enhancement of IGFs function by PSA and other proteases can play a critical role in modulating IGF bioavailability, further carcinogenesis and tumor development.

1.6.5 IGFBPrPs

Several low-affinity IGF binders, called IGFBP-related peptides, have also been discovered that exhibit significant structural homology to high-affinity IGFBPs. IGFBPrPs bind IGFs with low affinity and also play important roles in cell growth and differentiation [133]. IGFBPrP1 appears to be involved in diverse biological functions, including regulation of epithelial cell growth and stimulation of fibroblast cell growth. It can associate with type IV collagen [134], and also can bind IGFs and insulin [135]. IGFBPrP2 has a role in fibroblast and endothelial systems as well as in epithelial growth [136]. IGFBPrP4 has been shown to promote adhesion of fibroblasts and epithelial cells, to induce chemotaxis of fibroblasts [137], and to play a role in chondrogenesis [138]. IGFBPrP5 mRNA and protein expression are upregulated in osteoarthritis. Other peptides

including IGFBPrP3 and IGFBPrP6-10 also show low affinity for binding IGFs, however their biological function is still unclear [87, 95, 133, 139-144].

1.7 Prostate Cancer Progression from AD to AI

If primary PCa is not treated properly, PCa patients will eventually develop lymph nodes and bone metastasis. For patients with metastatic disease, androgen ablation is still the best palliative therapy. Upon androgen withdrawal, more cells undergo apoptosis and fewer cells proliferate so that the tumor regresses. Approximately 80% of patients have symptomatic response after treatment with antiandrogen or castration. Howeve, PCa will eventually progress to AI. Once PCa becomes AI, it indicates that tumor cells adapt to maintain their proliferative capacity and lose the apoptotic response to androgen withdrawal [145].

Androgen independence of PCa is a major obstacle to the treatment of PCa. How to prevent or block PCa progression from AD into AI remains a huge challenge for both urologists and medical researchers. Different hypotheses explaining the mechanism of this process have been proposed [146]. A number of mechanisms can possibly contribute to this AI [147]. The AI cell clones are selected from a heterogeneous population of AD and AI cells by androgen withdrawal. The AD stem cells that can adapt to self-renewal in the absence of androgen. Small residual amounts of androgen can stimulate androgen sensitive cells. AR is activated by other steroids due to AR mutation. AR is phosphorylated by growth factors, such as IGF, EGF, to become activated in the absence of androgen [7, 147]. It is also evident that androgen can regulate the expression of many prostate-related growth factors through AR [148]. The mechanism of androgen-independence in PCa is more complicated than expected, and is still unclear.

1.8 Prostate Cancer Bone Metastasis

PCa progression to AI is usually accompanied with cancer metastasis. Most patients with cancer die of incurable metastasis rather than the primary tumor. Bone is the most likely metastatic site for PCa, and lung or liver may also occasionally become affected. It is estimated that more than 350,000 people in the United States die with bone metastasis each year [149]. Bone is the third most common site of metastasis for all cancer types and is the most frequent metastatic organ for certain types of cancers, such as PCa [150]. It is estimated that in terminal patients, 95–100% of myelomas, 65-75% of breast and PCas, 60% of thyroid cancers, and 15-45% of bladder, lung, and renal cancers and melanomas suffer from bony metastasis.

It is important to understand how and why PCa cell are so likely to migrate to bone and survive, proliferate in the new bony environment. It has been over 100 years since Dr. Stephen Paget in 1889 published his famous "seed and soil" hypothesis [151]. He predicted that unique factors located at the site of metastasis served as fertile soil promoting proliferation of seeded tumor cells outside of their original environment. He hypothesized that it was the compatibility between the "seed" and the "soil" that determined whether tumors could survive and grow at a distant site. After many years of research into genetic deregulation inside the cancer cell, the "seeds", scientists and physicians are now focusing more on tumor environment, the "soil". This turn of focus is led by the unsatisfactory explanation of tumor development and progression, the increased knowledge of tumor microenvironment and therefore the demand to reassess of our previous assumption about the nature of cancer and how to control it [152-155].

Once regarded to be composed of a homogeneous population of cancer cells, tumors are now recognized as heterotypical and complex tissues containing not only malignant cancer cells but

also co-evolving normal neighboring cell types [156, 157]. The normal host cells found in the tumor microenvironment is a complex system of many cell types including stromal fibroblasts of various phenotypes, myofibroblasts, vascular cells (endothelial cells, pericytes, and smooth muscles), immune cells (lymphocytes, macrophages, dendritic cells, and mast cells) and their embedded ECM. In this complicated system, these different types of cells coexist and actively interact with each other with the invading malignant cells initiating and driving a vicious cycle of tumor expansion. The neoplastic cells induce the stromal cells to serve as active conspirators so that the activated stromal cells can reciprocally induce and maintain the growth of malignant cells. The dynamic expression of various genes is influenced by active interactions among these cells, surrounding matrix, and their local physical and biochemical microenvironment. The biological products encoded by these genes, such as growth factors [158, 159], cytokines [160], chemokines, hormone, transmembrane receptors [161, 162], cell adhesion molecules, and other proteins produced locally and/or systemically [163, 164], in turn, control the pathophysiological characteristics of the tumor. Tumor microenvironment has been implicated in the regulation of cell growth, determining metastatic potential and possibly determining location of metastatic disease.

It is assumed that inclination of cancer cells for bone is largely due to rich reticulate vasculature, uniquely abundant oxygen, nutrients and survival factors to tumor cells. Bone serves as a rich soil for the tumor cells to lodge and grow partly because it is a huge pool for growth regulatory factors. Bone accommodates a wide variety of growth factors, such as IGFs [165], TGF-β [166], bone morphogenetic proteins (BMPs) [167], FGFs [168, 169] and platelet-derived growth factor (PDGF) [170].

1.8.1 Bone Microenvironment

The factors listed here are responsible for regulation of the natural turnover of bone. This continuous remodeling is the result of the coupled and balanced action of bone resorbing osteoclasts and bone forming osteoblasts. Osteoblasts are derived from stromal stem cells of the bone marrow stroma and are responsible for bone formation by secreting new matrix. Osteoclasts are derived from hematopoietic stem cells and account for bone resorption by producing enzyme and acid to break down the matrix. Osteoblasts and osteoclasts interact with each other to control bone structure under a dynamic balance. This precisely balanced bone hemeostasis is completely disrupted when infiltrated by metastastic tumors.

Most cancer-causing bone metastases are a mixture of osteolytic and osteoblastic. However, breast cancer bone metastastic lesion is primarily osteolytic or osteoperotic disease, and PCa bone metastasis is dominated by osteoblastic lesion or osteoptropic disease. During a breast cancer metastasis development, a classical osteolytic disease, TGF-β is released from the bone matrix to stimulated cancer cells to secrete parathyroid hormone related protein (PTHrP). PTHrP cause osteoblasts and bone stromal cells to express receptor activator of NFκB ligand (RANKL). RANKL then activates its receptor RANK on the surface of osteoclast precursor cells to stimulate osteoclast differentiation. Increased number of osteoclasts resorb more bone and more TGF-β is released, resulting in a vicious cycle of bone destruction and tumor growth.

In PCa metastasis pathogenesis, a classical osteoblastic lesion, osteoblasts are overactive, producing more bone beyond the capability of break down by osteoclasts. Therefore, PCas are associated with profoundly osteoblastic lesions. The determining factors are those that stimulate proliferation or differentiation of the osteoblasts as well as osteoclast apoptosis. Numerous

factors have been identified that mediate osteoblastic lesions. These includes growth factor family (IGF-Is and IGF-IIs [171], FGFs [172] and PDGF [173]), TGF-β family (TGF-β [166], BMPs [167]), proteses and their activators (PSA [174] and uPA [175] [176-178]), and endothelin-1 [179]. Several TGF-β family members and both FGF1 and FGF2 were proved to strongly stimulate new bone formation in vivo [166]. Hydrolysis of IGFBPs by PSA leads to IGFs activation and freedom [174, 180]. Cleavage of TGF-β binding protein by uPA could activate and free TGF-β [181, 182]. These dynamic actions therefore indirectly result in stimulation of osteoblast proliferation and differentiation. Increased circulating concentration of endothelin-1 in patients with osteoblastic metastases indicates its stimulatory function in osteoblast proliferation and bone metastasis in vivo [179, 183], [184]. All these implied that this unbalanced osteoblasts/osteoclasts activity is a consequence of disordered regulatory factor homeostasis.

1.8.2 IGFs, IGF Receptors and Bone

IGF-I and IGF-II are the most abundant growth factors stored in bone. They are produced and secreted by osteoblasts and osteoblasts express IGF-IR and IGF-IIR [185]. The "seed and soil" theory has been supported in the case of PCa: tail vein-injected human PCa cells specifically metastasized to subcutaneously implanted human adult bone but not to other implanted human lung and mouse organs, indicating that human bone have a preferential microenvironment for the landing and subsequent growth of PCa cells [186]. Using a novel antibody directed against human IGF-I and IGF-II, Goya et al successfully inhibited the development of new bone tumors and the progression of established bone tumors in severe combined immunodeficient (SCID)

mice implanted with human adult bone [187]. It is obvious that IGFs played a central role in PCa bone metastasis.

1.8.3 Prostate Cancer Epithelium-Bone Stroma Interaction in Bone Metastasis

The tendency of PCa cells most likely metastasizing to bone and causing an osteoblastic lesion is a result of interactions between PCa cells and oesteoblasts. PCa cells can alter the normal balance between osteoblast and osteoclast activities, resulting in osteoblastic metastasis by means of secreting osteoblastic factors, such as IGF-I, FGF, TGF-β, PDGF, VEGF, PSA and uPA. These factors either directly promote activity of osteoblasts or remodel the bone matrix microenvironment. On the other hand, osteoblasts also secrete factors that accelerate progression of PCa in bone [188, 189]. However these bone-derived factors have not been identified [188]. To determine the role of tumor-stromal cell interaction and stoma-specific growth factors in PCa growth and metastasis, Gleave et al coinoculated poorly tumorigenic human PCa LNCaP cells and various tissue-specific fibroblasts subcutaneously in athymic mice. They found that LNCaP tumor induction rate is highest while inoculated with human bone fibroblasts (62%), followed by two prostate fibroblast cell lines (31% and 17%), but not with lung, kidney or embryonic 3T3 fibroblasts [190, 191]. Through mitogenic assays using mutual stimulation of serum-free CM from LNCaP and bone or prostate fibroblasts, and selecting several known fibroblast-derived growth factors to test, they observed that among them, FGF2 was the most potent mitogen that stimulates the LNCaP growth. However, it is difficult to draw a clear conclusion that FGF is the driving force for inducing these LNCaP tumors [61]. Identifying the key mediators contributing to survive and proliferate of PCa cells in the new environment, bone, becomes a question that needs to be immediately addressed in the field of PCa research.

1.9 Specific Experimental Objective

Bone metastatic PCa is an incurable disease. Patients at this stage may suffer from progressive severe bone pain, spinal cord compression, urination obstruction and poor general condition. All these symptoms lead to deprivation of quality of life from the patients. The bone metastasis of PCa definitely requires more attention. The explanation of compatibility between bone stroma cells and PCa cells is still unclear. The mechanisms of how bone metastatic PCa cells make their establishment in bone and how they further manage to survive androgen-ablation treatment and still proliferate are unknown.

We hypothesize that increased expression of IGFBP-5 in bone stroma in response to androgen ablation may be an important factor for promoting establishment of PCa metastatic lesions and AI progression in patients undergoing hormone withdrawal therapy through its ability to enhance IGF-mediated survival signaling.

2 MATERIALS AND METHODS

2.1 Tissue Culture

2.1.1 Cell Passage

LNCaP human PCa cells were obtained from American Type Culture Collection (ATCC), and maintained in RPMI supplemented with 10% FBS (Invitrogen Canada Inc. Burlington, Ontario). MG63 human osteosarcoma cells and PC3 human PCa cells were obtained from ATCC and maintained in DMEM supplemented with 10% FBS (Invitrogen Canada Inc. Burlington, Ontario). Cells were passaged at 70% confluency. Cells were cultured in 10 cm tissue culture plates (Nalge Nunc International, Rochester, NY) at 37°C and 5% CO_2. To passage cells, the media was aspirated and cells were washed once in 2 ml of phosphate buffered saline (PBS) and 1 ml of 1x Trypsin-EDTA [10% 10x Trypsin-EDTA (Invitrogen, Burlington, ON) and 90% Fetal Bovine Serum (FBS, Invitrogen, Burlington, ON)] was added to the plates and incubated for one to three minutes to loosen adherent cells. Cells were triturated from the plates with 5 ml of media and added to a larger volume of media for replating. Cells were passed at 1:4 ratio in 10 cm plate or from one 10 cm plate into one 6-well plate (Nalge Nunc International, Rochester, NY) for transfection.

2.1.2 Thawing Cells

Frozen cells stored at liquid nitrogen (-196°C) were thawed rapidly in a 37°C water bath and immediately added to 9 ml of media with 5% FBS in a 10 cm plate.

2.1.3 Plasmid Stable Transfection and Clone Selection

2.1.3.1 Plasmid Stable Transfection

24 hours before transfection, 6 x 10^5 MG63 were seeded in 6-well plates to make cells 90-95% confluent at the time of transfection. The following protocol was followed for each well. 4 μg of purified plasmid pRc/CMV/IGFBP5 or pRc/CMV (as a control) was gently mixed with 250 μl of OPTI-MEM I Reduced Serum Medium (clear, Invitrogen, Burlington, ON). 10 μl of Lipofectamine 2000 was gently mixed with 250 μl of OPTI-MEM I Reduced Serum Medium (clear, Invitrogen, Burlington, ON). Plasmid and Lipofectamine 2000 were gently mixed and incubated at room temperature for 20 minutes. The total 500 μl of mixture was then added to each well of MG63 cells. After 24 hours of incubation at 37°C, cells were lifted with Trypsin-EDTA (Invitrogen, Burlington, ON) and passed onto a fresh 6-well plate at ratio of 1:10. After 24 hours with approximately 15% confluency, 400 μg/ml of Genetisin (Invitrogen, Burlington, ON) was added the cells in each well. Cells were replaced with fresh Geneticin-containing medium every 3 to 4 days. 2 to 3 weeks after transfection, colonies were harvested using pipette tips onto 24-well plates. Subsequently colonies were transferred onto 12-well plates and eventually 6-well plates to expand to cell lines.

2.1.3.2 Clone Selection

After establishment of stable transfected cell lines, RNA and protein were extracted for test of positive transfection colonies. In all, thirty-one colonies were tested IGFBP-5 RNA and protein from concentrated CM by Reverse Transcriptase-Polymerase Chain Reaction (RT-PCR), northern blotting and western blotting. Four colonies were confirmed both expressing IGFBP-5 RNA and protein, however different levels of IGFBP-5 protein had been seen among these four

IGFBP-5 expression colonies. Based on the amount of IGFBP-5 protein that each IGFBP-5 expressing colony produced and later secreted into CM, the colony with the highest IGFBP-5 production was selected and used for the experiments. 70 μl of concentrated CM were concentrated from 1ml of CM using UFC800524 (Millipore Corporate, Billerica, MA, USA)

While CM was concentrated, proteins of each sample were harvested using the same volume of RIPA lysis buffer (20 mM of 1 M Tris-HCI/SDS, pH 7.4, 1% Triton-X-100, 0.1% deoxycholic acid, 1 mM of 0.5 M EDTA, 1x cocktail protease inhibitor (Roche Diagnostics, Mannheim, Germany), 1 mM sodium vanadate, 2 μM microcystin), 1ml for each 10 cm plate. BCA assay (Pierce, Rockford, IL) was performed. The protein concentration was calculated. 40 μl of each sample were loaded on a SDS-PAGE gel. Loading control strategy was used to make sure that CM of each sample is from the same amount of whole cell lysate protein for quantification of IGFBP-5 production.

2.2 Cell Stimulation

2.2.1 Reagents

Recombinant IGF-I (RDI Research Diagnostics Inc. Flanders, NJ), Recombinant IGFBP-5 (rBP5) (BioVision Research Products Inc. Mountain View, CA), R1881 (Perkin Elmer Boston, Massachusetts), LY294002 (Calbiochem, San Diago, CA) and E3R (Upstate, Tamecula, CA) were used in this study.

2.2.2 Antibodies

Anti-IGFBP-5 (rabbit, polyclonal, 1:1500), anti-IGFBP-2 (rabbit, polyclonal, 1:1000),

anti-IGFBP-3 (rabbit, polyclonal, 1:1000), anti-MAP Kinase2/Erk2 (clone 1b3b9, mouse monoclonal, 1:5000) were purchased from Upstate Biotechnology, Lake Placid, New York. Anti-Phospho-p44/42 MAP Kinase (Thr202/Tyr204), (rabbit, polyclonal, 1:1000), anti-Phospho-Akt (Ser473) (rabbit, polyclonal, 1:1000), anti-Akt (rabbit, polyclonal, 1:1000) were purchased from Cell Signaling Technology, Beverly, Massachussets. Anti-IGF-1Rβ (C-20) (rabbit, polyclonal, 1:200), anti-IGF-IR (3B7) (mouse, monoclonal, 1:1000), anti-Phospho-Tyr (PY99) (mouse, monoclonal, 1:1000) were purchased from Santa Cruz Biotechnology Santa Cruz, CA. Anti-β-actin (AC-15) (mouse, monoclonal, 1:7500) were purchased from Sigma-Aldrich St. Louis, Missori. Anti-Phospho-p44/42 MAP Kinase (Thr202/Tyr204) (rabbit, polyclonal, 1:1000), anti-Phospho-Akt (Ser473) (rabbit, polyclonal, 1:1000) and anti-Akt, (rabbit, polyclonal, 1:1000) were purchased from Cell Signaling Technology, Beverly, Massachussets,

2.2.3 Conditioned Medium (CM)

2.2.3.1 Collection of CM

2.4 x 10^6 MG63-mock (vector-transfected) and MG63-BP5 (IGFBP-5 transfected) were seeded in 10 cm plate. Next day, the cells were washed with PBS and starved in 5 ml serum-free RPMI 1640 for 48 hours. Conditioned media was collected in 15 ml centrifuge tubes (Newton, NC, USA) and centrifuged at 1,500 g for 3 minutes to be clear of cells.

2.2.3.2 Concentration of CM

Supernatant was collected from the above centrifuge tubes and transferred into 10K cut-off concentrator UFC801024 (Millipore Corporate, Billerica, MA, USA) and centrifuged at 3,650 g

for approximately 30 or 12 minutes. 14X or 5X conditioned media were achieved and used for quantification and cell treatment, respectively.

2.2.4 Cellular DNA Content Analysis

LNCaP cells were cultured for 48 hours in serum-free RPMI 1640 ± 40 μM LY294002, with ± 100 ng/ml IGF-I, or with ± 100 ng/ml E3R, or with ± 10^{-9} M R1881, or with ± 100 ng/ml IGF-I plus 10^{-9} M R1881, or with MG63-mock CM, or with MG63-BP5 CM, or with 100 ng/ml IGF-I plus MG63-mock CM, or with IGF-I plus MG63-BP5 CM, or with 10^{-9} M R1881 plus MG63-BP5 CM, or with 100 ng/ml E3R plus MG63-BP5 CM. Cells were detached in 5 mM EDTA in PBS [50 mmol/L sodium phosphate, 150 mmol/L NaCI (pH 7.4)], washed twice with PBS, fixed in ice-cold 70% ethanol for 10 minutes and stained in 1 μg/ml RNase A (Sigma) and 5 μg/ml Propidium Iodide (PI) (Sigma) for 20 minutes. The stained cells were analyzed for relative cellular DNA content on a flow cytometer (Beckman Coulter epics elite; Beckman, Inc., Miami, FL).

2.3 RNA Extraction and Northern Blotting

2.3.1 RNA Extraction

Total RNA was isolated by Trizol reagent (Invitrogen, Burlington, ON). The following protocol was followed. In order to lyse cells, 5 ml of Trizol reagent (Invitrogen, Burlington, ON) was added to a 10 cm dish (Nalge Nunc International, Rochester, NY). The cell lysate was passed through a pipette several times and transfered into a 13 ml centrifuge tube (Aktlengesellschaft & Co. Numbrecht Germany). The cell lysate was incubated for 5 minutes at 15 to 30°C to permit complete dissociation of nucleoprotein complexes. 0.2 ml of chloroform per 1 ml of Trizol

reagent was added. The sample tubes were capped securely and shaken vigorously by hand for 15 seconds and incubated at 15 to 30°C for 2 to 3 minutes. The samples were centrifuged at 10,000 g for 15 minutes at 4°C. Aqueous phase was transfered to a fresh centrifuge tube (Aktlengesellschaft & Co. Numbrecht Germany). RNA was precipitated from the aqueous phase by mixing with isopropyl alcohol (Fisher Scientific, Fair Lawn, NJ). 0.5 ml of isopropyl alcohol per 1 ml of Trizol reagent was used for the initial homogenization. The samples were incubated at 15 to 30°C for 10 minutes, and centrifuged at 10,000 g for 15 minutes at 4°C. The supernatant was removed and the RNA pellets were washed once with 75% ethanol (Fisher Scientific, Fair Lawn, NJ). 1 ml of 75% ethanol per 1 ml of Trizol reagent was added for the initial homogenization. The samples were mixed by vortexing and centrifuging at 7,000 g for 5 minutes at 4°C. The RNA pellets were briefly air-dried for 5 minutes. RNA was dissolved in DEPC (Diethyl Pyrocarbonate, Sigma-Aldrich, Oakville, ON)-treated RNase-free water by passing the solution a few times through a pipette tip, and incubated for 10 minutes at 60°C.

2.3.2 Northern Blotting

RNA concentration was measured by spectrometer. 15 to 20 μg of RNA was loaded on a 1.2 % gel and electrophoresed at 100V for 1 hour. The gel was then transferred onto a Biodyne B membrane (PALL Gelman Laboratory, East Hills, NY) for 20 hours. After the transfer, a picture was taken and the membrane was UV-crosslinked. cDNA probes were generated by RT-PCR from the total RNA of PC3 cells using primers 5'-TGCGACGAGAAAGCCCTCTCCAT-3' (sense) and 5'-AAGGTTTGCACTGCTTTCTCTT-3' (antisense) for IGFBP-5. Following the prehybridization using Ultrahyb (Ambion, Austin, TX, USA) at 68°C for 1 hour, 3 μl (ie 25 ng) of IGFBP-5 cDNA probe was added to 42 μl of 10 mM TE buffer (10mM Tris-CI, 1 mM EDTA,

pH 8.0). The probe was denatured at 95°C for 5 minutes and placed on ice for 1 minute. The cDNA probe was labeled with ^{32}P-α-dCTP using the Rediprime™ II Random Primer Labeling System (Amersham Biosciences, Priscataway, NJ, USA). 50 μCi of α-dCTP P^{32} was added to the labeling vial and mixed by pipetting up and down. The mixture was then incubated at 37°C for 10 minutes. 5 μl of 0.2M EDTA was added to the vial. The probe purification column was pre-spun at 3,000 g for 1 minute in 1.5 ml microcentrifuge tube. The column was transferred to a fresh microcentrifuge tube and the radioactive probe was added to the column, spun at 3,000 g for 2 minutes, and the elute was transferred to a fresh microcentrifuge tube, denatured at 95°C for 5 minutes and placed on ice for 5 minutes. β-actin cDNA probe is generated using primers 5'-GGCATCCTCACCCTGAAGTA-3' (sense) and 5'-CATCTCTTGCTCGAAGTCC-3'(antisense). The radioactive cDNA probe was added to the membrane and incubated at 42°C at low speed rotation for overnight in the hybridization oven. The membrane was washed at 44°C at high-speed rotation with 2X SSC/0.1% SDS solution for 30 minutes twice and 0.1X SSC/0.1%SDS solution 30 minutes twice. The membrane was exposed to a phosphor storage screen for appropriate length of time and the screen was scanned by the Typhoon scanner. Density of RNA band was calculated by the software on the Typhoon scanner (GE Healthcare Bio-Sciences Corp, Piscataway, NJ, USA).

2.4 Protein Extraction, Immunoprecipitation and Western Blotting

2.4.1 Protein Extraction

The media was aspirated from the cells and 200 μl of RIPA lysis buffer was added to each well and placed on ice for 5 minutes. Cells were scraped down, added to microcentrifuge tubes and

placed on ice for 5 minutes. Lysates were cleared by centrifugation at 10,000 g at 4°C and supernatant was assayed for protein content using a BCA assay (Pierce, Rockford, IL). 30 μg of protein were prepared for loading. 1/6 volume of 6x SDS sample buffer (35% 1 M Tris-HCI/SDS pH 6.8, 30% glycerol, 10% SDS, 9.3% DTT, 0.012% bromophenol blue) was added to each sample and boiled for 2 minutes at 100°C. Whole cell lysates were separated by sodium dodecyl sulphate-polyacrylamide gel electrophoresis (SDS-PAGE) and transferred to Immobilon™-P Transfer Membrane (Millipore Corporate, Billerica, MA, USA) for immunoblotting.

2.4.2 Immunoprecipitation

After indicated treatments, IGF-IR was immunoprecipitated from 1mg of whole cell lysates using the IGF-IR MAb 3B7 (Santa Cruz) and anti-mouse IgG-agarose (Sigma) and western blotted with PY99 anti-phosphotyrosine (upper panel) antibody or total anti-β subunit IGF-IR (lower panel) antibody (Santa Cruz). IRS-2 was coimmunoprecipitated from 500 ug of whole cell lysates using a p85 subunit of PI3K polyclonal antibody (UBI) and anti-rabbit IgG agarose (Sigma) and western blotted using anti-IRS-2 antibody (upper panel) or anti-p85 (lower panel) antibody (Upstate). The immunoprecipitates were separated by SDS-PAGE and transferred to Immobilon™-P Transfer Membrane (Millipore Corporate, Billerica, MA, USA) for immunoblotting.

2.4.3 Westen Blotting

After the membranes were placed in blocking buffer [100 ml of TBST pH 7.6 (2.42% Tris-HCI, 8% sodium choloride, 0.5% Tween-20) in 1000 ml dH_2O containing 5% milk for a minimum of 1 hour at room temperature or overnight at 4°C, the primary antibody was added to blocking buffer at the appropriate working concentration. The membranes were incubated for 1 hour at

room temperature or overnight at 4°C. Membranes were washed three times for 10 minutes in 1x TBST. The primary antibodies were detected with HRP-conjugated anti-rabbit or anti-mouse secondary antibodies (DAKO, Glostrup, Denmark). The secondary antibody was added to detect the primary antibody at a 1:2000 dilution in 1x TBST for 30 minutes at room temperature. Membranes were washed again three times for 10 minutes in 1x TBST and visualized by chemiluminescence (ECL, Amersham Pharmacia, Buckinghamshire, England).

2.5 Reverse Transcriptase Polymerase Chain Reaction (RT-PCR)

2.5.1 Preparation of Total RNA

Total RNA was prepared following the protocol of RNA extraction (see 2.3.1). RNA concentration was measured by spectrometer.

2.5.2 Reverse Transcriptase Reaction (RT)

2 μg of total RNA from each sample were used to make a corresponding cDNA using First-Strand cDNA Synthesis System (Invitrogen, Burlington, ON). The following protocol was followed to make cDNA. RNA/Primer mixtures were prepared in sterile 0.2 ml tubes (2 μg of total RNA, 1 μl of 10 mM dNTP mixture, 1 μl of Hexamer). DEPC-treated water was used to bring the volume up to 10 μl for each sample. A sample containing no RNA was used as negative control. Each sample was incubated at 65°C for 5 minutes, placed on ice for 1 minute. The following reaction mixture was prepared. Each reaction was composed of 2 μl of 10x RT buffer, 4 μl of 25 mM $MgCl_2$, 2 μl of 0.1 M DTT, 1 μl of RNaseOUT Recombinant RNase Inhibitor. 9 μl of reaction mixture was added to each RNA/Primer mixture, gently mixed, and collected by brief centrifugation. The mixtures were then incubated at 42°C for 2 minutes. 1 μl (50 units) of

SuperScript II RT was added to each tube, mixed, and incubated at 42°C for 50 minutes. The reactions were terminated at 70°C for 15 minutes, chilled on ice afterwards with final volume as 20 μl.

2.5.3 Polymerase Chain Reaction (PCR)

For each sample, 2 μl of the above 20 μl cDNA was used. Mixtures were prepared (2 μl of cDNA, 0.5 μl of 5'-primer (25μM), 1 μl of 3'-primer (25μM), 22 μl of SuperMix HiFi, Invitrogen, Burlington, ON). The following program was run for the reaction: 1. Initial Denaturation at 95°C for 2 minutes, 2. Cycling: Denaturation at 95°C for 1 minute, Annealing at 58°C for 1 minute, Extension at 72°C for 1 minute, totally 35 cycles, 3. Final extension at 72°C for 3 minutes, 4. Finish at 4°C. Product samples were run on a 1% Agarose gel for analysis.

2.6 Mice Xenograft Study

6-8-week-old male NU/NU mice (Harlan Sprague Dawley, Inc.) were randomly grouped into LNCaP/matrigel Matrigel (Collaborative Research, Bedford, MA), LNCaP/MG63-mock and LNCaP/MG63-BP-5 groups. They were subcutaneously inoculated with $2x10^6$ LNCaP cells plus matrigel (Becton Dickinson Labware, Lincoln Park, NJ), or $1x10^6$ MG63-mock cells or $1x10^6$ MG63-BP5 cells in 0.1 ml through a 16-gauge needle at left front, left rear, right front and right rear of flanks. Tumor take rate, tumor volume were measured and tail vein blood was drawn once weekly once tumors were palpable 4 to 5 weeks after inoculation. The blood was centrifuged and serum was collected for PSA measurement using a PSA enzymatic immunoassay (ELISA) kit (ClinPro International Co. LLC, TM-107, Union City, CA). Tumor take rate, tumor volume and PSA were plotted. Tumor volumes were calculated using the formula, length x width

x depth x 0.5236. In tumor take rate data plotting, nodules that were greater than 150 mm^3 (7 mm in length, width and depth, respectively) were defined to be active tumor and plotted. Comparison of tumor volume and serum PSA among three experimental groups using linear fit analysis. In our castrated mice xenograft study, when average serum PSA of a group reaches ~ 100 ng/ml, surgical castration was performed in all mice in that group. Kaplan-Meier curve was performed for serum PSA data using GraphPad Prism software (GraphPad Software, Inc). Tumors were considered to be AI once serum PSA reaches precastration level. Once tumor volume reached 10% of the body weight or PSA reached precastration level in castration series), mice were sacrificed and tumors were harvested and fixed in formalin for making tissue microarray (TMA).

2.6.1 Xenograft Tissue Microarray Preparation

A TMA was constructed using formalin-fixed, paraffin-embedded mice xenograft specimens. Deparaffinized and rehydreated TMA sections were steamed in citrate buffer for 30 minutes to enhance antigen retrieval.

2.6.2 Immunohistochemical (IHC) Studies

Immnunohistochemical labeling with apo-tag (Chemicon Inc. Billerica, MA), AR (Santa Cruz Biotechnology), vimentin (Santa Cruz Biotechnology) and Ki-67 (DAKO, Inc. Mississauga, ON) were performed overnight. Slides were washed with PBS and incubated with streptavidin-horseradish peroxidase-conjugated IgG secondary antibody (DAKO, Inc. Mississauga, ON) for 10 minutes at room temperature, developed with Nova-red, counterstained with hematoxylin and stained with staining blueing reagent. The TMA slides were imaged digitally and eventually reviewed by two independent pathologists. Visual scoring was performed using Image Pro Plus

(IPP), a digitalized immunohistochemistry scoring program (Media Cybernetics, San Diego, CA).

2.7 Data Analysis

All results of cell cycle analysis, cellular DNA content analysis and immunoblotting of signaling activation were from three different biological replicates. Representative immunoblots are provided to demonstrate the primary data. Statistical significance of data in cell cycle analysis, cellular DNA content analysis and immunoblotting of signaling as well as in tumor take rate analysis was assessed by student t test. Specifically, statistical significance of data in immunoblotting of signaling was analyzed with one sample test of the difference between two treatment with a hypothetical mean set as zero. A linear fit analysis was used to assess difference between xenograft growth and PSA kinetics. A logrank test was used to assess difference of survival between xenograft groups and a hazard ratio was used to assess difference of relative risk of serum PSA relapse between xenograft groups in Kaplan-Meier analysis.

3 INVESTIGATING THE ROLE OF BONE STROMA-PRODUCED IGFBP-5 IN PROSTATE CANCER CELL SIGNALING IN VITRO

3.1 Introduction

Epithelial-stromal crosstalk is essential to normal prostate differentiation and development as well as PCa carcinogenesis [9, 23]. Androgen is an indispensable factor for stroma-mediated prostate epithelial normal and cancer cell growth and survival [192]. PCa with bone or other site metastasis is treated with androgen withdrawal therapy. PCa cells undergo apoptosis and reduced proliferation at an early stage in response to androgen ablation. However, PCa cells eventually lose their response and become AI. In parallel to the role of andromedins in normal prostate development, AI progression is thought to be at least in part facilitated by increased responses of androgen-deprived tumor cells to microenvironment-derived andromedin growth factors, such as IGF-I axis [43, 44]. Bone contains a significant portion of IGF-I and IGF-II existing in the local microenvironment. IGF-I responsiveness is implicated in promoting androgen-independent progression of PCa.

The biological activity of IGFs is primarily regulated by IGFBPs. IGFBP-2 and IGFBP-5 upregulate and IGFBP-3 downregulates in less differentiated human PCa tissues versus more differentiated or benign tissues [193]. A significant increase in IGFBP-5, a slight increase in IGFBP-2 and an immediate decrease followed by increase in IGFBP-3 were observed in AD Shionogi tumor after castration [111]. Gleave et al observed that stable transfection of IGFBP-5 in LNCaP PCa cells resulted in faster growth of cells compared with vector-transfected controls

[109]. However this study could not definitely demonstrate whether they were the result of IGF-independent activities of autocrinely produced IGFBP-5 or IGF-dependent outcome, nor any above-mentioned studies investigate alteration of IGFBPs in PCa-invading bone stromal microenvironment.

The fact that PCa mostly metastasize to bone indicated that bone stroma is a favorable microenvironment for PCa cell to grow and proliferate. Bone-derived factors that contribute to PCa growth and survival have not been identified. IGFBP-5 is a potential candidate that mediates interaction of bone stroma and PCa cells. IGFBP-5 is unique to bone microenvironment. IGFBP-5 is found to be the richest IGFBP in bone [100]. IGFBP-5 binds to a number of ECM proteins and has the unique property of binding to hydroxyapatite, a component of the mineralized ECM of bone. IGFBP-5 is postulated to help sequester and concentrate IGFs in bone, thereby increasing local extracellular IGF concentrations to activate IGF-IR signaling [100, 102-104, 194]. Most importantly, recent study showed that IGFBP-5 is the most consistently increased gene in mouse bone marrow after castration [101].

Figure 3.1A shows possible IGF signaling in normal prostate epithelial cells through epithelial-stromal interaction. Testosterone enters cells, is converted to DHT by 5-α reductase and binds to AR. The DHT-AR complexes go into the nucleus and binds to AREs to transactivate target genes with decreases in IGFBPs and increases in IGF-IR and MMPs. Prostate stromal cells also secrete low level of IGFBPs and high level of IGFs. IGFs and IGFBPs produced by epithelial cells and stromal cells are secreted outside the cells and get into the vicinity of IGF-IR on the membrane of prostate epithelial cells, bind to IGF-IRs and initiates IGF-I-mediated survival and proliferative signaling. These events might contribute to normal prostate development.

Figure 3.1B raised a question: what is the function of increased bone stromal IGFBP-5 in response to castration in IGF signaling in bone metastatic PCa through prostate epithelial-bone stromal interaction. In response to androgen withdrawal, there is a dramatic increase in IGFBP-5 in bone stroma, as well as a decrease in IGF-IR and an increase in IGFBPs in PCa cells. However, the role of bone stromal increased IGFBP-5 in response to castration in bone stromal-PCa epithelial interaction, and the mechanism of how bone metastatic PCa cells manage to survive androgen-deprived stress and become AI, are still unknown.

Based on the above observations, and especially inspired by Xu et al's observation that IGFBP-5 is most consistently increased gene out of 159 genes in mouse bone marrow after castration [101], we wanted to investigate the hypothesis that increased expression of IGFBP-5 in bone stroma in response to castration maybe an important factor for promoting establishment of PCa bone metastatic lesions and AI progression in patients with bone metastasis undergoing hormone withdrawal therapy.

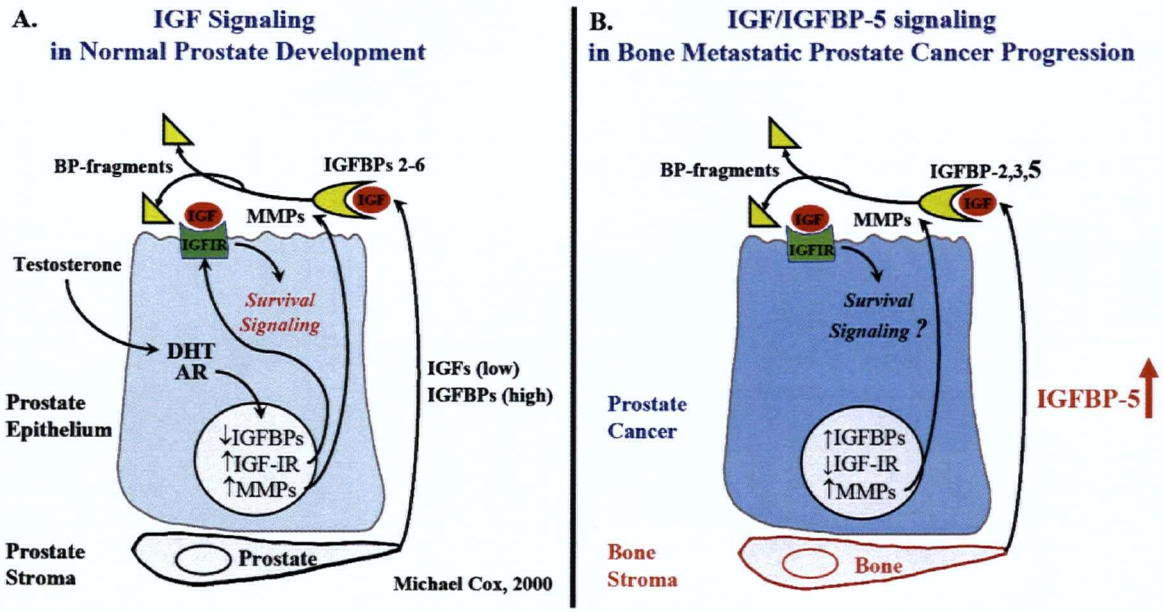

Figure 3.1 IGF Signaling in Normal Prostate Development and IGF/IGFBP-5 Signaling in Bone Metastasis Prostate Cancer Progression. A. In normal prostate epithelial cells, IGFs bind to the IGF-IR, which causes receptor auto-phosphorylation through the activation of its tyrosine kinase domain. Downstream Akt and MAP Kinase are subsequently activated, thereby a number of target genes are transactivated. Expression of IGF-IR, MMPs and IGFs are increased. The MMPs, together with IGFBP-binding IGFs from the prostate stromal cells, travel towards the epithelial cells surface. IGFBPs are cleaved by proteases such as PSA and MMPs, releasing IGFs and enabling them to interact with IGF-IRs. B. In response to castration, IGF-IR level decreases and IGFBPs level increase in PCa cells. Meanwhile, bone stromal IGFBP-5 is showed to consistantly increase upon castration. However, the answer to whether increased IGFBP-5 can provide prostate cancer cells survival signaling and what role(s) of bone stromal IGFBP-5 increased post castration might play in bone stromal-PCa epithelial interaction and the mechanism of how bone metastatic PCa cells manage to survive androgen-deprived stress and become AI, is still unknown.

3.2 IGFBP-5 is Undetectable in MG63 cells

Survival mechanisms of PCa cells occur through the interactions between epithelial tumor cells and stromal microenvironment of the host tissue. A major mediator of anti-apoptosis is the increased IGF-I bioavailability in the bone metastasis microenvironment [195].

Among over 100 genes tested in DNA microarray of mouse bone marrow after castration, IGFBP-5 is the most consistently increased gene [101]. IGFBP-5 is thought to play a key role in regulating IGFs bioavailability, further influencing the biological function of target cells. In order to assess how paracrine bone stromal IGFBP-5 might influence AI PCa progression, we required a human bone cell line that does not endogenously express IGFBP-5. MG63 is a human osteoblastic cell line that does not endogenously produce IGFBP-5. We planned to make a MG63 cell line that express IGFBP-5 using a stable transfection technique. By comparing mock-transfected MG63 cells with IGFBP-5-transfected MG63 cells, we would be able to investigate biological effects of bone stroma-derived IGFBP-5 on PCa cell biology. We may also be able to determine the mechanism of why bone is almost the first and frequently the only site of PCa metastases and why PCa cells can survive, grow and proliferate in the local bone microenvironment.

To determine whether MG63 cells express IGFBP-5, we first checked if there is IGFBP-5 mRNA expression in MG63 cells. Total RNA was collected from MG63, LNCaP and LNCAP/BP5 cells [107] and MG63 messanger RNA was processed from MG63 total RNA. All four RNAs were loaded onto a gel for Northern blotting. LNCaP cells are known not to express IGFBP-5, and were used as a negative control for IGFBP-5. LNCaP/BP5 is a LNCaP cell line transfected with IGFBP-5, and was used as a positive control for IGFBP-5 [107]. As shown in

Figure 3.2A, β-actin at 2.1 kb was used as a loading control for RNA. IGFBP-5 was detected in LNCaP/BP5 at 1.7 kb. No expression of IGFBP-5 was detected in mRNA or total RNA of MG63 cells and in LNCaP cells. Second, to determine whether IGFBP-5 protein is produced in in MG63 cells, we checked IGFBP-5 protein expression in MG63 cells. As mentioned above, LNCaP and LNCaP/BP5 were used as a negative and positive control for IGFBP-5, respectively [107]. We have screened a number of types of cell in order to assess IGFBP-5 production. All proteins were loaded onto a gel for western blotting. As shown in Figure 3.2B, β-actin at 42 kDa is used as a loading control. IGFBP-5 protein at 31 kDa is clearly detected in LNCaP/BP5, Shionogi tumor (mouse mammary gland carcinoma) and J82 (human bladder cancer) cell lines. IGFBP-5 expression is not detected in LNCaP, SaOS-2 (human osteosarcoma), PC3 (PCa), RT4 (human bladder cancer) and MSF (human bone fibroblast) cell lines. It is known that PC3 and SaOS-2 cells express IGFBP-5. This can be explained by the fact that IGFBP-5 is a secreted protein and that these proteins were extracted from whole cell lysates. A limitation of this experiment is that it is difficult to detect secreted proteins, such as IGFBP-5, because once IGFBP-5 is produced, it is secreted outside the cells. However, this discrepancy was noticed by my supervisor Dr. Cox. An idea of testing IGFBP-5 protein expression from CM rather than whole cell lysate of MG63 cells was suggested. The IGFBP-5 expression in MG63-BP5 CM will be shown and discussed in Section 3.3. These results indicate that MG63 cells might not express IGFBP-5, however, confirmed by MG63 CM western blotting in next Section 3.3.

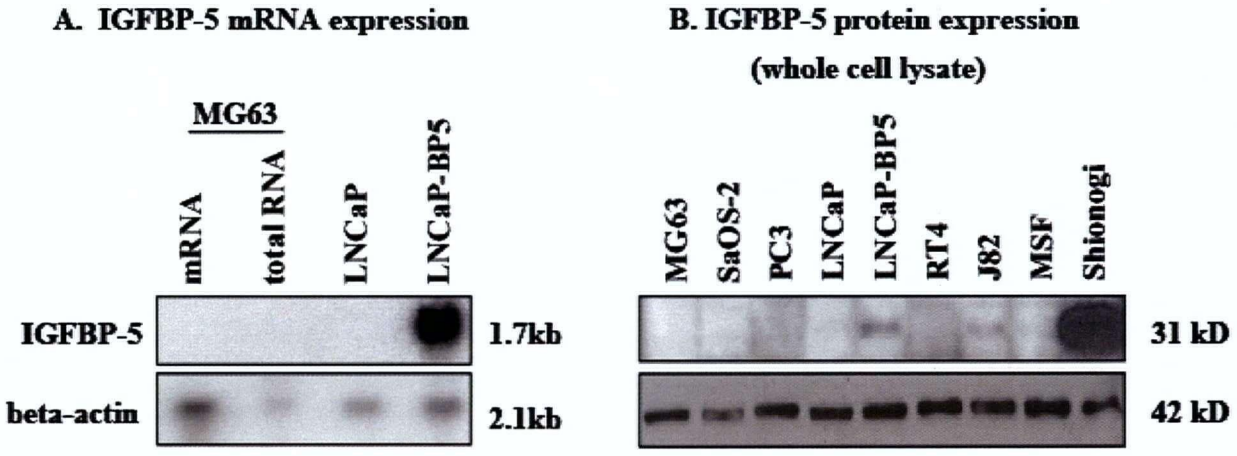

Figure 3.2 IGFBP-5 is Undetectable in MG63 cells. A panel of cell lines were cultured in 10% FBS DMEM. RNAs and proteins were extracted for Northern blotting and westernblotting. A. Total RNA and messenger RNA were loaded on agarose gel, transferred to Biodyne B membrane, hybridized with radioactive IGFBP-5 cDNA probe and exposed to a phosphor storage screen. The screen was scanned using a Typhoon scanner. RNA expression of IGFBP-5 (upper panel) and β-actin (lower panel) was detected. B. Proteins were extracted in whole cell lysate from the above cells, loaded on a SDS-PAGE gel, transferred to PVDF membrane and blotted with IGFBP-5 antibody. Protein expression of IGFBP-5 (upper panel) and β-actin (lower panel) was visualized by chemiluminescence.

3.3 Creation of Stable IGFBP-5-Expressing MG63 Cell Lines

In order to investigate the role of IGFBP-5 in PCa cell survival, proliferation and growth in the bone microenvironment, we established MG63 clones that can overexpress IGFBP-5. We thus stably transfected MG63 cells with IGFBP-5. pRc/CMV/IGFBP-5 was previously made by Dr. Miyake [107]. Plasmid pRc/CMV and pRc/CMV/IGFBP-5 were generously provided by Dr. Martin Gleave (Figure 3.3). Following the transfection protocol (Chapter 2, Section 2.1.3.1), we were able to create mock-transfected cell line with IGFBP-5-transfected cell line. After clones were harvested, RT-PCR, Northern blotting and westernblotting were performed in order to determine clones that express IGFBP-5. Again, LNCaP and LNCaP/BP5 were used as a negative and positive control for IGFBP-5, respectively. In all, thirty-one clones were first screened by RT-PCR. As in Figure 3.4 (top panel), four clones 5-4, 5a, 4-2 and 6-4 expressed IGFBP-5 with a product at 609 bp. Clones 5a and 4-2 appeared to have highest expression of IGFBP-5 compared with clones 5-4 and 6-4. IGFBP-5 was not detected in parental MG63 cells and clone 2-1, one of the clones that were transfected with empty vector. Second, RNA was collected from these clones and checked for IGFBP-5 RNA expression by Northern blotting analysis (Figure 3.4, middle panel), which showed consistent result with RT-PCR, with most expression of IGFBP-5 in clones 5a and 4-2, less expression in clones 5-4 and 6-4, and no expression clone 2-1 as well as parental MG63 cells. β-actin was used as a loading control for RNA at 2.1 kb Figure 3.4 (bottom panel). Subsequently, westernblot analysis (Figure 3.5) of CM from these clones confirmed that clones 5-4, 5a, 4-2 and 6-4 did produce and secrete IGFBP-5 protein into CM. While CM was prepared, proteins of each sample were harvested using the same volume of RIPA lysis buffer. BCA assay (Pierce, Rockford, IL) was performed and protein concentration is thereby calculated. Forty μl of concentrated CM from each clones was loaded. Calculation was

performed to adjust IGFBP-5 production in CM based on same amount of whole cell lysate protein from each clones. The IGFBP-5 protein production in CM is placed in the order from highest to lowest: clone 4-2 > 5a > 5-4 > 6-4. In the meanwhile, protein production of IGFBP-2 and IGFBP-3 was also tested in the CM from these clones. It is similar in levels of IGFBP-2 production, although slightly various in levels of IGFBP-3 production between these clones. Since highest IGFBP-5 production was detected in clone 4-2 CM in greatest contrast to its counterpart clone 2-1 CM, clone 4-2 was selected as the IGFBP-5-transfected MG63 cell line for the future experiments with clone 2-1 chosen as the mock-transfected MG63 cell line. Clone 2-1 and 4-2 were since referred to as MG63-mock and MG63-BP5. In addition, undetection in IGFBP-5 expression in RT-PCR, Northern blotting and CM westernblotting clearly demonstrated that MG63 indeed does not express IGFBP-5.

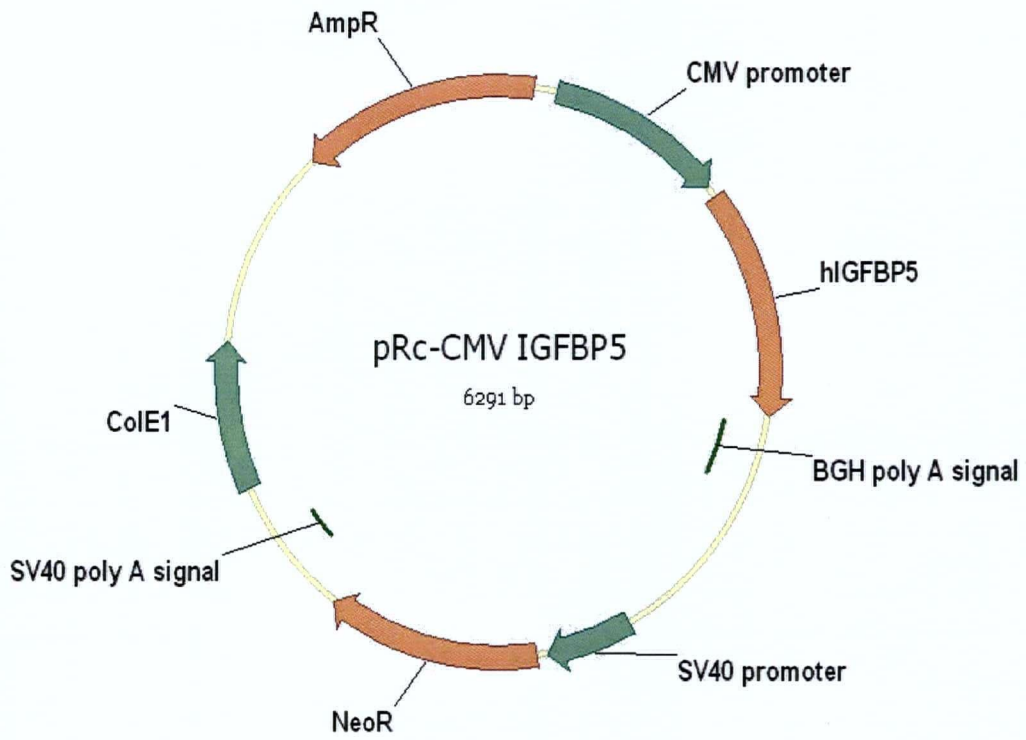

Figure 3.3 Schematic Structure of Plasmid pRc-CMV IGFBP5. Stable clonal cell lines were created from MG63 cells by transfection with a plasmid encoding constitutive IGFBP-5 expression cassette (pRc-CMV IGFBP5) or empty vector (pRc-CMV).

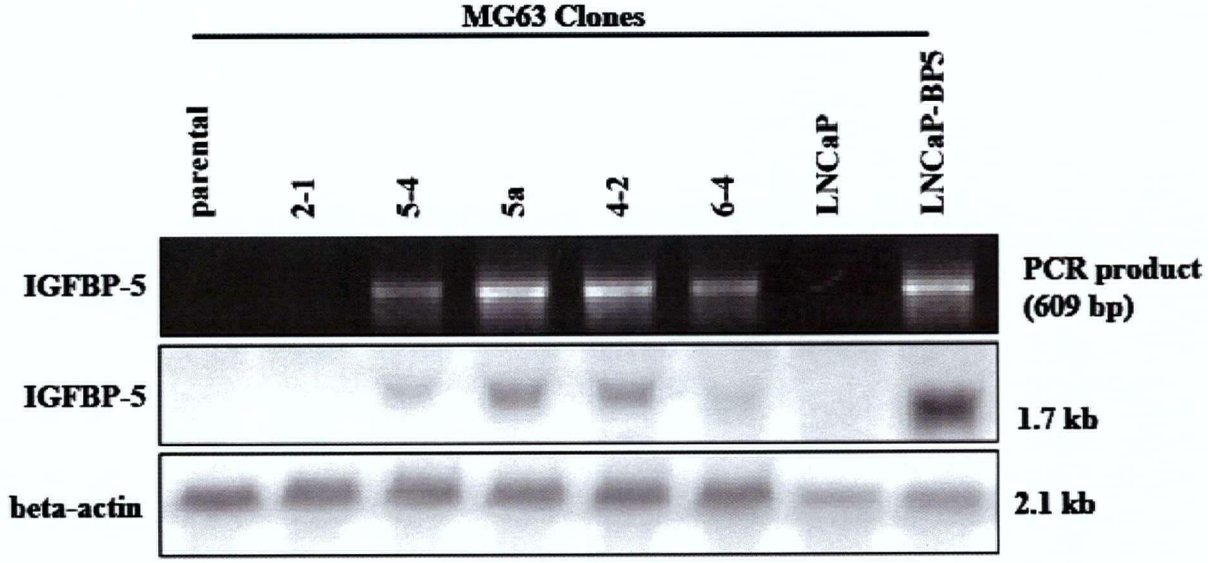

Figure 3.4 RT-PCR and Northern Blot Analysis of IGFBP-5 Expression in MG63-BP5 Clones. Human IGFBP-5 and β-actin cDNA probes were generated by Reverse Transcription (RT) from total RNA of PC3 cells using primers listed in Materials and Methods. RT- analysis (top panel). RNAs were extracted from each clones using Trizol extraction method. Reverse Transcription (RT) was performed and cDNAs of each clones were obtained. Subsequently reaction was performed using the program as described in Materials and Methods. Product samples were run on a 1% Agarose gel and scanned for analysis Northern blot analysis (middle and bottom panel): Total RNA from each clone was loaded on agarose gel, transferred to Biodyne B membrane, hybridized with radioactive IGFBP-5 cDNA probe and exposed to a phosphor storage screen. The screen was scanned using a Typhoon scanner. RNA expression of IGFBP-5 (middle panel) and β-actin (bottom panel) was detected. Density of bands for IGFBP-5 was normalized against that of beta-actin by densitometric analysis.

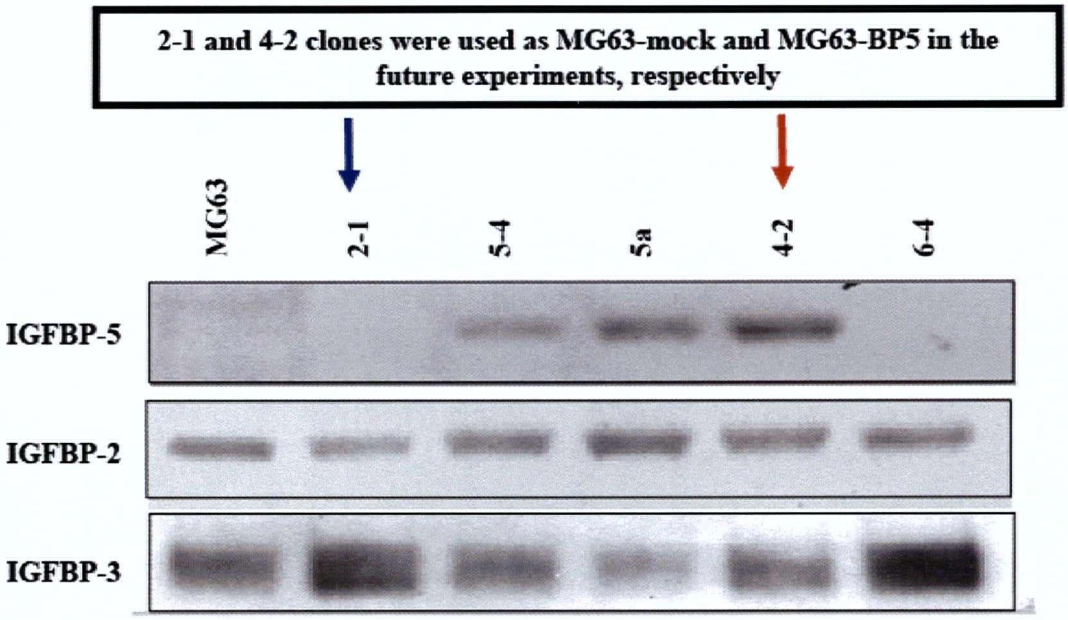

Figure 3.5 Western Blot Analysis of IGFBP-5 Expression In MG63-BP5 CM. 2.4×10^6 cells were seeded in a 10 cm plate. Next day the plate was rinsed with PBS and cells were starved in 5 ml serum-free RPMI 1640 for 48 hours. CM was collected and concentrated up to 14X using centrifuge concentrator UFC801024 (Millipore). In the meantime, whole cell lysate was harvested using the same amount of RIPA lysis buffer. The protein concentration is analyzed by BCA assay. 40 µl concentrated CM from each samples were loaded on a SDS-PAGE gel and transferred to PVDF membrane for westernblot analysis. The membrane was blotted by IGFBP-5 from Upstate (# 06-110 anti-rabbit) at 1:1500. IGFBP-5 expression was evaluated by densitometry and adjusted further by protein concentration as loading control. IGFBP5 protein production in the above clones in the order from most to least is: 4-2 > 5a > 5-4 > 6-4. Therefore, clone 4-2 was chosen to use in future experiment and referred to as MG63-BP5. clone 2-1 was referred to as MG63-mock.

3.4 Quantification of IGFBP-5 Produced in MG63-BP5 CM

To determine how much IGFBP-5 protein there is in MG63-BP5 CM, we quantified the amount IGFBP-5 produced and secreted into MG63-BP5 CM. Following the protocol in Chapter 2.2.3.2, 6 x 10^6 MG63-BP5 cells were seeded and starved in 12 ml serum-free RPMI 1640 for 48 hours. CM was concentrated up to 50X. In parallel with 1.5, 3, 6, 12, 25, 50, 100 ng of rBP5, 2.5, 5, 10, 20, 40μl of concentrated MG63-BP5 CM were loaded for westernblotting analysis. Densitometry for each band is calculated. A standard curve of rBP5 in ng versus density in unit was established, upon which amount of IGFBP-5 in MG63-BP5 CM is calculated. 10 μl of 50X concentrated MG63-BP5 CM or 0.5 ml of MG63-BP5 CM contains approximately 35 ng of IGFBP-5. It also indicates the concentration of IGFBP-5 in unconcentrated MG63-BP5 CM is 70 ng/ml. At the beginning, we used 1X CM (ie unconcentrated) for LNCaP cell treatment, we did not observe any effect of IGFBP-5. Upon a suggestion from Dr. Duronio, one of my committee members, we tried 5X CM for the LNCaP cell treatment and started observing effect of IGFBP-5. The IGFBP-5 concentration in 5X concentrated CM is 350 ng/ml. The concentration of IGF-I used in our experiment is 100 ng/ml. The concentration ratio of IGFBP-5 to IGF-I is approximately 1:4. Considering that the molecular weight of IGFBP-5 and IGF-I is approximately 30 kDa and 7 kDa (ratio 4:1), respectively, we may easily reason that one IGFBP-5 molecule is needed to carry one IGF-I molecule in order to observe effect of IGFBP-5 on activation of IGF-IR mediated signaling. In fact, our observation is consistent with Jones et al's work [196]. They used a concentration of 80ng/ml for IGFBP-5 and 20 ng/ml for IGF-I to observe the biological effect of IGFBP-5 in their ECM experiments.

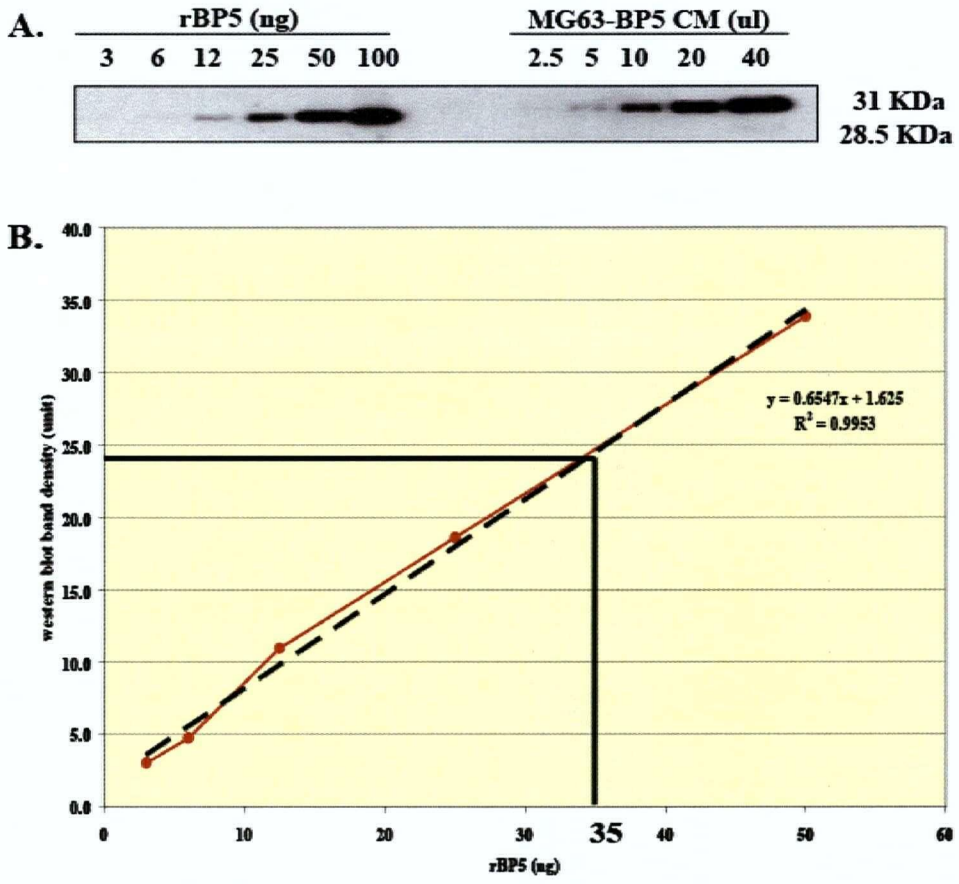

35 ng of recombinant BP5 = 10 ul of concentrated MG63-BP5 CM

Figure 3.6 Quantification of IGFBP-5 produced in MG63-BP5 CM. 6×10^6 MG63-BP5 cells were seeded for overnight attachment. The cells were starved in 12 ml serum free RPMI 1640 for 48 hours. CM was concentrated up to 50X. In parallel with 1.5, 3, 6, 12, 25, 50, 100 ng of rBP5, 2.5, 5, 10, 20, 40µl of concentrated MG63-BP5 CM were loaded for westernblotting analysis in Figure 3.6A. Densitometry for each band is calculated. A standard curve of rBP5 in ng versus density in unit was established, upon which amount of IGFBP-5 in MG63-BP5 CM is calculated (Figure 3.6B).

3.5 IGFBP-5 from MG63-BP5 CM Protects LNCaP Cells from LY294002-induced Apoptosis

Several studies indicated that autocrine IGFBP-5 has an anti-apoptotic function in PCa growth progression [107-109]. IGF-I prevented only IGFBP-5-transfected cells from apoptosis [109]. To determine whether paracrine IGFBP-5 produced by human bone stroma-derived MG63-BP5 cells has an anti-apoptotic function in LNCaP cells, cellular DNA content analysis was performed on cells cultured for 48 hours in MG63-mock, or MG63-BP5 CM (Figure 3.7). Because IGFs and IGFBP-5 have a molecular weight of 7 kDa and 30 kDa, so 10K cut-off concentrator was used in order to remove any MG63-BP5 produced free IGFs and keep all IGFBPs (molecular weight range from 24 to 36 KDa), particularly IGFBP-5. As shown in the cell cycle profiling, LNCaP cells treated with MG63-mock or MG63-BP5 CM exhibited indistinguishable G_0/G_1 or $S+G_2/M$ cell cycle fractions as well as G_0/G_1 or $S+G_2/M$ ratio, indicating no difference in mitotic index. However, we did observe a difference in the sub G_0/G_1 fraction (12% in MG63-mock CM vs. 4.4% in MG63-BP5 CM, respectively). These results indicate that MG63-BP5 CM alone might confer LNCaP cells a decreased apoptotic index fraction under androgen-deprived condition. We went on further to investigate whether MG63-BP5 CM can modulate IGF-I-mediated signaling.

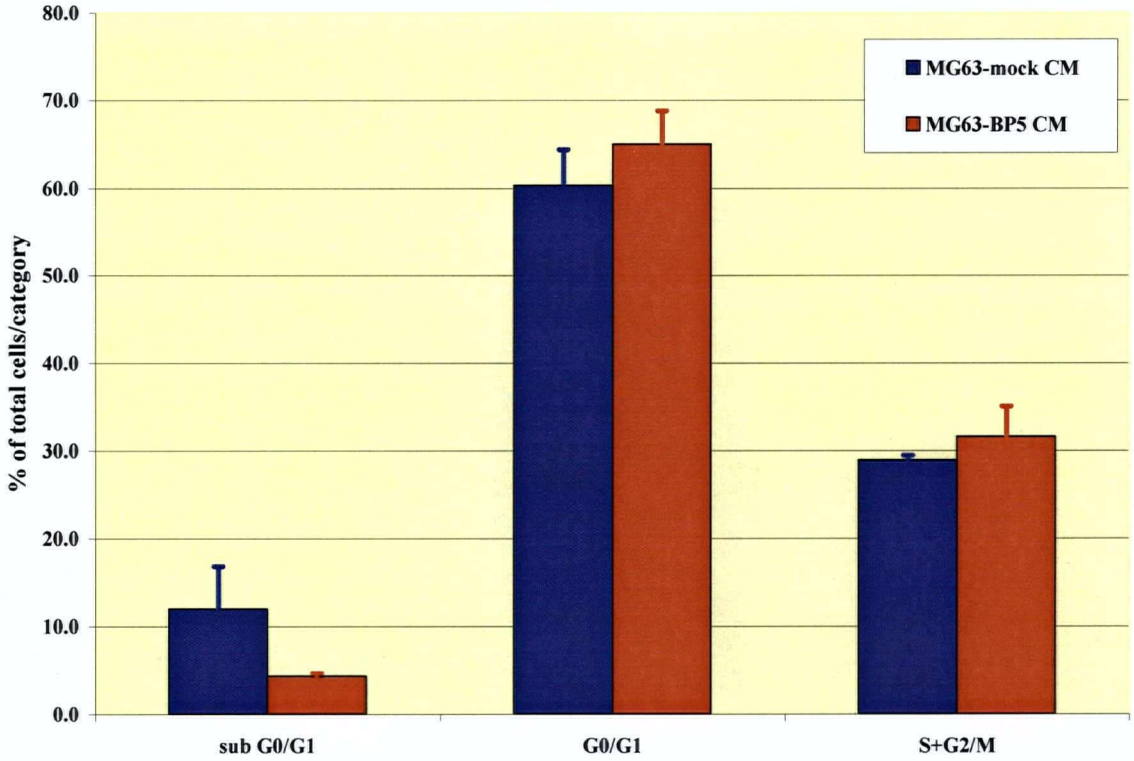

Figure 3.7 Decrease in Apoptotic/Necrotic Fraction in LNCaP cells Treated with MG63-BP5 CM under Serum-Free Conditions (n=3). MG63-mock and MG63-BP5 cells were seeded and starved in serum-free RPMI 1640 for 48 hours. MG63-mock and MG63-BP5 CM were prepared as described in Materials and Methods. LNCaP cells were incubated in MG63-mock and MG63-BP5 CM for 48 hours. Apoptosis was measured by cellular DNA content of PI stained cells and % apoptosis calculated as the fraction of cells with sub-G0/G1 DNA content. The sub-G0/G1 fraction in MG63-mock and MG63-BP5 CM was compared by student t test ($p < 0.05$). Data is representative of three independent biological replicates.

To determine whether paracrine IGFBP5 protects LNCaP cells from LY294002-induced apoptosis, PI staining was performed on LNCaP with a series of treatment (Figure 3.8A). LNCaP cells in serum-free media had a consistent basal apoptosis index (9%) (lane 1). IGF-I and R1881 (a synthetic androgen) slightly reduced basal apoptosis (lane 3 and lane 5). LY294002 induced an 80% apoptosis (lane 2). Further addition of IGF-I and androgen exhibited 20 to 33% protection (lane 4 and lane 6). Dramatic protection (66%) was observed when both IGF-I and androgen were added (lane 8). These results indicate that combination of IGF-I and androgen has a synergistic effect on anti-apoptotic function against LY294002-induced apoptosis. MG63-mock CM alone (lane 9), or MG63-mock CM plus IGF-I (lane 13) had no effect on basal apoptosis. However, MG63-BP5 CM (lane 11), or MG63-BP5 CM plus IGF-I (lane 15) had moderate protection from basal apoptosis. MG63-mock CM (lane 10), MG63-BP5 CM (lane 13) and MG63-mock CM plus IGF-I (lane 14) protected LY294002-induced apoptosis by 20 to 30%. However, 50% protection from LY294002-induced apoptosis was observed in LNCaP cells treated with MG63-BP5 CM plus IGF-I (lane 16). A synergistic function in protection from LY294002-induced apoptosis was observed in LNCaP cells treated with combination of IGFBP-5 containing CM, but not with combination of MG63-mock CM. Recalling that MG63-mock CM contains IGFBP-2 and IGFBP-3, as does MG63-BP5 CM, therefore we concluded that IGF-I signaling is potentiated by the addition of IGFBP-5 in MG63-BP5 CM.

In order to determine whether the ability of IGFBPs to bind IGF-I is required to promote anti-apoptotic signaling, cellular DNA content analysis was performed on LNCaP cells using E3R (a mutant IGF-I that does not bind to IGFBPs) instead of IGF-I. Similar to IGF-I, E3R alone (lane 17), with addition of androgen (lane 19) or MG63-BP5 CM (lane 21) exhibited a slight protection from basal apoptosis. E3R alone had a slight protection from LY294002-induced

apoptosis (lane 18). E3R plus androgen also had a dramatic protection (55%) from LY294002-induced apoptosis (lane 20). However, E3R plus MG63-BP5 CM (lane 22) exhibited a 20% protection from LY294002-induced apoptosis, much less than that of IGF-I plus MG63-BP5 CM (50%). These results indicate that interaction, probably binding between IGFBP5 and IGF-I is essential to performing anti-apoptotic function against LY294002-induced apoptosis. Our data is in accordance with observed consistent increase in IGFBP5 expression in mice bone stroma after castration [101].

Studies from our lab and others showed that one mechanism of enhancing protection from apoptosis is to increase IGF-IR expression and subsequently augment the downstream anti-apoptotic signaling [34, 83]. To determine whether this anti-apoptotic function is due to elevated IGF-IR level, immunoprecipitation and western blotting were performed. LNCaP cells were prestarved for 48 hours and were cultured in MG63-mock CM or MG63-BP5 CM, with or without R1881 for 15 minutes. Same amount of lysis buffer were added to harvest whole cell lysates. Protein concentration were assessed using BCA protein assay kit. IGF-IR was immunoprecipitated from 1 mg protein of each sample and western blotted with total IGF-IR antibody. β-actin was used as a loading control. Each treatment has three biological replicates and was shown in Figure 3.8B. R1881 is dissolved in 100% ethanol, which was used as control for R1881. R1881 increased IGF-IR expression both in cells treated with MG63-mock and MG63-BP5 CM. However, no difference in IGF-IR expression was observed in LNCaP cells treated with MG63-mock and MG63-BP5 CM. These results concur with and confirm the above work [34, 83], indicating that MG63-BP5 CM did not alter IGF-IR expression compared with MG63-mock CM.

The increased anti-apopototic function observed in LNCaP treated with MG63-BP5 CM plus IGF-I is not due to increase in IGF-IR expression, but because of IGFBP-5 produced and secreted into MG63-BP5 CM. IGFBP-5 might serve in substitute of androgen to perform anti-apoptotic function against LY294002-induced apoptosis in an androgen-deprived environment. This switch of utilization from androgen to IGFBP5 might be an adaptive mechanism for PCa cells to survive androgen withdrawal-induced apoptosis.

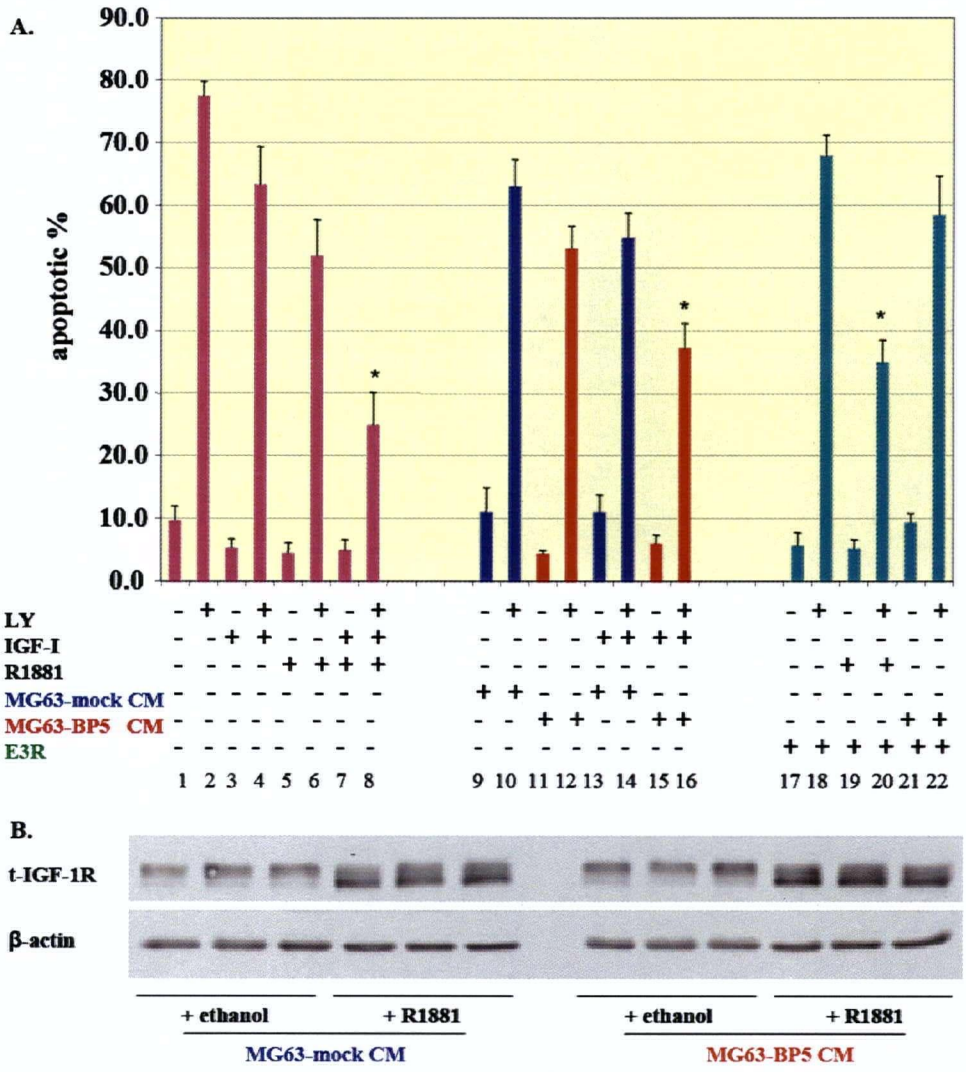

Figure 3.8 MG63-BP5 CM protection of LNCaP cells from LY294002-Induced Apoptosis under Androgen-Deprived Conditions is IGF-Dependent (n=3). (Lane 1 to 22 is from left to right). A. Cellular DNA content analysis. MG63-mock and MG63-BP5 CM were prepared as described in Materials and Methods. LNCaP cells were incubated for 48 hours with ± 40 μM LY294002, or ± 100 ng/ml IGF-I, or ± 100 ng/ml E3R, or ± 10^{-9} M R1881, or MG63-mock and MG63-BP5 CM. Apoptosis was measured by PI stained cells and % apoptosis calculated as the fraction of cells with sub-G0/G1 DNA content. Apoptosis rates in LNCaP treated with 40 μM LY294002 (lane 2), and 40 μM LY294002 plus 100 ng/ml IGF-I plus 10^{-9} M R1881 (lane 8), or LY294002 plus 100 ng/ml IGF-I plus MG63-BP5 CM (lane 16), or 40 μM LY294002 plus 100 ng/ml E3R plus 10^{-9} M R1881 (lane 20) were compared by student's t test (* $p < 0.05$). B. Total IGF-IRs were immunoprecipitated and immunoblotted as described in Materials and Methods. β-actin was used as a loading control. Data is representative of three independent biological samples per treatment (n = 3). Band densities were calculated and compared by student t test (* $p < 0.05$).

3.6 IGFBP-5 Production from MG63-BP-5 CM Promotes Activation of IGF-I-mediated Survival Signaling in LNCaP cells

To determine whether the anti-apoptotic function exhibited by MG63-BP5 CM plus IGF-I is through IGF-I-mediated survival signaling, activities of several important nodes of IGF-I-mediated signaling were investigated by immunoprecipitation and immnoblotting. LNCaP cells were prestarved for 48 hours and stimulated with 100 ng/ml IGF-I plus 5X MG63-mock CM or 5X MG63-BP5 CM, with or without 10^{-9} M R1881 at 0, 20 minutes, 2, 4, 8, 16 hours . Activation of IGF-IR, as well as downstream factors IRS-2, Akt and Erk, were detected. IGF-IR activation was assessed by immunoprecipitation and anti-phospho-tyrosine immunoblotting of the IGF-IR β–subunit (Figure 3.9A and Figure 3.10A). IRS-2 activation was assessed by immunoprecipitation using anti-PI3K-p85-subunit antibody and immunoblotting using anti-IRS-2 antibody (Figure 3.10B). Akt (Figure 3.9B and Figure 3.10C) and Erk (Figure 3.9C and Figure 3.10C) activations were assessed by anti-phospho S473-Akt and anti-phospho p42/p44-Erk immunoblotting, respectively. In the absence of androgen, peak activation of IGF-IR in LNCaP cells treated with IGF-I plus MG63-BP5 CM is only half of that in LNCaP cells treated with IGF-I plus MG63-mock CM. However, peak activation of Akt and Erk in LNCaP cells treated with IGF-I plus MG63-BP5 CM is 1.5-fold of that in LNCaP cells treated with IGF-I plus MG63-mock CM. Statistically significant difference between treatments of IGF-I plus MG63-mock CM and IGF-I plus MG63-BP5 CM in the absence of androgen was found for activation of IGF-IR and Akt ($p < 0.01$), but not for Erk activation. In the presence of androgen, peak activation of IGF-IR in LNCaP cells treated with IGF-I plus MG63-BP5 CM is also only half of that in LNCaP cells treated with IGF-I plus MG63-mock CM. However, peak activation of IRS-2, Akt and Erk in LNCaP cells treated with IGF-I plus MG63-BP5 CM is also 1.5-fold of that in

LNCaP cells treated with IGF-I plus MG63-mock CM. Statistically significant difference between treatments of IGF-I plus MG63-mock CM and IGF-I plus MG63-BP5 CM in the presence of androgen was found for activation of IGF-IR, IRS-2, Akt and Erk ($p < 0.05$). Both in the presence and absence of androgen, decreased peak activation of IGF-IR and interestingly increased peak activation of Akt were observed in LNCaP cells treated with IGF-I plus MG63-BP5 CM, compared to that treated with IGF-I plus MG63-mock CM. These results indicate that the anti-apoptotic function exhibited by IGF-I plus MG63-BP5 CM under androgen-deprived condition might be due to increased Akt activation, rather than increased Erk activation in IGF-I-mediated signaling.

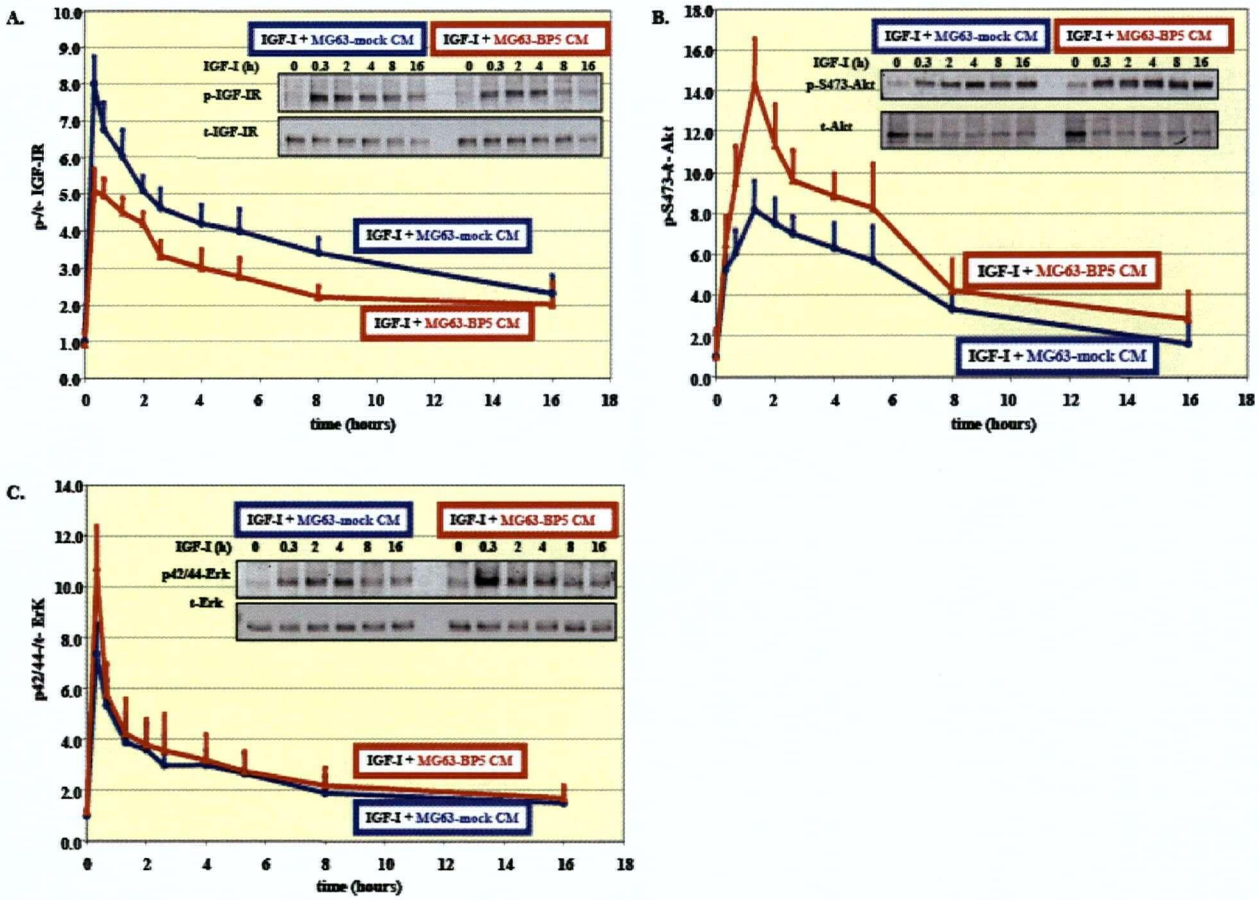

Figure 3.9 Kinetics of IGF-I plus MG63-BP5 CM on Activation of IGF-IR, IRS-2, Akt and Erk in LNCaP cells in the Absence of R1881. LNCaP cells were prestarved in serum-free RPMI 1640 for 48 h and stimulated with 100 ng/ml IGF-I plus MG63-BP5 or MG63-mock CM for up to 16 h. A. IGF-IR was immunoprecipitated from 1mg of whole cell lysates using the IGF-IR MAb 3B7 (Santa Cruz) and anti-mouse IgG-agarose (Sigma) and westernblotted with PY99 anti-phosphotyrosine (upper panel) antibody or total anti-β subunit IGF-IR (lower panel) antibody (Santa Cruz). B. Whole cell lysates were immunoblotted for phospho S^{473} Akt (upper panel) and total Akt (lower panel) antibodies (Cell Signaling). C. Whole cell lysates were immunoblotted with phospho p42/p44 Erk (upper panel) and total Erk (lower panel) antibodies (Cell Signaling). Quantitation was performed on triplicate experiments by densitometry and expressed as the ratio ± SD were performed. Statistical analysis between IGF-I plus MG63-mock and IGF-I plus MG63-BP5 groups was performed with student t test. Significant difference was found for activation of IGF-IR and Akt ($p < 0.01$), but not for Erk activation.

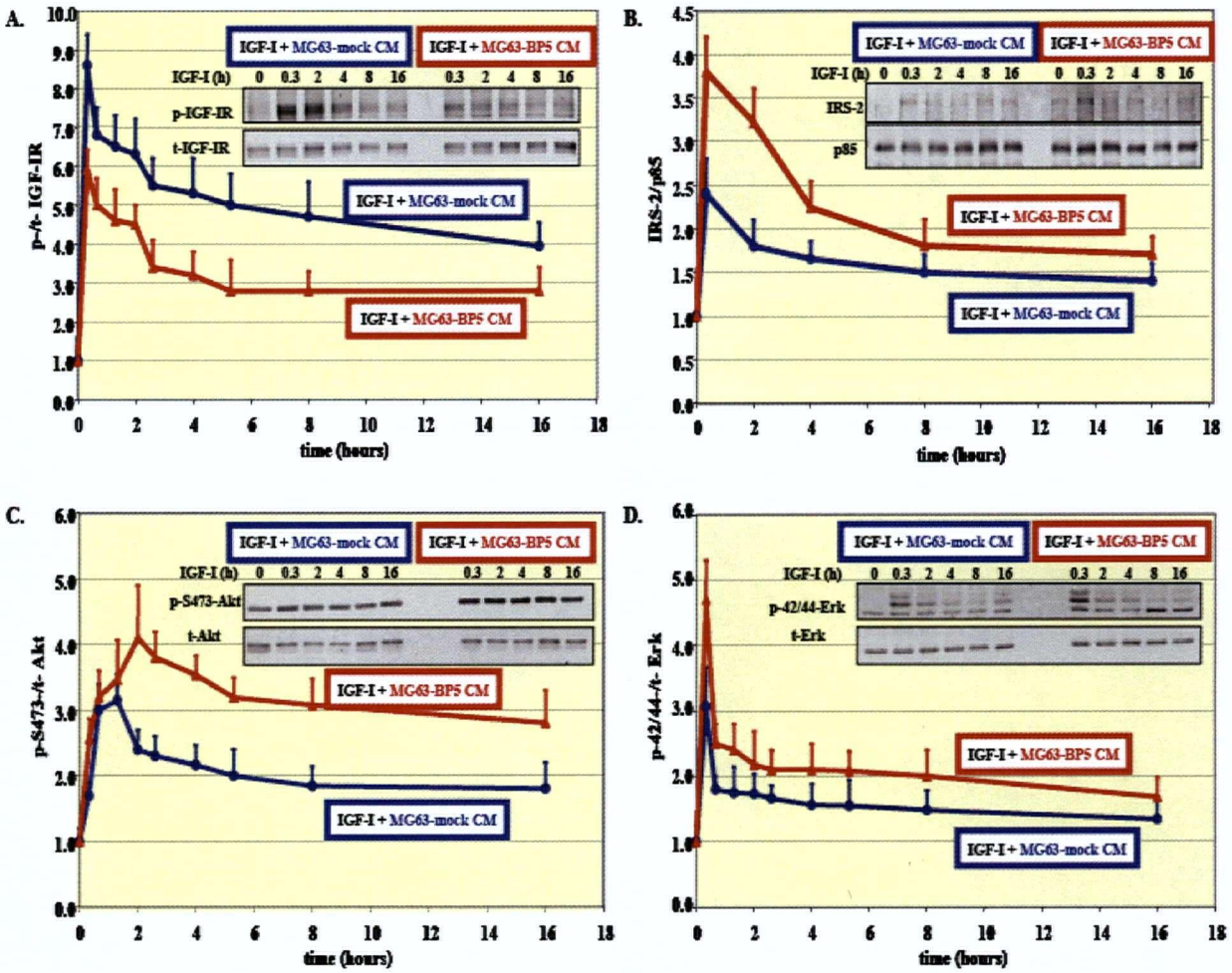

Figure 3.10 Kinetics of IGF-I plus MG63-BP5 CM on activation of IGF-IR, Akt and Erk in LNCaP cells in the Presence of R1881. LNCaP cells were prestarved in serum-free RPMI 1640 for 48 h and stimulated in addition to 10^{-9} M R1881 with IGF-I plus MG63-BP5 or MG63-mock CM for up to 16 h. A. IGF-IR was immunoprecipitated and westernblotted using antibodies as described in Figure 3.9. B. IRS-2 was coimmunoprecipitated from 500 ug of whole cell lysates using a p85 subunit of PI3K polyclonal antibody (UBI) and anti-rabbit IgG agarose (Sigma) and westernblotted using anti-IRS-2 antibody (upper panel) or anti-p85 (lower panel) antibody (Upstate). Akt (C.) and Erk (D.) were detected using antibodies as described in Figure 3.9. Quantitation was performed on triplicate experiments by densitometry. Statistical analysis between IGF-I plus MG63-mock and IGF-I plus MG63-BP5 groups was performed with student t test. Significant difference was found for activation of IGF-IR, Akt, Erk ($p < 0.01$).

3.7 Summary

Both northern blotting and western blotting confirmed that MG63 does not express IGFBP-5. A cell line MG63-BP5 that can stably express IGFBP-5 was established by stable transfection with pRc-CMV IGFBP5. Northern blotting, and western blotting showed that MG63-BP5 cells produce and secrete IGFBP-5 into the conditioned media. Further, IGFBP-5 was quantified by western blotting. Cell cycle analysis showed that a difference in the sub G_0/G_1 fraction of LNCaP treated with MG63-mock CM and MG63-BP5 CM, indicating that MG63-BP5 CM reduces apoptotic index in LNCaP. Cellular DNA content analysis indicated that IGFBP-5 containing CM protects LNCaP cells in the absence of androgen from LY494002-induced apoptosis in an IGF-dependent fashion. Binding of IGFBP-5 and IGF-I is essential for IGFBP-5 to exert this anti-apoptotic function. Western blotting demonstrated that IGFBP-5 produced in MG63-BP5 CM reduced the peak activation of IGF-IR, acting in a submaximal fashion. Interestingly, peak activation of the downstream targets, IRS-2, Akt were enhanced by IGFBP-5 compared to that stimulated by MG63-mock CM. The anti-apoptotic function of IGFBP-5 under androgen-deprived condition might be mediated through increased Akt activation of IGF-I-mediated signaling. This increase in survival signaling is thought to result from slow release of IGF-I for receptor interaction by increased concentration of IGFBP-5. All these implied that stroma-produced paracrine IGFBP-5 played a role in protecing LNCaP cells from apoptosis.

4 INVESTIGATING THE ROLE OF BONE STROMA-PRODUCED IGFBP-5 IN PROSTATE CANCER XENOGRAFT IN VIVO

4.1 Introduction

It has been previously reported that castration-induced apoptosis in the normal rat prostate gland is associated with an increased expression of IGFBPs, and that IGFBP-5 expression is directly regulated by apoptosis-inducing stimuli rather than androgen [117]. The same phenomenon were also found in the Shionogi carcinoma, a well-characterized model of AD neoplasia [108, 197]. IGFBP-5 expression changes most substantially among the IGFBPs in prostate tissues after androgen withdrawal [105, 110, 112, 113, 117]. IGFBP-5 expression is significantly up-regulated in the bone stroma of castrated mice [101]. Although various functional roles of IGFBP-5 expression have been suggested in different model systems, these data are varying and conflicting. For example, IGFBP-5 has been reported to either stimulate or inhibit cell proliferation under different experimental conditions [87, 102, 198-202], and these effects are exerted dependent and /or independent of its well-characterized actions associated with modulation of IGF bioavailability [87, 198]. Up-regulation of IGFBP-5 after castration serves to enhance IGF bioactivity by the findings that antisense IGFBP-5 ODN treatment resulted in decreased Erk activity and number of cells in the S + G_2/M phases of the cell cycle that directly correlated with reduced proliferation rate of Shionogi tumor cells. Systemic administration of antisense IGFBP-5 oligodeoxynucleotide in mice bearing Shionogi tumors after castration significantly delayed time to progression to androgen independence and inhibited growth of AI recurrent tumors. However, to date, there has been no data demonstrating the functional

significance of IGFBP-5 up-regulation in bone stroma after androgen ablation in PCa progression. We showed in Chapter 3 that in vitro MG63-produced IGFBP-5 has a protective effect on LNCaP cells undergoing LY294002-induced cytotoxic stress. This protection might be due to IGFBP-5's prolonged activation of IGF-I-mediated survival signaling. We are interested in assessing whether, in the mouse xenograft model, paracrine IGFBP-5 produced by bone stroma cells can also promote LNCaP cell growth. The observation that LNCaP tumor formation is supported by human bone fibroblasts (62%), followed by two prostate fibroblasts (31% and 17%), not by lung, kidney or embryonic fibroblasts, indicated that human bone fibroblast is most supportive stromal cells so far tested [203]. However, MG63, a human osteosarcoma cell line commonly used for osteoblastic models, has not been tested for the ability to support LNCaP tumor formation. In addition, compared to MG63-mock cells, IGFBP-5 produced by MG63-BP5 cells was shown to have an anti-apoptotic effect on LNCaP cells undergoing LY294002-induced apoptosis in our in vitro data. All these led us to examine whether MG63 cells can support LNCaP tumor formation and growth, if can, whether MG63-BP5 cell-derived IGFBP-5 can enhance this supportive ability.

4.2 Xenograft Study in Intact Mice Coinoculated with LNCaP Prostate Cancer Cells and MG63-mock or MG63-BP5 Cells

4.2.1 MG63 Produced IGFBP-5 does not Affect Xenograft Tumor Take Rate in Mice

To determine whether MG63 cells can support LNCaP tumor formation and growth, mice were randomly grouped into LNCaP/matrigel, LNCaP/MG63-mock and LNCaP/MG63-BP5 arms and subcutaneously inoculated. At week 5 post inoculation, nodules at inoculation sites were

observed and palpable. Tumor size and serum PSA were monitored and measured once weekly as described in Materials and Methods. At this time, mice skin at inoculation sites just appeared as nodules due to inoculation. However, tumors did grow and their sizes increased over time. In order to have tumor take rate determined in an accurate fashion, xenografts were defined to be active tumors when they achieve a size of greater than or equal to 150 mm^3 (7 mm in length, width and depth). Tumor take rate was calculated as a ratio of the number of total tumors at a certain timepoint to the number of total inoculation sites in each group. From week 7 post inoculation, some nodules started to achieve the size of 150 mm^3 and data was plotted (Figure 4.1). The positive control in this experiment was comparison to tumor take rate of matrigel-inoculated tumors. The tumor take rate is 63% in LNCaP/matrigel group, which is in accordance with other's observation of 60% LNCaP tumor take rate [204], indicating that LNCaP cells used in the inoculations were capable of establishing xenografts. At week 7 post inoculation, 30% take rate was observed in LNCaP/matrigel xenografts compared to 7% in LNCaP/MG63-mock and LNCaP/MG63-BP5 xenografts, indicating that matrigel has a function for early tumor formation. Increases in tumor take rate in all three groups are similar between week 8 and week 10 post inoculation. However, at week 10 post inoculation, a plateau was observed in tumor take rate in LNCaP/matrigel xenografts (63%) compared to 37% in LNCaP/MG63-mock and LNCaP/MG63-BP5 xenografts, indicating that matrigel has an enhancing effect on tumor take rate. At week 11 post inoculation, a saturation was observed in tumor take rate in LNCaP/MG63-BP5 xenografts (46%) compared to 40% in LNCaP/MG63-mock xenografts, however, with no significant difference. Tumor take rate reached 44% at week 12 post inoculation and 46% at week 13 post inoculation in LNCaP/MG63-mock xenografts. Tumor take rates in both LNCaP/MG63-mock and LNCaP/MG63-BP5 xenografts reached same level (46%). These

results indicate that while not as efficient as matrigel, MG63 cells could indeed support LNCaP xenografts in nude mice. It was also clear that exogenous IGFBP-5 production by MG63 cells did not alter the tumor take rates. It seems that the ability of MG63 cells to support LNCaP tumor formation (46%) falls between that of human bone fibroblasts (61%) and two UGM cells (31% and 17%) [203].

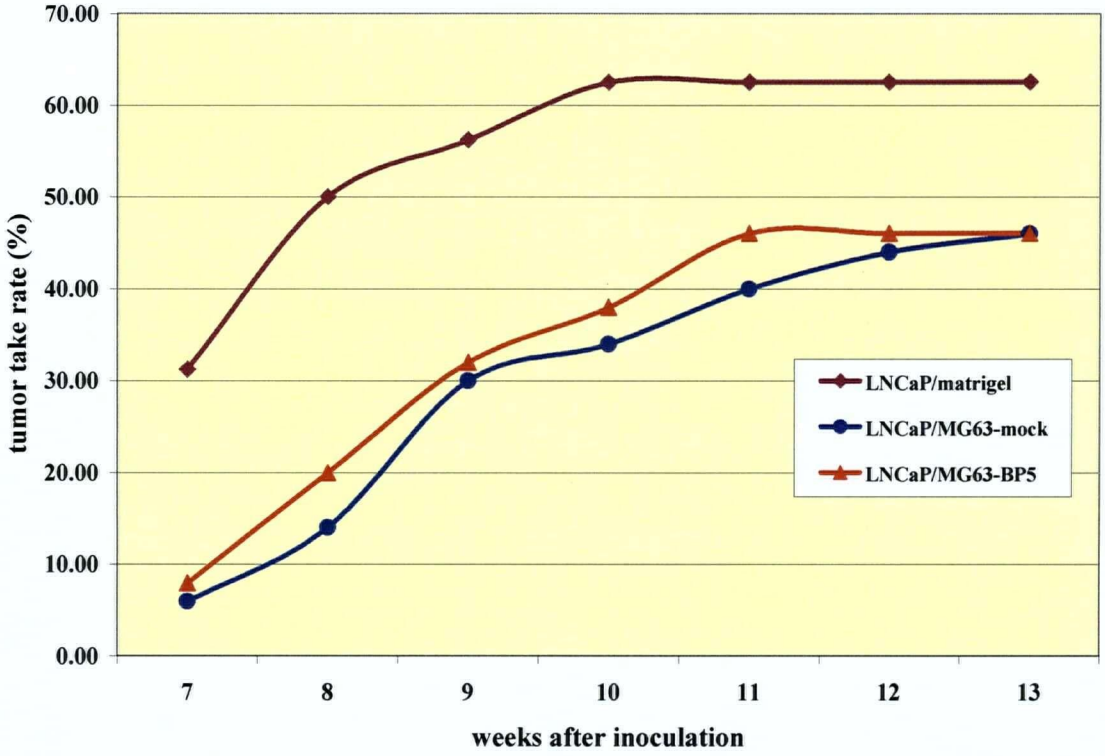

Figure 4.1 LNCaP/MG63 Xenograft Tumor Take Rate in Intact Mice. 4, 14, 14 6-8-week-old male NU/NU mice were randomly grouped into LNCaP/matrigel, LNCaP/MG63-mock and LNCaP/MG63-BP5 arms and subcutaneously inoculated as described in Materials and Methods. Once tumors were palpable 5 weeks after inoculation, tumor size were measured once weekly and calculated using the formula, length x width x depth x 0.5236. Xenografts were considered to be active tumors when they achieved a size of greater than or equal to 150 mm^3. The tumor take rates in LNCaP/matrigel, LNCaP/MG63-mock and LNCaP/MG63-BP5 groups were plotted and compared by student t test.

4.2.2 Tumor Growth Rate in LNCaP/MG63-BP5 Xenografts of Intact Mice is Increased Relative to LNCaP/MG63-mock Xenografts

To determine whether MG63-BP5-produced IGFBP-5 has an effect on tumor growth, xenograft growth rates were measured. The above-mentioned tumor volume data was plotted in Figure 4.2. Differences in tumor growth were compared by assessing average tumor growth rate for experimental arms. For this analysis all inoculation sites were included even if the xenograft size was less than 150 mm^3. LNCaP/matrigel tumors grew fastest from early stage (week 7) up to week 8 post inoculation, then plateaued. Over the course of the experiment, LNCaP/MG63-mock tumors grew slowest throughout the experiment and at similar rate to that of LNCaP/matrigel tumors at the end. LNCaP/MG63-BP5 tumors grew at a rate of 124.55 mm^3/week to an average volume of ~1000 mm^3 by 12 weeks post-inoculation. LNCaP/MG63-mock and LNCaP/matrigel tumors grew at distinguishable rates of 72.36 mm^3/week and 81.29 mm^3/week, respectively, both achieving a final volume of < 700 mm^3. The LNCaP/MG63-BP5 tumor growth rate was nearly twice that of LNCaP/MG63-mock and LNCaP/matrigel tumors ($p < 0.0001$). However, undistinguishable difference was observed between LNCaP/MG63-mock and LNCaP/matrigel groups. These results indicate that paracrine IGFBP-5 production enhances the ability of MG63 cells to support LNCaP tumor growth over that of matrigel or mock MG63 coinoculations.

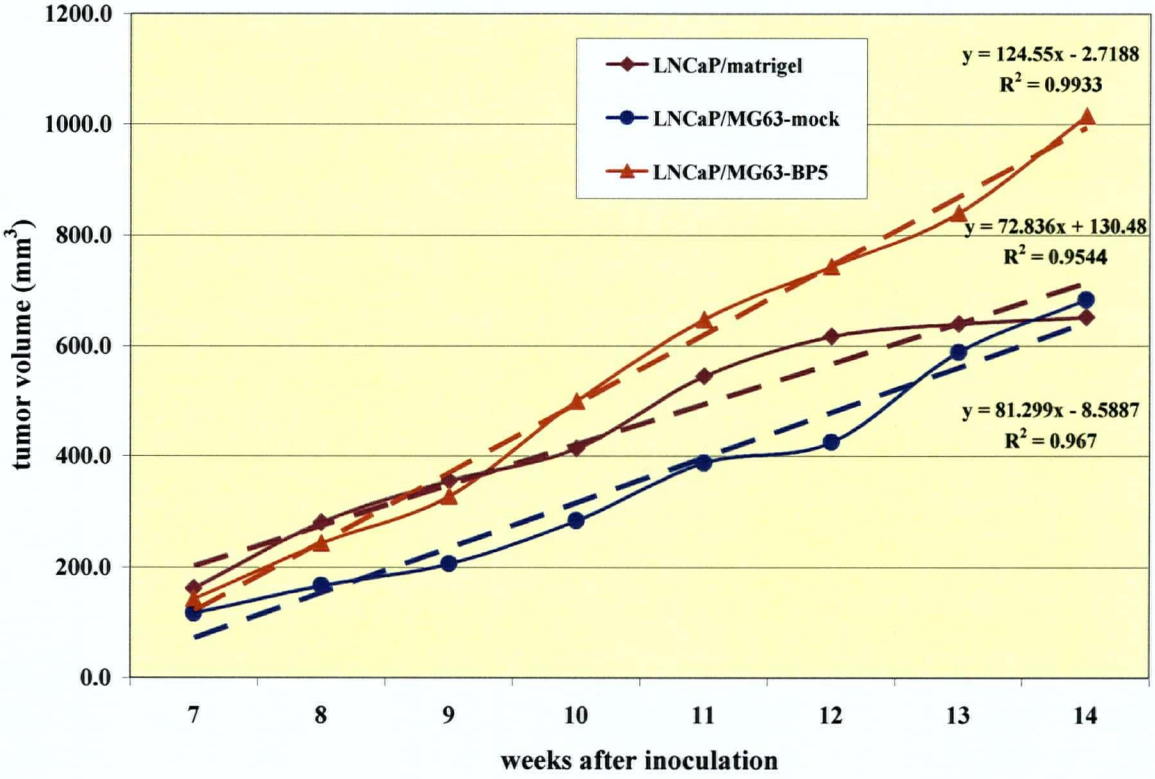

Figure 4.2 Increase in Growth Rate of LNCaP/MG63-BP5 Xenografts Relative to LNCaP/MG63-mock Xenografts in Intact Mice. Tumor volume was determined by caliper measurements and calculated with formula 0.5236 (LxWxD). Nodules that were greater than 150 mm^3 were defined to be active tumors and taken into calculation. Tumor volume data was collected and plotted. Tumor growth rates in LNCaP/MG63-BP5 tumors, LNCaP/matrigel tumors and LNCaP/MG63-mock tumors were compared by linear fit analysis ($p < 0.0001$) with an order of LNCaP/MG63-BP5 > LNCaP/MG63-mock and LNCaP/matrigel.

4.2.3 PSA Rise Rate in LNCaP/MG63-BP5 Xenografts of Intact Mice is Increased Relative to LNCaP/MG63-mock Xenografts

To determine whether MG63-BP5-produced IGFBP-5 has an effect on serum PSA in xenografts, tail vein blood was drawn and PSA values were measured as described in Materials and Methods. Measurement of PSA levels was not initiated until obvious xenograft growth was detected, so assessment of serum PSA levels was performed at week 8 post inoculation. Between week 8 and week 9 post inoculations, paralleling the observed differences in tumor growth rates, PSA levels increased at higher rate in mice bearing LNCaP/MG63-BP5 tumors compared to lower rate in mice bearing LNCaP/matrigel and LNCaP/MG63-mock tumors, indicating that LNCaP cells in LNCaP/MG63-BP5 tumors had an early fast growth. Between week 9 and week 11 post inoculation, PSA in LNCaP/MG63-BP5 tumors continued to increase at a higher rate compared to a lower rate in LNCaP/matrigel and LNCaP/MG63-mock tumors. Between week 11 and week 12 post inoculation, PSA rise at a higher rate in LNCaP/matrigel and LNCaP/MG63-mock tumors compared to a high rate in LNCaP/MG63-BP5 tumors, indicating a late surge in LNCaP cell growth in LNCaP/matrigel and LNCaP/MG63-mock tumors. Throughout the course, serum PSA levels increased at a rate of 127.69 ng/ml/week, reaching a maximal concentration of ~ 700 ng/ml in LNCaP/MG63-BP5 groups, compared to 87.80 ng/ml/week with a maximal concentration of < 600 ng/ml in LNCaP/matrigel groups and 51.28 ng/ml/week with a maximal concentration of < 400 ng/ml in LNCaP/MG63-mock groups, at 12 weeks post inoculation. Serum PSA levels rose as 2.5-fold faster and terminated at a 2-fold higher level in LNCaP/MG63-BP5 tumors bearing mice as in LNCaP/MG63-mock tumors bearing mice ($p < 0.0001$), indicating more LNCaP cells grew in LNCaP/MG63-BP5 tumors than in LNCaP/MG63-mock tumors. This indicates that MG63 cell-derived IGFBP-5 can initiate

quicker increase in serum PSA and eventually help PSA reach higher level in LNCaP/MG63-BP5 xenografts compared to LNCaP/matrigel and LNCaP/MG63-mock xenografts. Knowing that secretion of PSA is a characteristic of LNCaP cells, and that PSA level increase pattern was in accordance with the above mentioned tumor growth rate, these results indicate that the xenografts were indeed LNCaP dominant tumors, however, supported by either MG63 cells or matrigel and further confirmed that IGFBP-5 can enhances the ability of MG63 cells to support LNCaP tumor growth.

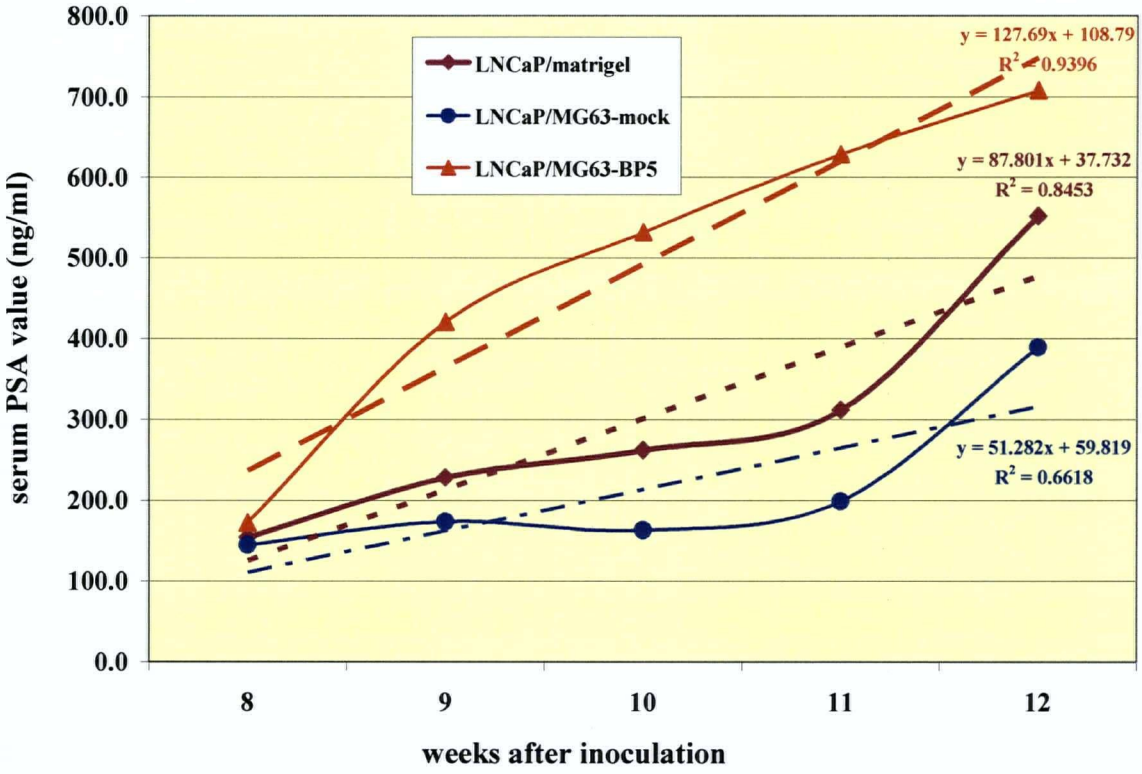

Figure 4.3 Increase in Serum PSA of Intact Mice bearing LNCaP/MG63-BP5 Xenografts Relative to Mice bearing LNCaP/MG63-mock Xenografts. Serum PSA was determined as described in Materials and Methods and plotted. PSA increase rates in LNCaP/MG63-BP5 group, LNCaP/matrigel and LNCaP/MG63-mock groups were compared by linear fit analysis ($p < 0.0001$) with an order of LNCaP/MG63-BP5 > LNCaP/MG63-mock and LNCaP/matrigel.

4.2.4 Immunohistochemical Staining in Intact Mice Xenografts

To evaluate the relative composition of LNCaP and MG63 cells in the xenografts, tumor TMA was created from 25 tumors in this experiment and IHC staining of AR, vimentin and Ki-67 was performed. Figure 4.4 clearly showed the expression of AR in all xenografts, including LNCaP/matrigel tumors, LNCaP/MG63-mock tumors and LNCaP/MG63-BP5 tumors. Ubiquitous staining of AR in positive control LNCaP/matrigel tumors, and dominant staining of AR in LNCaP/MG63 tumors, indicating that majority of cells were LNCaP cells and these xenografts were indeed LNCaP or LNCaP dominant tumors. Though vimentin staining can not distinguish between murine and MG63 mesenchyml cells invading the tumor, however, vimentin, a mesenchymal marker, was sparsely detected in LNCaP/MG63 tumors, but none in LNCaP/matrigel tumors, indicating that these vimentin-positive cells were most likely the coinoculated MG63 cells. The observation that vimentin staining density was indistinguishable between the LNCaP/MG63-mock tumors and LNCaP/MG63-BP5 tumors suggested that there was no difference in the number of MG63 cells inoculated or grown in the MG63-mock or MG63-BP5 inoculated xenografts. Ki-67, a cell proliferation marker, was detected with indistinguishable expression in all three tumor groups, indicating that change in LNCaP proliferation rate was unlikely to contribute to the significant difference of tumor growth between LNCaP/MG63-BP5 tumors and LNCaP/MG63-mock tumors. Since no difference in proliferation was observed, in combination with our in vitro data indicating that CM from MG63-BP5 cells could enhance prosurvival signaling and not proliferative potential of LNCaP cells, we suggest that anti-apoptotic function of IGFBP-5 from MG63-BP5 cells most likely accounts for faster growth of LNCaP/MG63-BP5 xenografts.

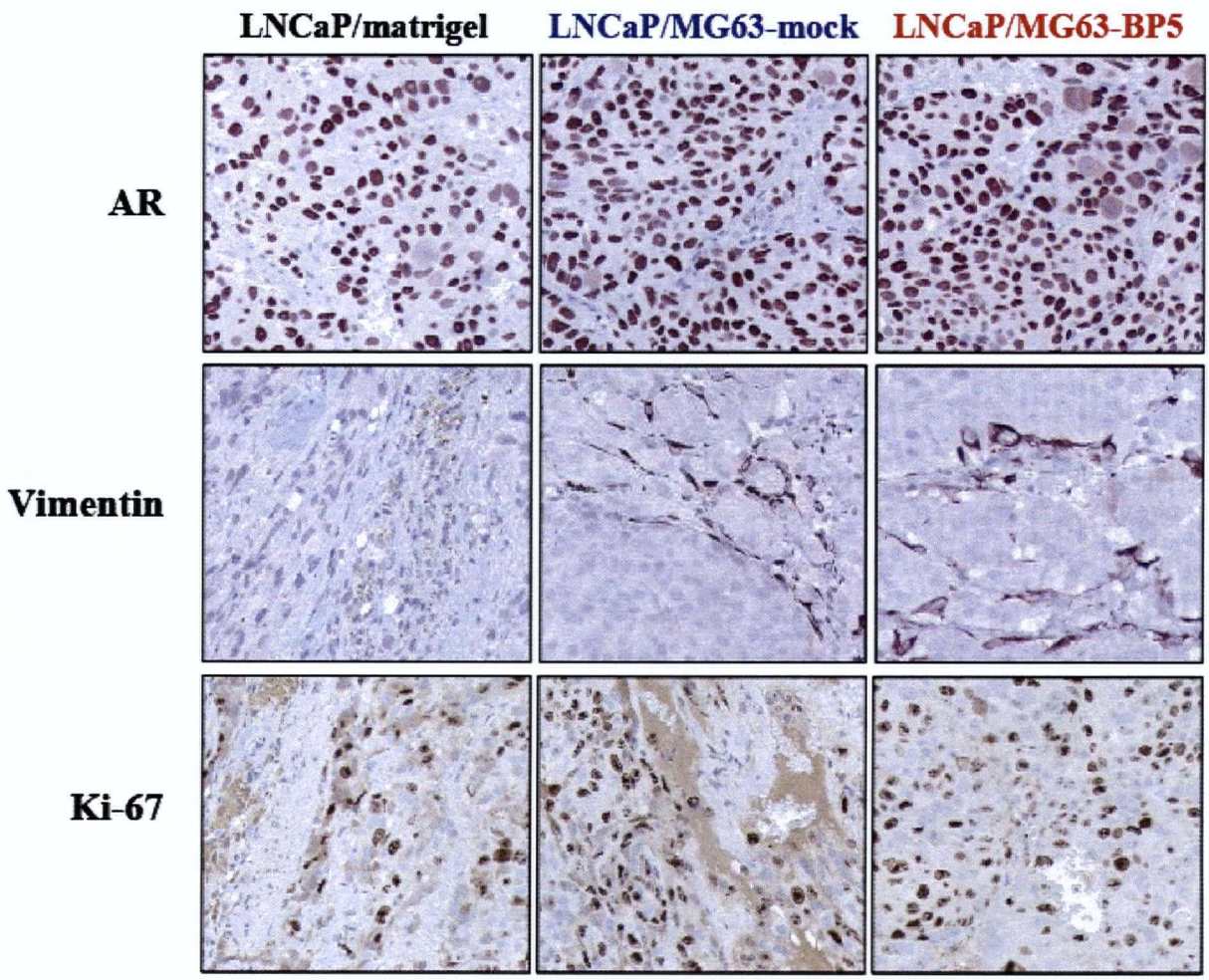

Figure 4.4 Immunohistochemical Staining of Xenografts from Intact Mice. Tumors were harvested, formalin fixed and used to create a TMA as described in Materials and Methods. Representative images of each treatment group with different marker expression are shown. AR expression in LNCaP was identified based on AR-positive stained nuclei (top panel). Vimentin-positive mesenchymal cells is detected (middle panel). Proliferation marker Ki-67 staining was restricted to LNCaP nuclei (bottom panel). IHC staining intensity was quantified using the BLISS analysis system of the Prostate Centre Pathology Core with help from Dr. Ladan Fazli and Dr. Antonio Hurtado-Coll.

4.3 Xenograft Study in Castrated Mice with LNCaP/MG63-mock Tumors and LNCaP/MG63-BP5 Tumors

4.3.1 PSA Relapse Rate in LNCaP/MG63-BP5 Xenografts of Castrated Mice is Increased Relative to LNCaP/MG63-mock Xenografts

In its early stages, PCa is AD, relying on androgen to survive and grow. Serum PSA rises proportional to tumor growth. Patients are normally treated with androgen withdrawal therapy once they developed metastasis. Following castration, PSA drops to a dramatically low or undetected level but eventually patients suffer relapse and serum PSA levels begin to rise again. In the meanwhile, tumors grow at a slow rate. However, once PSA relapse, tumors start to be grow fast and even faster when they become AI. Rising PSA in PCa patients after androgen ablation treatment is considered as relapse to AI. However, the threshold of rising PSA to precastration levels was just a convention we used in the LNCaP xenograft model. Considering our observation that anti-apoptotic function of bone stroma-derived IGFBP5 is likely responsible for faster growth of LNCaP/MG63 xenograft in the intact mice study, we are keen to determine whether IGFBP-5 has an effect on PSA relapse and LNCaP/MG63 xenografts progression to AI in castrated mice.

6, 18 and 18 mice were inoculated with LNCaP/matrigel, LNCaP/MG63-mock and LNCaP/MG63-BP5 groups, respectively. Once tumors were palpable, PSA was measured as described in Materials and Methods. Tumors became palpable at week 4 post inoculation. At week 5 post inoculation, average PSA was ~ 100 ng/ml in all xenograft groups and castration was performed (Figure 4.5A). At week 5 post inoculation, average PSA reached a higher level at 140 ng/ml in LNCaP/MG63-BP5 groups compared to 80 ng/ml in LNCaP/matrigel or

LNCaP/MG63-mock groups in accordance with observation in our intact host xenograft experiment. Following castration, average PSA dropped and reached its nadir at week 1.5 post castration. PSA nadir was a 70% reduction in LNCaP/MG63-BP5 and LNCaP/matrigel tumors, compared to a 90% reduction in LNCaP/MG63-mock tumors. PSA started to relapse at week 2 post castration at a significantly higher rate of 47.03 ng/ml/week to a maximum of ~ 350 ng/ml in LNCaP/MG63-BP5 tumors than at 36.19 ng/ml/week and < 280 ng/ml in LNCaP/matrigel, and 15.76 ng/ml/week and < 120 ng/ml in LNCaP/MG63-mock tumors at week 9 post castration, indicating that average serum PSA relapsed faster and accumulated to a higher level in LNCaP/MG63-BP5 group than in LNCaP/MG63-mock and LNCaP/matrigel groups. Tumors were defined to became AI once serum PSAs reached their precastration levels. As shown in Figure 4.5A, it took only 4 to 5 weeks for LNCaP/MG63-BP5 tumors and LNCaP/matrigel tumors to become AI, compared to 6-7 weeks for LNCaP/MG63-mock tumors.

Based on the above PSA data, precent AI was also performed with Kaplan-Meier analysis using the defined AI threshold for each group. Once serum PSA reach its precastration level, tumors were defined as becoming AI. As shown in Figure 4.6A, at week 3 post castration, 23% of total mice had become AI in LNCaP/MG63-BP5 group compared to none in LNCaP/MG63-mock group, indicating a quicker PSA relapse in LNCaP/MG63-BP5 group. At week 4 post castration, already more than half of total mice (62%) had become AI in LNCaP/MG63-BP5 group compared to only 23% in LNCaP/MG63-mock group. At week 5, 6 and 7 post castration, 84%, 89% and 96% of total mice had become AI in LNCaP/MG63-BP5 group compared to 50%, 56% and 56% in LNCaP/MG63-mock group, indicating continued increase in becoming AI. At week 8 post castration, all mice in the LNCaP/MG63-BP5 group had become AI compared to 62% in LNCaP/MG63-mock group. At week 9 post castration, 73% of mice had become AI in

LNCaP/MG63-mock group. At week 10 post castration, 27% of mice had still not achieved precastration PSA levels in the LNCaP/MG63-mock group. Serum PSA in some of these alive mice was in fact undetectable, indicating that tumors in these mice might start their growth later or never be able to grow. The time to AI progression in the LNCaP/MG63-BP5 group was significantly earlier than that in the LNCaP/MG63-mock group ($p < 0.0001$). The relative risk of serum PSA relapse in LNCaP/MG63-BP5 group is 2.5-fold that in LNCaP/MG63-mock group (Hazard ratio is 0.39). These results indicate that paracrine IGFBP-5 can promote LNCaP tumor progression to AI.

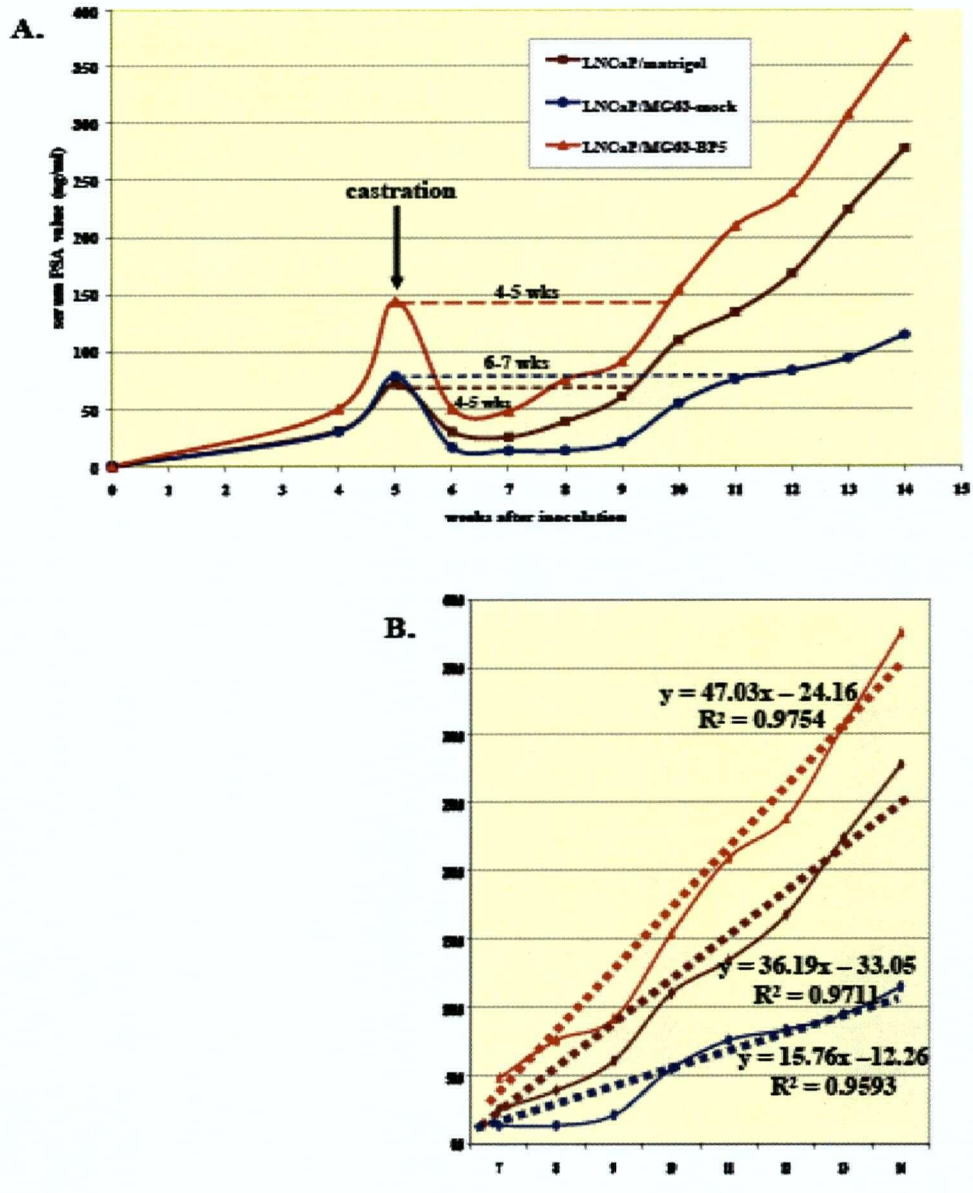

Figure 4.5 Increase in PSA Relapse Rate of Castrated Mice Bearing LNCaP/MG63-BP5 Xenografts Relative to Mice Bearing LNCaP/MG63-mock Xenografts. A. As described in Materials and Methods, 6, 18 and 18 mice were inoculated with LNCaP/matrigel, LNCaP/MG63-mock and LNCaP/MG63-BP5, respectively. Once tumor became palpable at week 4 post inoculation, PSA was measured once weekly. When PSA reached ~ 100 ng/ml in all xenograft groups at week 5 post inoculation, mice were castrated and subsequently tumor were measured. B. Linear trendlines showed difference in PSA relapse rates between LNCaP/MG63-BP5 group and LNCaP/MG63-mock group tested by linear fit analysis ($p < 0.0001$) with an order of LNCaP/MG63-BP5 > LNCaP/MG63-mock and LNCaP/matrigel.

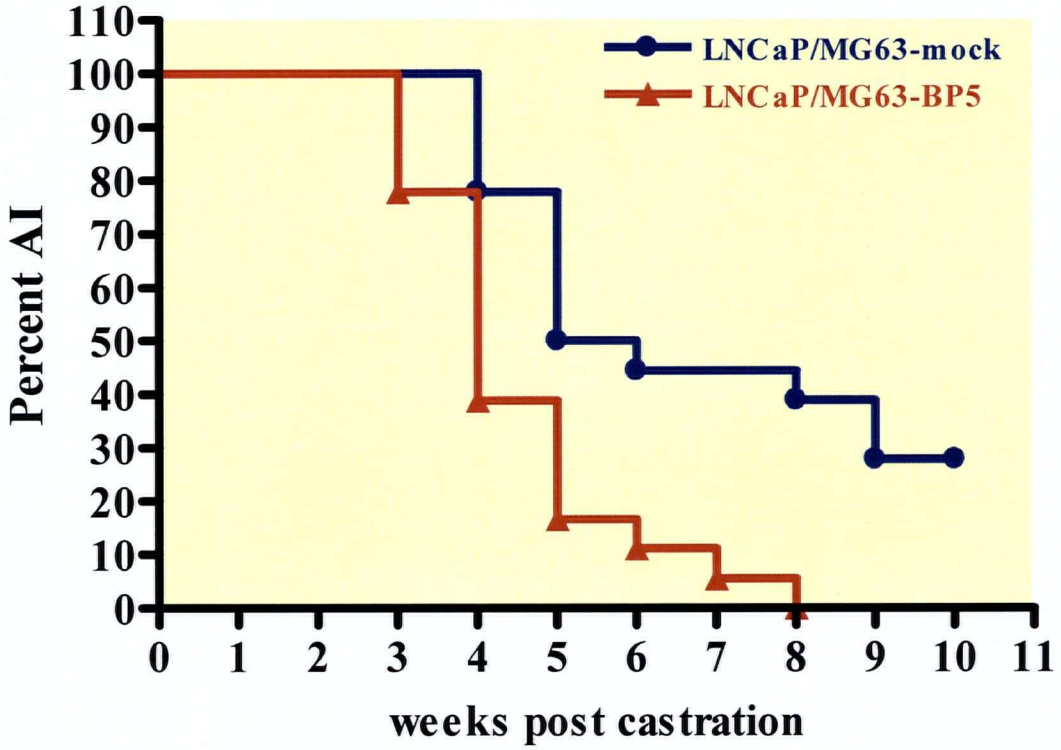

Figure 4.6 Time for LNCaP/MG63 Xenografts to become AI following Castration. Kaplan-Meier survival curve was performed with the PSA data using GraphPad Prism software (GraphPad Software, Inc). Once PSA reached its precastration level, xenografts were defined as becoming AI. At week 3, 4, 5, 6, 7, 8 post castration, 23%, 62%, 84%, 89%, 96%, 100% of mice had become AI in LNCaP/MG63-BP5 group compared to 0%, 23%, 50%, 56%, 62%, 73% in LNCaP/MG63-mock group. At week 9 post castration, 73% of mice had become AI in LNCaP/MG63-mock group. At week 10 post castration, 27% of mice had still not achieved precastration PSA levels in the LNCaP/MG63-mock group. Significance of difference was assessed by Logrank test ($p < 0.001$). The relative risk is also tested (Hazard ratio is 0.39).

4.3.2 Tumor Growth Rate in LNCaP/MG63-BP5 Xenografts of Castrated Mice is Increased Relative to LNCaP/MG63-mock Xenografts

At week 4 post inoculation, nodules were palpable. According to the serum PSA level, mice were castrated and tumor volumes were then measured once weekly from week 5 post inoculation. Following castration, tumors grew at a relatively slow rate. However, during the week immediately after castration, LNCaP/MG63-BP5 xenografts grew faster than LNCaP/MG63-mock xenografts, indicating delayed response to castration-induced apoptosis in LNCaP/MG63-BP5 tumors than in LNCaP/MG63-mock tumors. Between week 2 to week 5 post castration, LNCaP/MG63-BP5 xenografts grew slightly faster than LNCaP/MG63-mock xenografts. In accordance with our above-mentioned PSA data, a dramatic growth increase from week 5 post castration in LNCaP/MG63-BP5 xenografts is observed compared to week 7 post castration in LNCaP/MG63-mock xenografts, indicating a faster tumor growth when becoming AI and an early onset of AI by LNCaP/MG63-BP5 xenografts. Through the course of castration, tumors grew at a higher rate of 61.66 mm^3/week, achieving a maximal average volume of 900 mm^3 in LNCaP/MG63-BP5 group compared to 36.83 mm^3/week and 500 mm^3 in LNCaP/MG63-mock xenografts ($p < 0.0001$). These results confirm that MG63-derived IGFBP-5 can promote LNCaP tumor growth and progression to AI in castrated mice.

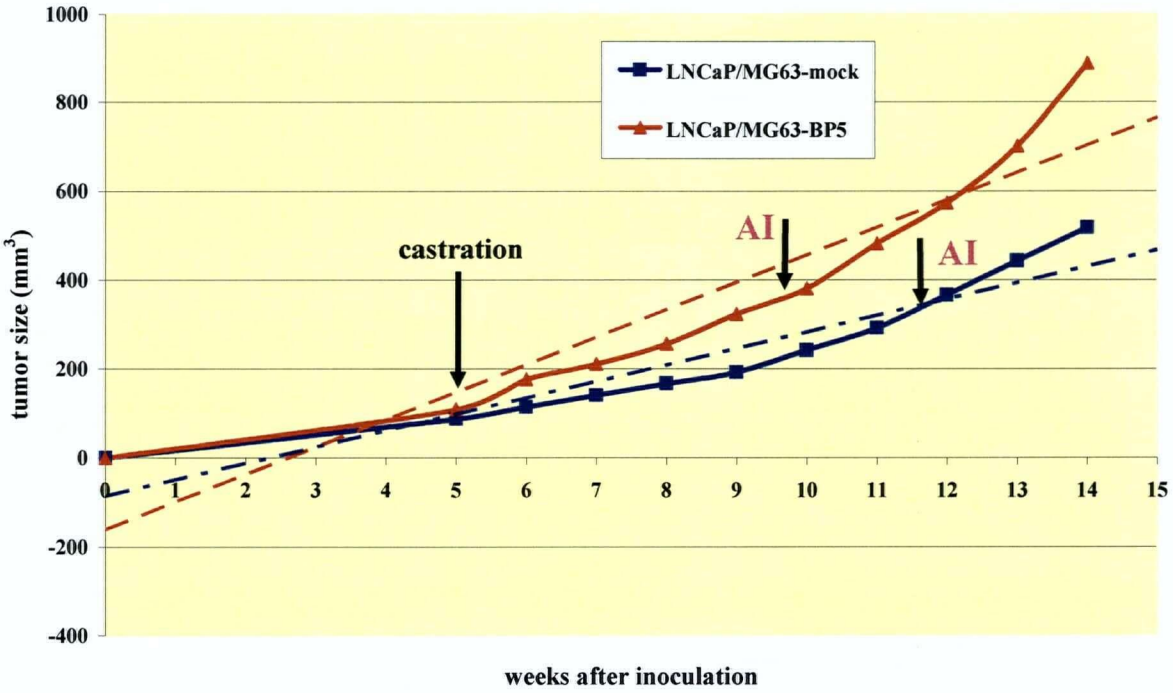

Figure 4.7 Increase in Grwoth Rate of LNCaP/MG63-BP5 Xenografts Relative to LNCaP/MG63-mock Xenografts in Castrated Mice. Tumor volumes were monitored and measured once weekly starting at the time of castration. As describe in our intact mice xenograft study, tumor volume was determined by caliper measurements as 0.5236 (Length x Width x Depth). Tumors growth rates in LNCaP/MG63-BP5 and LNCaP/MG63-mock groups were compared by linear fit analysis ($p < 0.0001$ with an order of LNCaP/MG63-BP5 > LNCaP/MG63-mock.

4.3.3 Immunohistochemical Staining in Castrated Mice Xenografts

To assess the relative composition of LNCaP and MG63 cells in the tumors, IHC staining of AR and vimentin were performed. These measurements were made at termination from 31 tumors. Then we used Ki-67 and Apo-tag staining to measure potential differences in mitotic and/or apoptotic activity in the tumors. As in our intact mice xenograft study, the expression of AR was detected in all xenografts, including LNCaP/matrigel, LNCaP/MG63-mock and LNCaP/MG63-BP5, confirming that the vast majority of cells in the xenografts these were indeed LNCaP cells. Vimentin expression was again sparsely detected in both LNCaP/MG63 tumors, but not in negative control LNCaP/matrigel tumors, indicating that these cells were likely to be the MG63 cells, rather than murine mesenchymal cells invading the tumor. The observation that vimentin density was approximately the same in LNCaP/MG63-mock tumors and LNCaP/MG63-BP5 tumors suggested no difference in the number of MG63 cells inoculated or grown over the course of the experiment and that differences in tumor growth rates were predominantly due to changes in LNCaP cell number. Ki-67 staining exhibited indistinguishable expression in all three tumor groups, indicating that proliferation unlikely contributes to the significant difference of tumor growth between LNCaP/MG63-BP5 tumors and LNCaP/MG63-mock tumors. However, expression of Apo-tag, an apoptosis marker, was clearly detected in LNCaP/matrigel and LNCaP/MG63-mock tumors, but hardly detected in LNCaP/MG63-BP5 tumors, indicating that faster growth of LNCaP/MG63-BP5 tumors most likely was not due to increased proliferation, but decreased apoptosis of LNCaP cells. Taken together with our in vitro data and intact mice xenograft study, these results further strengthen the conclusion that anti-apoptotic function of paracrine MG63-BP5-produced IGFBP-5 is likely responsible for growth increase and earlier progression to AI in LNCaP/MG63-BP5 xenografts.

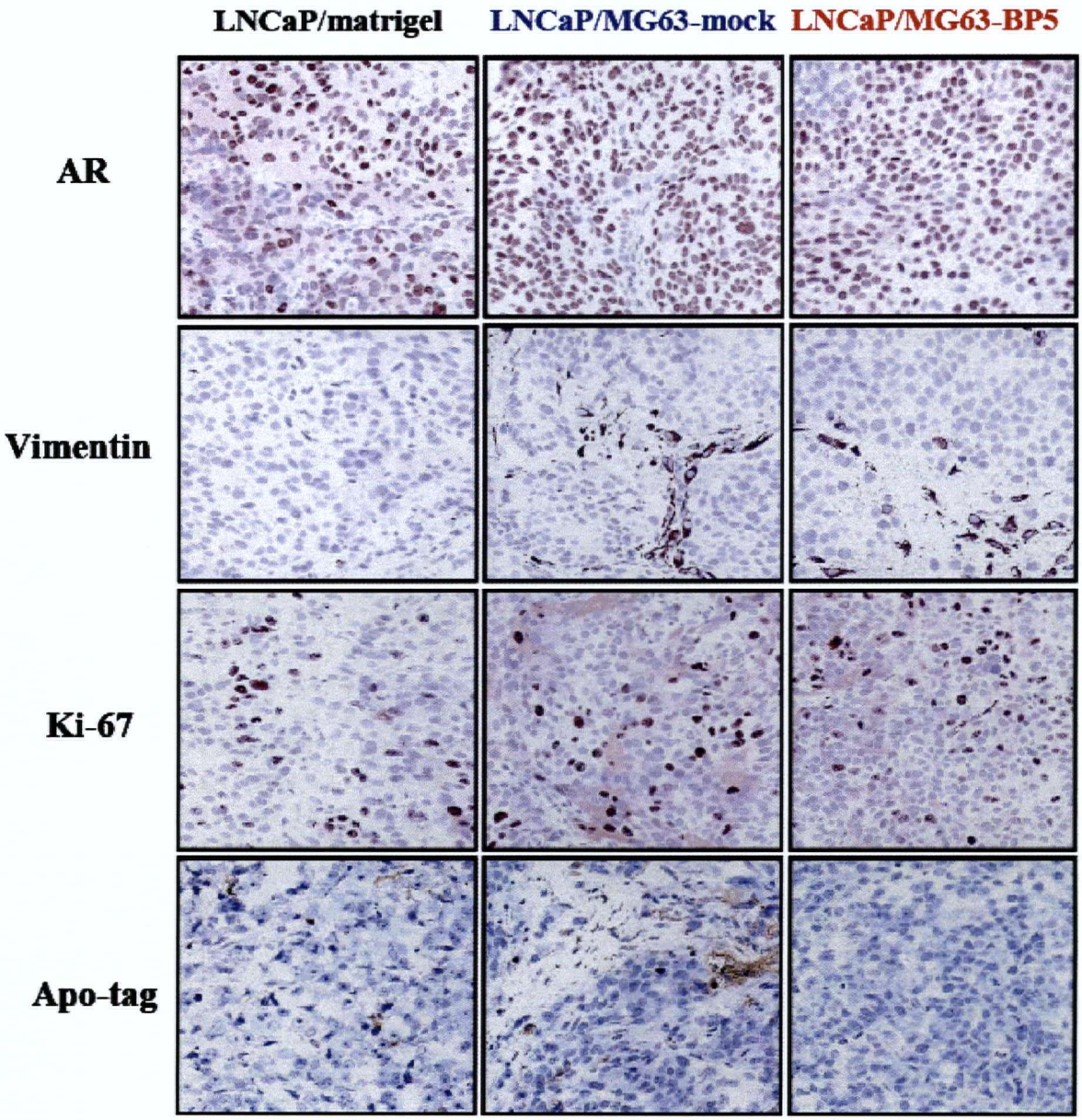

Figure 4.8 Immunohistochemical Staining of Xenografts from Castrated Mice. TMA was created as described in Materials and Methods. 1st row: AR staining was detected in majority of cells in all xenograft groups. 2nd row: Vimentin staining was detected in LNCaP/MG63 xenografts, but not in LNCaP/matrigel xenografts. 3rd row: Ki-67 staining was detected in all three xenograft groups. Bottom row: Apo-tag staining was detected in LNCaP/Matrigel and LNCaP/MG63-BP5 xenografts and hardly detected in LNCaP/MG63-BP5 xenografts.

4.4 Summary

The intact mice xenograft experiments showed that tumor take rate was indistinguishable between LNCaP/MG63-BP5 and LNCaP/MG63-mock groups, indicating IGFBP-5 did not affect the ability of MG63 cells to support LNCaP tumor formation. Tumors in LNCaP/MG63-BP5 group grew twice as fast as those in LNCaP/MG63-mock and LNCaP/matrigel groups, indicating paracrine IGFBP-5 enhanced LNCaP cell growth. Serum PSA followed the same pattern as the tumor growth among these three groups and was proportional to tumor growth, confirming that these xenografts were LNCaP dominant tumors. IHC staining showed no difference in proliferation between these xenograft groups, indicating increased growth in LNCaP/MG63-BP5 tumors was unlikely due to altered proliferation in LNCaP cells in LNCaP/MG63-BP5 tumors .

The castrated mice xenograft study demonstrated that LNCaP/MG63-BP5 tumors grew twice as fast as LNCaP/MG63-mock tumors following castration, indicating MG63 cell-produced IGFBP-5 protected LNCaP cells from castration-induced apoptosis in LNCaP/MG63 tumors. Serum PSA relapsed earlier and reached precastration level faster in LNCaP/MG63-BP5 group than those in LNCaP/MG63-mock group after castration indicating that paracrine IGFBP-5 promoted tumor growth as well as progression to AI. IHC staining showed no difference in proliferation, however, obvious differences in apoptosis, solidified our conclusion that increased growth of LNCaP/MG63-BP5 tumors was most likely due to decreased apoptosis in LNCaP cells in LNCaP/MG63-BP5 tumors.

Taken together, the xenograft studies demonstrated that paracrine IGFBP-5 can promote tumor growth in LNCaP/MG63 xenografts, delayed castration-induced apoptosis and accelerated progression to AI of LNCaP/MG63 xenografts in castrated mice.

5 DISCUSSION AND CONCLUSIONS

5.1 Discussion

It has long been a tough challenge for the urologists and medical researchers to deal with PCa patients at advanced stage with bone metastasis. Approximately 90% of advanced stage PCa patients develop bone lesions causing significant morbidity and mortality. Most patients died of bone metastasis and incurable androgen-independence of PCa. This phenomenon leads to critical questions. How do PCa cells interact with metastatic bone stromal microenvironment? What factors in the bone stroma prompt migratory PCa cells to initiate growth and survival in a new microenvironment? How PCa becomes AI from AD after androgen withdrawal in the bone local microenvironment? All these questions require us to understand the biological processes leading to the establishment of clinical relevant bone metastasis.

Stroma-epithelial interaction plays a critical role in PCa carcinogenesis, progression, metastasis and androgen-independence. The widely accepted "seed and soil" theory described distal metastases that are organ-specific, explaining that the bone microenvironment provides a rich "soil" for the PCa cell "seeds" and PCa cells utilize the "soil" for their survival and growth [151]. IGF-I is a major andromedin mediating the transition from androgen-dependence to androgen-independence of bone metastatic PCa. The bioavailability of IGF-I in the bone microenvironment of PCa metastasis is increased [195]. IGF-I responsiveness is implicated in promoting AI progression of PCa [43]. IGFBP-5 and IGF-I are categorized as genes associated with invasive PCa [205]. Serum IGFBP-5 concentrations are significantly higher in PCa than in benign prostatic hyperplasia [206]. IGFBP-5 expression is significantly up-regulated in the bone stroma of castrated mice [101]. It is indicated that IGFBP5 may involve in the bone metastasis of

PCa. However, it is not completely understood that how IGFBP-5 regulates IGF-induced PCa cell survival and proliferation in bone metastatic microenvironment. We hypothesized that increased expression of IGFBP-5 produced by bone stroma may be an important factor for promoting establishment of PCa metastatic lesions and AI progression in patients undergoing hormone withdrawal therapy.

In my thesis, we have examined the role of MG63 bone stromal cell-derived IGFBP-5 in PCa growth under androgen-deprived condition and progression to AI. LNCaP is an androgen-responsive PCa cell line derived from a lymph node metastasis [4]. Even under castrated condition, LNCaP continues tosecrete a basal level of PSA, which can be used as a surrogate for tumor volume. LNCaP was poorly tumorigenic in nude mice unless coinoculated with tissue-specific mesenchymal or stroma cells [203] or matrigel [207], suggesting that stroma and stroma-derived growth factors play a role in PCa growth and site-specific metastasis [39]. When injected subcutaneously, LNCaP cells form tumors in SCID or nude mice with serum PSA levels proportional to tumor volume [208]. Following castration, LNCaP tumors typically undergo a period of growth arrest after which there is a return of growth and rise in PSA correlating with androgen independence. Prolonged androgen withdrawal leads to AI growth of LNCaP tumors, which is presented by PSA rising [44]. MG63 is a human osteosarcoma-derived cell line that is easy to proliferate for cell culture study. In addition, MG63 cells have some osteoblastic features, such as expression of many osteoblastic proteins, for examples, osteonectin, osteopontin, osteoproterin, collagen-III and collagen V, mimicking osteoblastic bone microenvironment in PCa [209]. Normal human bone osteoblast can theoretically be an option for this study due to its ability of mimicking human normal bone microenvironment. However, as mentioned in the introduction, stroma cells can undergo alteration induced by reacting to surrounding prostate

cancer cells, indicating these carcinoma associated fibroblasts are no longer normal stromal cells [28, 29]. Lastly, MG63 cell was selected for this study because it was screened to be IGFBP-5 negative, which allowed us to have MG63-mock and MG63-BP5 in parallel in order to compare their biological functions. Therefore, bone stromal MG63 cell and PCa LNCaP cell were chosen for this IGFBP-5 study.

First, in order to establish a model to study the role of IGFBP-5 produced by MG63-BP5 cells on PCa LNCaP cell growth in vitro and in vivo, both LNCaP and MG63 cells were tested for expression of IGFBP-5 by Northern blotting (Figure 3.3A) and westernblotting (Figure 3.3B). Our results showed that neither of them endogenously expresses IGFBP-5. Taking MG63 as an IGFBP-5 negative parental cell line, we were able to build a MG63 cell line with IGFBP-5 expression, MG63-BP5 and its vector transfected counterpart, MG63-mock. IGFBP5 expression in MG63-BP5 cells was confirmed by Northern blotting (Figure 3.4) and western blotting (Figure 3.5). Quantification of IGFBP-5 secreted into MG63-BP5 CM was also be performed (Figure 3.6). This gave us the opportunity to investigate the role IGFBP-5 might play in PCa biology.

The biological function of IGFBP-5 produced by MG63-BP5 bone stromal cells on LNCaP cells was investigated by cell cycle profiling analysis (Figure 3.7). We observed a decreased apoptotic index in the LNCaP cells treated with MG63-BP5 CM compared to MG63-mock CM under androgen-deprived condition. Further we performed cellular DNA content analysis on LNCaP cells treated with PI3K inhibitor LY294002, also in various combination with IGF-I, R1881, E3R and MG63-BP5 or MG63-mock CM (Figure 3.8A). R1881 plus IGF-I or R1881 plus E3R protected LNCaP cells from LY294002-induced apoptosis, which can be explained by the report that androgen increases IGF-IR expression, thus increases IGF-I-mediated survival signaling

[34]. The observation that MG63-BP5 CM plus IGF-I protected LNCaP from LY294002-induced apoptosis in the absence of androgen implied that IGFBP-5 might be a substitute candidate for androgen in protecting LNCaP from apoptosis. MG63-BP5 CM plus IGF-I, but not MG63-BP5 CM plus E3R, has anti-apoptotic function in LNCaP cells, indicating interaction between IGFBP-5 and IGF-I is essential for IGFBP-5 to perform this protection. This protection against apoptosis by paracrine IGFBP-5 produced MG63-BP5 cells may be due to augmentation in activation of key nodes, such as Akt, of IGF-IR signaling pathway. Our result is in agreement with Gleave et al's previous work that IGFI-I prevented only IGFBP-5 transfected LNCaP cells from androgen ablation induced apoptosis, not mock cells, implying IGFBP-5 has an ability to enhance the anti-apoptotic action of IGF-I [109]. Both paracrine and autocrine IGFBP-5 seems to function as an anti-apoptotic agent. Regarding the anti-apoptotic mechanism, AR can perform IGF-I-dependent protection from apoptotic stress in LNCaP cells by means of increasing IGF-IR expression [34]. Our immunoblotting result confirmed that androgen increased IGF-IR in LNCaP cells treated with or without R881, and showed that MG63-BP5 CM did not increase IGF-IR expression compared to MG63-mock CM (Figure 3.8B), further implying that the protection of LNCaP from LY294002-induced apoptosis is not due to increased IGF-IR expression, but submaximal stimulation of IGF-IR by slow release of IGF-I from IGFBP-5 and subsequently increased activation of downstream targets, such as Akt. However, it needs further investigation to confirm.

To examine whether IGFBP-5 indeed does so, we looked into IGF-I-mediated signaling activation in a time-dependent fashion (Figure 3.9). To our surprise, both in presence and absence of androgen, an approximate 1.5-fold decrease in peak activation of IGF-IR was observed in LNCaP cell treated with MG63-BP5 CM compared to that with MG63-mock CM.

However, within our expectation, an approximate 1.5-fold increase in peak activation of IRS-2, Akt and Erk downstream IGF-IR was observed in LNCaP cell treated with MG63-BP5 CM compared to that with MG63-mock CM. This increased Akt peak activation subsequent to slow release of IGF-Is by paracrine IGFBP-5 for IGF-IRs contributed to protection of LNCaP cells from apoptosis. Our findings were in accordance with Conover et al's observation that IGFBPs can enhance IGF effects by presenting and slowly releasing IGF-I for receptor interactions [210].

MG63-BP5 CM contains IGFBP-5, however, both MG63-BP5 CM and MG63-mock CM also contains IGFBP2 and IGFBP-3 (Figure 3.5). Apoptosis protection was only observed in LNCaP cells treated with IGF-I plus MG63-BP5 CM, but not in LNCaP cells treated with IGF-I plus MG63-mock CM (Figure 3.8), suggesting that IGFBP-5, not IGFBP-2 nor IGFBP-3, is the major IGFBP to present IGF-Is to IGF-IRs for activation of IGF-I signaling in bone stromal microenvironment. This observation is in agreement with report that IGFBP-5 is the most abundant IGFBP in bone stroma [100] and that IGFBP5 is the most consistent upregulated gene in mice bone stroma following castration [101].

The functional role of IGFBP-5 in in vivo study is not fully understood. PCa bone metastasis is associated with loss of dynamic balance between osteoblast and orthoclase activities. Osteoblastic factors secreted by PCa cells activate osteoblasts to break down bone matrix, release growth factors stored and form a favorite microenvironment for PCa cells. In return, unknown factors produced by activated osteoblasts can accelerate growth and progression of PCas [189]. Gleave's work has shown that LNCaP tumor is most likely induced by coinoculation of LNCaP with human bone fibroblasts and rat prostate fibroblasts, not with lung, kidney or embryonic fibroblasts [203]. Unfortunately, his group was unable to identify the factor(s) that contribute to this phenomenon.

Further, we performed xenograft study to examine paracrine IGFBP-5's anti-apoptotic function in vivo. We first observed that bone stromal MG63 cells did support LNCaP tumor formation. We also observed a tumor take rate of 63% in LNCaP/matrigel group, which is agreement with other's work [204]. An indistinguishable tumor take rate of 46% was observed in LNCaP/MG63-BP5 and LNCaP/MG63-mock groups, which falls between 62% and 31% or 17% of tumor take rate in LNCaP tumor supported by human bone fibroblasts and rat prostate fibroblast from Gleave's work [203]. Xenografts in LNCaP/MG63-BP5 group grew 1.5-fold as fast as that in LNCaP/MG63-mock and LNCaP/matrigel groups, indicating a growth-promotive role for MG63-BP5-produced IGFBP-5. Following serum PSA dynamics from the same mice study matched the above-mentioned growth rate change, confirming that these xenografts were indeed LNCaP tumors, not MG63 sarcomas nor any other types of stromal cell tumors. We inclined to contribute this faster growth to primarily an anti-apoptotic function, rather a pro-proliferative effect of paracrine IGFBP-5. IHC staining of xenografts further confirmed that these tumors were AR positive LNCaP tumors supported by vimentin positive mesenchymal cells. While the vimentin staining can not distinguish between murine and MG63 mesenchyml cells invading the tumor, the staining of the matrigel co-inoculated xenografts show no sign of vimentin-positive invading cells in the xenografts. We therefore conclude that the most likely source for the vimentin –positive cells was the co-inoculated MG63 cells. Proliferative difference was not observed between LNCaP/MG63-mock group and LNCaP/MG63-BP5 group, strengthening our above thought that most likely paracrine IGFBP-5 exerted an anti-apoptotic function. However, further experiment need to be performed in order to characterize the function of bone stromal cell-dervied IGFBP-5 in this context.

In our second xenograft study, we examined change of tumor growth rate, serum PSA level in castrated mice and analyzed the rate for PSAs to reach their precastration levels, becoming AI. We observed a 2-fold growth rate in LNCaP/MG63-BP5 tumors compared to that in LNCaP/MG63-mock tumors in castrated mice (Figure 4.7). Immediately after castration, the average PSAs in mice of all three groups dripped off, reached their nadir between week 1 and week 2 post castration and were able to bounce back up to overpass their precastration levels. It took 6-7 weeks for serum PSA reach its precastration level in mice bearing LNCaP/MG63-mock tumors compared to only 4-5 weeks in mice bearing LNCaP/MG63-BP5 tumors and mice bearing LNCaP/matrigel tumors (Figure 4.5A). The average PSA relapsed from its nadir 3-fold as fast in mice in LNCaP/MG63-BP5 group as that in LNCaP/MG63-mock group (Figure 4.5B). At week 8 post castration, serum PSAs reached their precastration levels in all mice bearing LNCaP/MG63-BP5 tumors and most mice bearing LNCaP/MG63-mock. It was within our expectation that even at week 10 post castration, serum PSAs still not reached their precastration levels in a few mice bearing LNCaP/MG63-mock tumors, indicating that MG63-BP5 cell-produced IGFBP-5 accelerated PSA relapse from castration-induced apoptosis in LNCaP/MG63-BP5 group compared to LNCaP/MG63-mock group (Figure 4.6). In correspondence with this difference in PSA relapse rate, we observed that xenografts grew almost 2-fold as fast in LNCaP/MG63-BP5 group as in LNCaP/MG63-mock group following castration. Considering our in vitro data, we thought that paracrine IGFBP5 in these LNCaP tumors contributed their faster growth by protecting LNCaP cells from apoptosis post castration. Further IHC staining supported our reasoning (Figure 4.8). Difference in expression of proliferation marker, Ki-67, is not detected in LNCaP/MG63-mock group and LNCaP/MG63-BP5 group. However, a decreased expression of Apo-tag, an apoptotic marker is observed in LNCaP/MG63-BP5 group than in

LNCaP/MG63-mock group and LNCaP/matrigel group. The data is in agreement with our in vitro data that IGFBP-5 protects LNCaP cells from apoptosis under androgen-deprived condition (Figure 4.8). These results indicate stroma-deprived IGFBP-5 indeed perform an anti-apoptotic function in LNCaP tumors post castration.

To our best knowledge, our report is the first to demonstrate that bone stroma-produced paracrine IGFBP-5 played a role in bone environment that favors PCa cell survival as well as AI progression both in vitro and in vivo. Dramatic up-regulation of IGFBP-5 after castration helps potentiate the anti-apoptotic activity of IGF-I. IGFBP-5 protects LNCaP cells from LY294002- and castration-induced apoptosis both in vitro and in vivo. The anti-apoptotic function performed by IGFBP-5 is IGF-I-dependent and thus probably through IGF-I-mediated signaling. IGFBP-5 has a reductive function towards IGF-IR activation and conversely enhancing effect on IRS-2, Akt and Erk activation in IGF-I signaling pathway in PCa cells. It is assumed that increased Akt activation may contribute to IGFBP-5's anti-apoptotic function. The mechanism might be that paracrine IGFBP-5 in bone stroma presents more IGF-Is for interaction with IGF-IRs in a slow-releasing and prolonged manner. It might be an adaptive approach for PCa cells to utilize bone-rich IGFBP-5 in substitute of androgen, survive and maybe still proliferate in an androgen-deprived microenvironment. Therefore, IGFBP-5 should continue to be a therapeutic target of downregulation in treatment of PCa patients with bone metastasis and androgen-independence.

5.2 Conclusions

Our in vitro data showed that bone stromal MG63-BP5 cell-produced IGFBP-5 has an IGF-I-dependent anti-apoptotic function in LNCaP cells under androgen-deprived condition. Paracrine

IGFBP-5 decreases peak activation of IGF-IR, however, increases peak activation of downstream targets IRS-2, Akt and Erk both in the absence and presence of androgen.

In our xenograft study, no difference in tumor take rate is observed in mice bearing LNCaP/MG63-mock tumors and in mice bearing LNCaP/MG63-BP5 tumors, indicating IGFBP-5 does not affect the ability of MG63 cells to support LNCaP tumor take rate. However, LNCaP/MG63-BP5 tumors grew 1.5-fold as fast as LNCaP/MG63-mock tumors and LNCaP/matrigel tumors. In accordance with differences in tumor growth rate, PSA increased at a 2-fold higher rate in mice in LNCaP/MG63-BP5 group as in LNCaP/MG63-mock group and LNCaP/matrigel group. IHC staining confirmed that these xenografts were LNCaP dominant tumors supported by MG63 cells. No difference in proliferation was detected between LNCaP/MG63-BP5 tumors, LNCaP/MG63-mock tumors and LNCaP/matrigel tumors.

At early stage of PCa, cancer cells are AD, relying on androgen to survive and grow. Serum PSA rises proportional to tumor growth. Following castration, PSA drops to a dramatically low or undetected level and relapses. Once PSA reaches its precastration level, PCa cells are defined to be AI. In our castrated mice xenograft experiment, no difference was observed in serum PSA post castration drop rate in mice bearing LNCaP/MG63-mock tumors, mice bearing LNCaP/MG63-BP5 tumors and mice bearing LNCaP/matrigel tumors. Average PSAs dropped to its nadir at week 1.5 post castration in all three groups. However, serum average PSA relapse from its nadir three-fold as fast in mice in LNCaP/MG63-BP5 group and two-fold as fast in LNCaP/matrigel group as in LNCaP/MG63-mock group. In addition, it took 4-5 weeks for xenografts to become AI in mice in LNCaP/MG63-BP5 group and in LNCaP/matrigel group compared to 6-7 weeks in mice LNCaP/MG63-mock group. At week 8 post castration, all mice became AI in LNCaP/MG63-BP5 group compared to 73% of mice in LNCaP/MG63-mock

group. At week 9 and week 10 post castration, 27% of mice have not yet reached its precastration level in LNCaP/MG63-mock group. In accordance with PSA change, tumors grew as 2-fold fast in LNCaP/MG63-BP5 group as in LNCaP/MG63-mock group. Difference in proliferation was not observed in LNCaP/MG63-BP5 xenografts and in LNCaP/MG63-mock xenografts. However, a decrease in apoptosis was detected in LNCaP/MG63-BP5 xenografts compared to LNCaP/MG63-mock xenografts and LNCaP/MG63-matrigel xenografts, indicating faster growth in LNCaP/MG63-BP5 xenografts post castration is indeed due to reduced apoptosis in LNCaP cells protected by paracrine IGFBP-5.

All these results indicate that bone stroma-derived IGFBP-5 has an active role in protection of PCa LNCaP cells from castration-induced apoptosis . This protective function is primarily an anti-apoptotic, rather a pro-proliferative effect.

5.3 Proposed Model for How IGFBP-5 Producing Bone Stromal Cells can Modulate IGF-I Signaling Kinetics in Bone Metastatic Prostate Cancer.

Bone is a major site of PCa metastasis. In early stage of PCa bone metastasis, AD PCa cells primarily utilize androgen, such as functioning through upregulation of IGF-IR [34] or transactivation of andromedins [17], to survive and proliferate in a new microenvironment. Upon androgen ablation, circulating as well as local androgen concentration, such as in bone, drops to a significantly low or maybe zero level. Androgen concentration is not sufficient to survival and proliferation of PCa cells. At this time, PCa cell normally undergo castration-induced apoptosis or growth arrest. However, some PCa cells can survive androgen withdrawal stress and become AI. The mechanism is still unclear.

We are here proposing a model that might explain the above-mentioned mechanism. Prior to androgen withdrawal, in addition to androgen, PCa cells may also use IGFBPs, especially IGFBP-5 in bone, as a supplementation for their growth and survival. However, when androgen is withdrawn, IGFBP-5 expression is dramatically increased in bone stroma [101]. High concentration of IGFBP-5 and low or zero level of androgen in bone stroma make PCa cells to switch to utilization of surrounding IGFBP-5 from androgen. High concentration of IGFBP-5 can act as a buffer system restricting IGF-Is access to cell surface IGF-IRs in a slow and prolonged release fashion. This constant, sub-acute activation of IGF-IR results in amplification of downstream signaling pathways mediated by IRS-2 and Akt which promotes cell survival (Figure 5.1). This is thought to be an adaptive mechanism for PCa cells to resist undergoing apoptosis and survive under androgen deprivation stress.

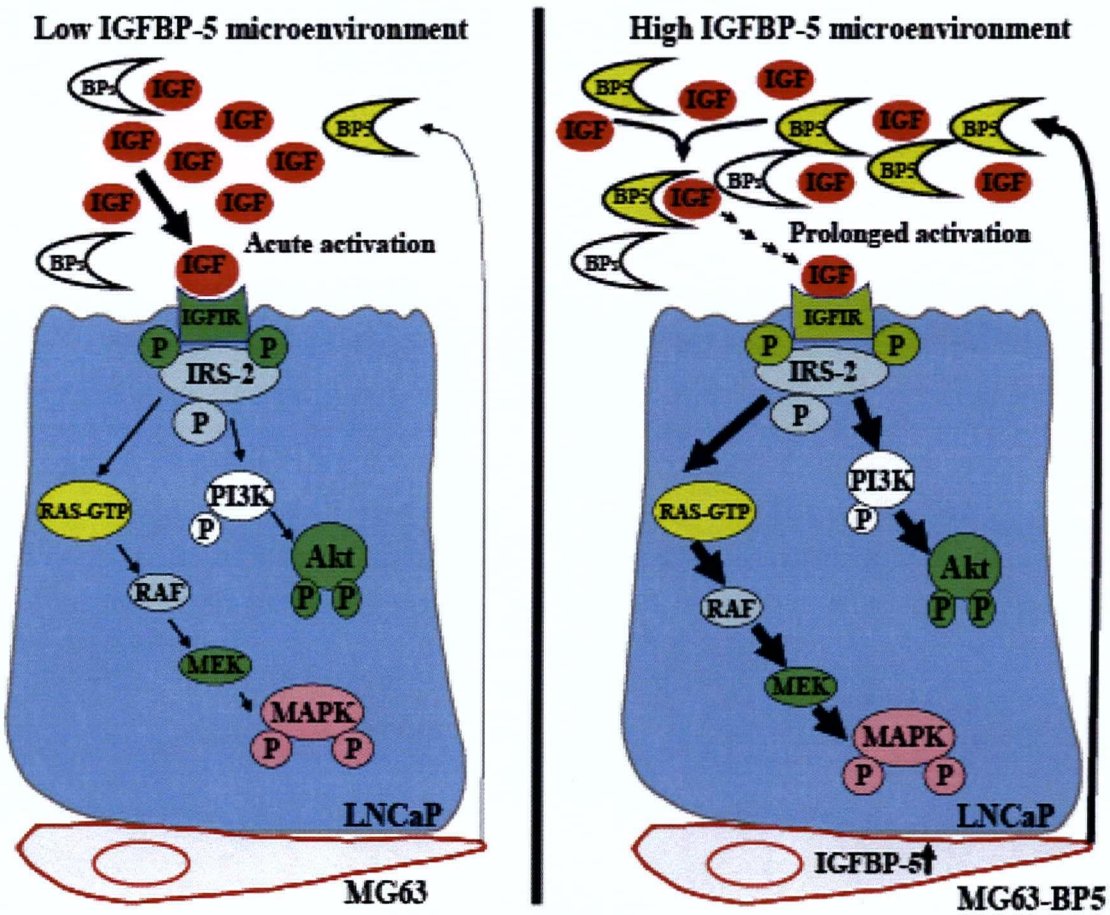

Figure 5.1 Proposed Model for How IGFBP-5 Producing Bone Stromal Cells can Modulate IGF-I Signaling Kinetics in Bone Metastatic Prostate Cancer.
High concentration of IGFBP-5 can act as a sink for IGF-I that allows presentation of IGF-I for IGF-IR interactions in a slow and prolonged release fashion. This constant, sub-acute activation of IGF-IR results in amplification of downstream signaling pathways mediated by IRS-2 and Akt which promotes cell survival. This is thought to be an adaptive mechanism for PCa cells to resist undergoing apoptosis and survive under androgen deprivation stress.

5.4 Future Directions

We have determined that stoma-derived IGFBP-5 enhances pro-survival signaling under androgen-deprived condition by assessing the ability of MG63-BP5 CM to alter magnitude and/or kinetics of IGF-1R activation in LNCaP cells in the absence of R1881. We have also shown that MG63-BP5 cells protect LNCaP cells from LY294002 and castration-induced apoptosis.

We will investigate the dependence on IGF-1R for any increased growth or survival signaling mediated by IGFBP-5 in MG63-BP5 CM by inhibiting the IGF-1R tyrosine kinase activity with the small molecule inhibitor NVP-AEW541(Novartis Pharma AG), or the tyrphostin AG1024 (Calbiochem). Alternatively, IGF-1R expression will be suppressed by siRNA transfection (Dharmacon) or expression of shRNA constructs. We will also examine whether downregulation of bone stroma-derived IGFBP-5 using RNAi or antisense techniques can reverse the difference in tumor growth and PSA dynamics we observed in our xenograft mice study.

All in all, a better understanding of association of IGFBP-5, osteoblasts and androgen withdrawal will help clarify the predominant osteoblastic metastasis in PCa and AI progression of PCa.

BIBLIOGRAPHY

1. Society, C.C., *Prostate cancer statistics*. 2007.
2. Coffey, D., *The molecular biology of the prostate.* Prostate diseases, 1993. **Lepor, H, Lawson, RK**(Philadelphis, Sauders): p. 28-56.
3. Collins, A.T. and N.J. Maitland, *Prostate cancer stem cells.* Eur J Cancer, 2006. **42**(9): p. 1213-8.
4. Bonkhoff, H. and K. Remberger, *Differentiation pathways and histogenetic aspects of normal and abnormal prostatic growth: a stem cell model.* Prostate, 1996. **28**(2): p. 98-106.
5. Coffery, D., *The molecular biology, endocrinology and physiology of the prostate and seminal vesicles.* . Campbell's urology, 1992. **Walsy PC, Refik AB, Stamey TA, Vaughan ED**(6th edition): p. 367-378.
6. Russell, P.J., S. Bennett, and P. Stricker, *Growth factor involvement in progression of prostate cancer.* Clin Chem, 1998. **44**(4): p. 705-23.
7. Feldman BJ, F.D., *The development of androgen-independent prostate cancer.* Nat Rev Cancer., 2001. **1**(1): p. 34-45.
8. McNeal, J.E., D.G. Bostwick, R.A. Kindrachuk, E.A. Redwine, F.S. Freiha, and T.A. Stamey, *Patterns of progression in prostate cancer.* Lancet, 1986. **1**(8472): p. 60-3.
9. Cunha, G.R., E. Battle, P. Young, J. Brody, A. Donjacour, N. Hayashi, and H. Kinbara, *Role of epithelial-mesenchymal interactions in the differentiation and spatial organization of visceral smooth muscle.* Epithelial Cell Biol, 1992. **1**(2): p. 76-83.
10. Cunha, G.R., L.W. Chung, J.M. Shannon, and B.A. Reese, *Stromal-epithelial interactions in sex differentiation.* Biol Reprod, 1980. **22**(1): p. 19-42.
11. Cunha, G.R., E.T. Alarid, T. Turner, A.A. Donjacour, E.L. Boutin, and B.A. Foster, *Normal and abnormal development of the male urogenital tract. Role of androgens, mesenchymal-epithelial interactions, and growth factors.* J Androl, 1992. **13**(6): p. 465-75.
12. Cooke, P.S., P. Young, R.A. Hess, and G.R. Cunha, *Estrogen receptor expression in developing epididymis, efferent ductules, and other male reproductive organs.* Endocrinology, 1991. **128**(6): p. 2874-9.
13. Cunha, G.R., B.A. Reese, and M. Sekkingstad, *Induction of nuclear androgen-binding sites in epithelium of the embryonic urinary bladder by mesenchyme of the urogenital sinus of embryonic mice.* Endocrinology, 1980. **107**(6): p. 1767-70.
14. Cunha, G.R. and P. Young, *Inability of Tfm (testicular feminization) epithelial cells to express androgen-dependent seminal vesicle secretory proteins in chimeric tissue recombinants.* Endocrinology, 1991. **128**(6): p. 3293-8.
15. Glanton, J.B., R.J. Fitzpatrick, L.M. Orr, and J.C. Hayward, *Palliative treatment of prostatic cancer.* South Med J, 1952. **45**(11): p. 1094-9.
16. Cunha, G.R., A.A. Donjacour, P.S. Cooke, S. Mee, R.M. Bigsby, S.J. Higgins, and Y. Sugimura, *The endocrinology and developmental biology of the prostate.* Endocr Rev, 1987. **8**(3): p. 338-62.
17. Donjacour, A.A., A.A. Thomson, and G.R. Cunha, *FGF-10 plays an essential role in the growth of the fetal prostate.* Dev Biol, 2003. **261**(1): p. 39-54.
18. Steiner, M.S., *Role of peptide growth factors in the prostate: a review.* Urology, 1993. **42**(1): p. 99-110.

19. Tanji, N., K. Aoki, and M. Yokoyama, *Growth factors: roles in andrology.* Arch Androl, 2001. **47**(1): p. 1-7.
20. Cohen, P., D.M. Peehl, and R.G. Rosenfeld, *The IGF axis in the prostate.* Horm Metab Res., 1994. **26**(2): p. 81-4.
21. Cohen, P., D.M. Peehl, G. Lamson, and R.G. Rosenfeld, *Insulin-like growth factors (IGFs), IGF receptors, and IGF-binding proteins in primary cultures of prostate epithelial cells.* J Clin Endocrinol Metab., 1991. **73**(2): p. 401-7.
22. Fiorelli, G., A. De Bellis, A. Longo, S. Giannini, A. Natali, A. Costantini, G.B. Vannelli, and M. Serio, *Insulin-like growth factor-I receptors in human hyperplastic prostate tissue: characterization, tissue localization, and their modulation by chronic treatment with a gonadotropin-releasing hormone analog.* J Clin Endocrinol Metab, 1991. **72**(4): p. 740-6.
23. Cunha, G.R., S.W. Hayward, Y.Z. Wang, and W.A. Ricke, *Role of the stromal microenvironment in carcinogenesis of the prostate.* Int J Cancer, 2003. **107**(1): p. 1-10.
24. Cooke, P.S., P. Young, and G.R. Cunha, *Androgen receptor expression in developing male reproductive organs.* Endocrinology, 1991. **128**(6): p. 2867-73.
25. Takeda, H. and C. Chang, *Immunohistochemical and in-situ hybridization analysis of androgen receptor expression during the development of the mouse prostate gland.* J Endocrinol, 1991. **129**(1): p. 83-9.
26. Pisters, L.L., X.H. Wang, L.W. Chung, and J.T. Hsieh, *Differential expression of c-erb B2/neu, epidermal growth factor receptor, cytokeratin 8, and the prostatic steroid-binding protein gene in rat ventral prostate during postnatal development.* Prostate, 2001. **47**(3): p. 164-71.
27. Wang, Y., S.W. Hayward, A.A. Donjacour, P. Young, T. Jacks, J. Sage, R. Dahiya, R.D. Cardiff, M.L. Day, and G.R. Cunha, *Sex hormone-induced carcinogenesis in Rb-deficient prostate tissue.* Cancer Res, 2000. **60**(21): p. 6008-17.
28. Tuxhorn, J.A., G.E. Ayala, and D.R. Rowley, *Reactive stroma in prostate cancer progression.* J Urol, 2001. **166**(6): p. 2472-83.
29. Olumi, A.F., G.D. Grossfeld, S.W. Hayward, P.R. Carroll, T.D. Tlsty, and G.R. Cunha, *Carcinoma-associated fibroblasts direct tumor progression of initiated human prostatic epithelium.* Cancer Res, 1999. **59**(19): p. 5002-11.
30. Rovere-Querini, P., A. Capobianco, P. Scaffidi, B. Valentinis, F. Catalanotti, M. Giazzon, I.E. Dumitriu, S. Muller, M. Iannacone, C. Traversari, M.E. Bianchi, and A.A. Manfredi, *HMGB1 is an endogenous immune adjuvant released by necrotic cells.* EMBO Rep., 2004. **5**(8): p. 825-30. Epub 2004 Jul 23.
31. Brawley, O.W., S. Barnes, and H. Parnes, *The future of prostate cancer prevention.* Ann N Y Acad Sci, 2001. **952**: p. 145-52.
32. Borgono, C.A. and E.P. Diamandis, *The emerging roles of human tissue kallikreins in cancer.* Nat Rev Cancer, 2004. **4**(11): p. 876-90.
33. Wu, J.D., K. Haugk, L. Woodke, P. Nelson, I. Coleman, and S.R. Plymate, *Interaction of IGF signaling and the androgen receptor in prostate cancer progression.* J Cell Biochem, 2006. **99**(2): p. 392-401.
34. Krueckl, S.L., R.A. Sikes, N.M. Edlund, R.H. Bell, A. Hurtado-Coll, L. Fazli, M.E. Gleave, and M.E. Cox, *Increased insulin-like growth factor I receptor expression and signaling are components of androgen-independent progression in a lineage-derived prostate cancer progression model.* Cancer Res, 2004. **64**(23): p. 8620-9.

35. Gnanapragasam, V.J., C.N. Robson, D.E. Neal, and H.Y. Leung, *Regulation of FGF8 expression by the androgen receptor in human prostate cancer.* Oncogene, 2002. **21**(33): p. 5069-80.
36. Gregory, C.W., K.G. Hamil, D. Kim, S.H. Hall, T.G. Pretlow, J.L. Mohler, and F.S. French, *Androgen receptor expression in androgen-independent prostate cancer is associated with increased expression of androgen-regulated genes.* Cancer Res, 1998. **58**(24): p. 5718-24.
37. Tan, J., Y. Sharief, K.G. Hamil, C.W. Gregory, D.Y. Zang, M. Sar, P.H. Gumerlock, R.W. deVere White, T.G. Pretlow, S.E. Harris, E.M. Wilson, J.L. Mohler, and F.S. French, *Dehydroepiandrosterone activates mutant androgen receptors expressed in the androgen-dependent human prostate cancer xenograft CWR22 and LNCaP cells.* Mol Endocrinol, 1997. **11**(4): p. 450-9.
38. Nelson, P.S., W.L. Ng, M. Schummer, L.D. True, A.Y. Liu, R.E. Bumgarner, C. Ferguson, A. Dimak, and L. Hood, *An expressed-sequence-tag database of the human prostate: sequence analysis of 1168 cDNA clones.* Genomics, 1998. **47**(1): p. 12-25.
39. Chung, L.W., M.E. Gleave, J.T. Hsieh, S.J. Hong, and H.E. Zhau, *Reciprocal mesenchymal-epithelial interaction affecting prostate tumour growth and hormonal responsiveness.* Cancer Surv., 1991. **11**: p. 91-121.
40. Lee, C., *Role of androgen in prostate growth and regression: stromal-epithelial interaction.* Prostate Suppl, 1996. **6**: p. 52-6.
41. Sadi, M.V., P.C. Walsh, and E.R. Barrack, *Immunohistochemical study of androgen receptors in metastatic prostate cancer. Comparison of receptor content and response to hormonal therapy.* Cancer, 1991. **67**(12): p. 3057-64.
42. Chodak, G.W., D.M. Kranc, L.A. Puy, H. Takeda, K. Johnson, and C. Chang, *Nuclear localization of androgen receptor in heterogeneous samples of normal, hyperplastic and neoplastic human prostate.* J Urol, 1992. **147**(3 Pt 2): p. 798-803.
43. Krueckl, S.L., R.A. Sikes, N.M. Edlund, R.H. Bell, A. Hurtado-Coll, L. Fazli, M.E. Gleave, and M.E. Cox, *Increased insulin-like growth factor I receptor expression and signaling are components of androgen-independent progression in a lineage-derived prostate cancer progression model.* Cancer Res., 2004. **64**(23): p. 8620-9.
44. Nickerson, T., F. Chang, D. Lorimer, S.P. Smeekens, C.L. Sawyers, and M. Pollak, *In vivo progression of LAPC-9 and LNCaP prostate cancer models to androgen independence is associated with increased expression of insulin-like growth factor I (IGF-I) and IGF-I receptor (IGF-IR).* Cancer Res., 2001. **61**(16): p. 6276-80.
45. Khandwala, H.M., I.E. McCutcheon, A. Flyvbjerg, and K.E. Friend, *The effects of insulin-like growth factors on tumorigenesis and neoplastic growth.* Endocr Rev., 2000. **21**(3): p. 215-44.
46. Daughaday, W.H., K.A. Parker, S. Borowsky, B. Trivedi, and M. Kapadia, *Measurement of somatomedin-related peptides in fetal, neonatal, and maternal rat serum by insulin-like growth factor (IGF) I radioimmunoassay, IGF-II radioreceptor assay (RRA), and multiplication-stimulating activity RRA after acid-ethanol extraction.* Endocrinology., 1982. **110**(2): p. 575-81.
47. Rechler, M.M., S.P. Nissley, G.L. King, A.C. Moses, E.E. Van Obberghen-Schilling, J.A. Romanus, A.B. Knight, P.A. Short, and R.M. White, *Multiplication stimulating activity (MSA) from the BRL 3A rat liver cell line: relation to human somatomedins and insulin.* J Supramol Struct Cell Biochem., 1981. **15**(3): p. 253-86.

48. Rosenfeld, R.G. and R.L. Hintz, *Characterization of a specific receptor for somatomedin C (SM-C) on cultured human lymphocytes: evidence that SM-C modulates homologous receptor concentration.* Endocrinology., 1980. **107**(6): p. 1841-8.
49. Baxter, R.C. and J.L. Martin, *Binding proteins for insulin-like growth factors in adult rat serum. Comparison with other human and rat binding proteins.* Biochem Biophys Res Commun., 1987. **147**(1): p. 408-15.
50. Binkert, C., J. Landwehr, J.L. Mary, J. Schwander, and G. Heinrich, *Cloning, sequence analysis and expression of a cDNA encoding a novel insulin-like growth factor binding protein (IGFBP-2).* Embo J., 1989. **8**(9): p. 2497-502.
51. Brinkman, A., C. Groffen, D.J. Kortleve, A. Geurts van Kessel, and S.L. Drop, *Isolation and characterization of a cDNA encoding the low molecular weight insulin-like growth factor binding protein (IBP-1).* Embo J., 1988. 7(8): p. 2417-23.
52. Martin, J.L., K.E. Willetts, and R.C. Baxter, *Purification and properties of a novel insulin-like growth factor-II binding protein from transformed human fibroblasts.* J Biol Chem., 1990. **265**(7): p. 4124-30.
53. Shimasaki, S., M. Shimonaka, H.P. Zhang, and N. Ling, *Identification of five different insulin-like growth factor binding proteins (IGFBPs) from adult rat serum and molecular cloning of a novel IGFBP-5 in rat and human.* J Biol Chem., 1991. **266**(16): p. 10646-53.
54. Shimonaka, M., R. Schroeder, S. Shimasaki, and N. Ling, *Identification of a novel binding protein for insulin-like growth factors in adult rat serum.* Biochem Biophys Res Commun., 1989. **165**(1): p. 189-95.
55. Rajah, R., L. Katz, S. Nunn, P. Solberg, T. Beers, and P. Cohen, *Insulin-like growth factor binding protein (IGFBP) proteases: functional regulators of cell growth.* Prog Growth Factor Res., 1995. **6**(2-4): p. 273-84.
56. Valentinis, B. and R. Baserga, *IGF-I receptor signalling in transformation and differentiation.* Mol Pathol., 2001. **54**(3): p. 133-7.
57. Gluckman, P., N. Klempt, J. Guan, C. Mallard, E. Sirimanne, M. Dragunow, M. Klempt, K. Singh, C. Williams, and K. Nikolics, *A role for IGF-1 in the rescue of CNS neurons following hypoxic-ischemic injury.* Biochem Biophys Res Commun., 1992. **182**(2): p. 593-9.
58. Zapf, J., C. Schmid, and E.R. Froesch, *Biological and immunological properties of insulin-like growth factors (IGF) I and II.* Clin Endocrinol Metab, 1984. **13**(1): p. 3-30.
59. Scott, C.D., J.L. Martin, and R.C. Baxter, *Rat hepatocyte insulin-like growth factor I and binding protein: effect of growth hormone in vitro and in vivo.* Endocrinology., 1985. **116**(3): p. 1102-7.
60. Lowe, W.L., Jr., M. Adamo, H. Werner, C.T. Roberts, Jr., and D. LeRoith, *Regulation by fasting of rat insulin-like growth factor I and its receptor. Effects on gene expression and binding.* J Clin Invest, 1989. **84**(2): p. 619-26.
61. Straus, D.S. and C.D. Takemoto, *Effect of dietary protein deprivation on insulin-like growth factor (IGF)-I and -II, IGF binding protein-2, and serum albumin gene expression in rat.* Endocrinology, 1990. **127**(4): p. 1849-60.
62. Stoving, R.K., A. Flyvbjerg, J. Frystyk, S. Fisker, J. Hangaard, M. Hansen-Nord, and C. Hagen, *Low serum levels of free and total insulin-like growth factor I (IGF-I) in patients with anorexia nervosa are not associated with increased IGF-binding protein-3 proteolysis.* J Clin Endocrinol Metab, 1999. **84**(4): p. 1346-50.

63. Kassem, M., R. Okazaki, S.A. Harris, T.C. Spelsberg, C.A. Conover, and B.L. Riggs, *Estrogen effects on insulin-like growth factor gene expression in a human osteoblastic cell line with high levels of estrogen receptor.* Calcif Tissue Int, 1998. **62**(1): p. 60-6.
64. Favelyukis, S., J.H. Till, S.R. Hubbard, and W.T. Miller, *Structure and autoregulation of the insulin-like growth factor 1 receptor kinase.* Nat Struct Biol, 2001. **8**(12): p. 1058-63.
65. Kulik, G., A. Klippel, and M.J. Weber, *Antiapoptotic signalling by the insulin-like growth factor I receptor, phosphatidylinositol 3-kinase, and Akt.* Mol Cell Biol., 1997. **17**(3): p. 1595-606.
66. Li, J., K. DeFea, and R.A. Roth, *Modulation of insulin receptor substrate-1 tyrosine phosphorylation by an Akt/phosphatidylinositol 3-kinase pathway.* J Biol Chem., 1999. **274**(14): p. 9351-6.
67. Motyka, B., G. Korbutt, M.J. Pinkoski, J.A. Heibein, A. Caputo, M. Hobman, M. Barry, I. Shostak, T. Sawchuk, C.F. Holmes, J. Gauldie, and R.C. Bleackley, *Mannose 6-phosphate/insulin-like growth factor II receptor is a death receptor for granzyme B during cytotoxic T cell-induced apoptosis.* Cell, 2000. **103**(3): p. 491-500.
68. LeRoith, D., H. Werner, D. Beitner-Johnson, and C.T. Roberts, Jr., *Molecular and cellular aspects of the insulin-like growth factor I receptor.* Endocr Rev, 1995. **16**(2): p. 143-63.
69. Pollak, M., W. Beamer, and J.C. Zhang, *Insulin-like growth factors and prostate cancer.* Cancer Metastasis Rev, 1998. **17**(4): p. 383-90.
70. Djavan, B., M. Waldert, C. Seitz, and M. Marberger, *Insulin-like growth factors and prostate cancer.* World J Urol, 2001. **19**(4): p. 225-33.
71. Wolk, A., C.S. Mantzoros, S.O. Andersson, R. Bergstrom, L.B. Signorello, P. Lagiou, H.O. Adami, and D. Trichopoulos, *Insulin-like growth factor 1 and prostate cancer risk: a population-based, case-control study.* J Natl Cancer Inst., 1998. **90**(12): p. 911-5.
72. Reiss, K., C. D'Ambrosio, X. Tu, C. Tu, and R. Baserga, *Inhibition of tumor growth by a dominant negative mutant of the insulin-like growth factor I receptor with a bystander effect.* Clin Cancer Res, 1998. **4**(11): p. 2647-55.
73. Reiss, K., X. Tu, G. Romano, F. Peruzzi, J.Y. Wang, and R. Baserga, *Intracellular association of a mutant insulin-like growth factor receptor with endogenous receptors.* Clin Cancer Res, 2001. **7**(7): p. 2134-44.
74. Burfeind, P., C.L. Chernicky, F. Rininsland, J. Ilan, and J. Ilan, *Antisense RNA to the type I insulin-like growth factor receptor suppresses tumor growth and prevents invasion by rat prostate cancer cells in vivo.* Proc Natl Acad Sci U S A, 1996. **93**(14): p. 7263-8.
75. Hellawell, G.O., G.D. Turner, D.R. Davies, R. Poulsom, S.F. Brewster, and V.M. Macaulay, *Expression of the type 1 insulin-like growth factor receptor is up-regulated in primary prostate cancer and commonly persists in metastatic disease.* Cancer Res, 2002. **62**(10): p. 2942-50.
76. Zhang, M., D.E. Latham, M.A. Delaney, and A. Chakravarti, *Survivin mediates resistance to antiandrogen therapy in prostate cancer.* Oncogene, 2005. **24**(15): p. 2474-82.
77. Culig, Z., A. Hobisch, M.V. Cronauer, C. Radmayr, J. Trapman, A. Hittmair, G. Bartsch, and H. Klocker, *Androgen receptor activation in prostatic tumor cell lines by insulin-like growth factor-I, keratinocyte growth factor, and epidermal growth factor.* Cancer Res, 1994. **54**(20): p. 5474-8.

78. Orio, F., Jr., B. Terouanne, V. Georget, S. Lumbroso, C. Avances, C. Siatka, and C. Sultan, *Potential action of IGF-1 and EGF on androgen receptor nuclear transfer and transactivation in normal and cancer human prostate cell lines.* Mol Cell Endocrinol, 2002. **198**(1-2): p. 105-14.
79. Plymate, S.R., M.K. Tennant, S.H. Culp, L. Woodke, M. Marcelli, I. Colman, P.S. Nelson, J.M. Carroll, C.T. Roberts, Jr., and J.L. Ware, *Androgen receptor (AR) expression in AR-negative prostate cancer cells results in differential effects of DHT and IGF-I on proliferation and AR activity between localized and metastatic tumors.* Prostate, 2004. **61**(3): p. 276-90.
80. Lin, H.K., S. Yeh, H.Y. Kang, and C. Chang, *Akt suppresses androgen-induced apoptosis by phosphorylating and inhibiting androgen receptor.* Proc Natl Acad Sci U S A, 2001. **98**(13): p. 7200-5.
81. Bakin, R.E., D. Gioeli, R.A. Sikes, E.A. Bissonette, and M.J. Weber, *Constitutive activation of the Ras/mitogen-activated protein kinase signaling pathway promotes androgen hypersensitivity in LNCaP prostate cancer cells.* Cancer Res, 2003. **63**(8): p. 1981-9.
82. Mohler, J.L., C.W. Gregory, O.H. Ford, 3rd, D. Kim, C.M. Weaver, P. Petrusz, E.M. Wilson, and F.S. French, *The androgen axis in recurrent prostate cancer.* Clin Cancer Res., 2004. **10**(2): p. 440-8.
83. Pandini, G., R. Mineo, F. Frasca, C.T. Roberts, Jr., M. Marcelli, R. Vigneri, and A. Belfiore, *Androgens up-regulate the insulin-like growth factor-I receptor in prostate cancer cells.* Cancer Res, 2005. **65**(5): p. 1849-57.
84. Nickerson, T., F. Chang, D. Lorimer, S.P. Smeekens, C.L. Sawyers, and M. Pollak, *In vivo progression of LAPC-9 and LNCaP prostate cancer models to androgen independence is associated with increased expression of insulin-like growth factor I (IGF-I) and IGF-I receptor (IGF-IR).* Cancer Res, 2001. **61**(16): p. 6276-80.
85. Kawada, M., H. Inoue, T. Masuda, and D. Ikeda, *Insulin-like growth factor I secreted from prostate stromal cells mediates tumor-stromal cell interactions of prostate cancer.* Cancer Res, 2006. **66**(8): p. 4419-25.
86. Jones, J.I. and D.R. Clemmons, *Insulin-like growth factors and their binding proteins: biological actions.* Endocr Rev., 1995. **16**(1): p. 3-34.
87. Rajaram, S., D.J. Baylink, and S. Mohan, *Insulin-like growth factor-binding proteins in serum and other biological fluids: regulation and functions.* Endocr Rev., 1997. **18**(6): p. 801-31.
88. Macaulay, V.M., *Insulin-like growth factors and cancer.* Br J Cancer, 1992. **65**(3): p. 311-20.
89. Arai, T., A. Parker, W. Busby, Jr., and D.R. Clemmons, *Heparin, heparan sulfate, and dermatan sulfate regulate formation of the insulin-like growth factor-I and insulin-like growth factor-binding protein complexes.* J Biol Chem., 1994. **269**(32): p. 20388-93.
90. Mohan, S., Y. Nakao, Y. Honda, E. Landale, U. Leser, C. Dony, K. Lang, and D.J. Baylink, *Studies on the mechanisms by which insulin-like growth factor (IGF) binding protein-4 (IGFBP-4) and IGFBP-5 modulate IGF actions in bone cells.* J Biol Chem., 1995. **270**(35): p. 20424-31.
91. Unterman, T.G., D.T. Oehler, L.J. Murphy, and R.G. Lacson, *Multihormonal regulation of insulin-like growth factor-binding protein-1 in rat H4IIE hepatoma cells: the dominant role of insulin.* Endocrinology, 1991. **128**(6): p. 2693-701.

92. Murphy, L.J., K. Rajkumar, and P. Molnar, *Phenotypic manifestations of insulin-like growth factor binding protein-1 (IGFBP-1) and IGFBP-3 overexpression in transgenic mice.* Prog Growth Factor Res, 1995. **6**(2-4): p. 425-32.
93. Hasegawa, T., P. Cohen, Y. Hasegawa, P.J. Fielder, and R.G. Rosenfeld, *Characterization of the insulin-like growth factors (IGF) axis in a cultured mouse Leydig cell line (TM-3).* Growth Regul, 1995. **5**(3): p. 151-9.
94. Baxter, R.C. and H. Saunders, *Radioimmunoassay of insulin-like growth factor-binding protein-6 in human serum and other body fluids.* J Endocrinol, 1992. **134**(1): p. 133-9.
95. Kelley, K.M., Y. Oh, S.E. Gargosky, Z. Gucev, T. Matsumoto, V. Hwa, L. Ng, D.M. Simpson, and R.G. Rosenfeld, *Insulin-like growth factor-binding proteins (IGFBPs) and their regulatory dynamics.* Int J Biochem Cell Biol., 1996. **28**(6): p. 619-37.
96. Cohen, P., D.M. Peehl, T.A. Stamey, K.F. Wilson, D.R. Clemmons, and R.G. Rosenfeld, *Elevated levels of insulin-like growth factor-binding protein-2 in the serum of prostate cancer patients.* J Clin Endocrinol Metab., 1993. **76**(4): p. 1031-5.
97. Moore, M.G., L.A. Wetterau, M.J. Francis, D.M. Peehl, and P. Cohen, *Novel stimulatory role for insulin-like growth factor binding protein-2 in prostate cancer cells.* Int J Cancer, 2003. **105**(1): p. 14-9.
98. Holman, S.R. and R.C. Baxter, *Insulin-like growth factor binding protein-3: factors affecting binary and ternary complex formation.* Growth Regul, 1996. **6**(1): p. 42-7.
99. Thissen, J.P., J.M. Ketelslegers, and L.E. Underwood, *Nutritional regulation of the insulin-like growth factors.* Endocr Rev, 1994. **15**(1): p. 80-101.
100. Bautista, C.M., D.J. Baylink, and S. Mohan, *Isolation of a novel insulin-like growth factor (IGF) binding protein from human bone: a potential candidate for fixing IGF-II in human bone.* Biochem Biophys Res Commun., 1991. **176**(2): p. 756-63.
101. Gudmundsson, J., P. Sulem, A. Manolescu, L.T. Amundadottir, D. Gudbjartsson, A. Helgason, T. Rafnar, J.T. Bergthorsson, B.A. Agnarsson, A. Baker, A. Sigurdsson, K.R. Benediktsdottir, M. Jakobsdottir, J. Xu, T. Blondal, J. Kostic, J. Sun, S. Ghosh, S.N. Stacey, M. Mouy, J. Saemundsdottir, V.M. Backman, K. Kristjansson, A. Tres, A.W. Partin, M.T. Albers-Akkers, J. Godino-Ivan Marcos, P.C. Walsh, D.W. Swinkels, S. Navarrete, S.D. Isaacs, K.K. Aben, T. Graif, J. Cashy, M. Ruiz-Echarri, K.E. Wiley, B.K. Suarez, J.A. Witjes, M. Frigge, C. Ober, E. Jonsson, G.V. Einarsson, J.I. Mayordomo, L.A. Kiemeney, W.B. Isaacs, W.J. Catalona, R.B. Barkardottir, J.R. Gulcher, U. Thorsteinsdottir, A. Kong, and K. Stefansson, *Genome-wide association study identifies a second prostate cancer susceptibility variant at 8q24.* Nat Genet, 2007. **39**(5): p. 631-7.
102. Jones, J.I., A. Gockerman, W.H. Busby, Jr., C. Camacho-Hubner, and D.R. Clemmons, *Extracellular matrix contains insulin-like growth factor binding protein-5: potentiation of the effects of IGF-I.* J Cell Biol., 1993. **121**(3): p. 679-87.
103. Nicolas, V., S. Mohan, Y. Honda, A. Prewett, R.D. Finkelman, D.J. Baylink, and J.R. Farley, *An age-related decrease in the concentration of insulin-like growth factor binding protein-5 in human cortical bone.* Calcif Tissue Int., 1995. **57**(3): p. 206-12.
104. Mohan, S., J.R. Farley, and D.J. Baylink, *Age-related changes in IGFBP-4 and IGFBP-5 levels in human serum and bone: implications for bone loss with aging.* Prog Growth Factor Res., 1995. **6**(2-4): p. 465-73.
105. Thomas, L.N., P. Cohen, R.C. Douglas, C. Lazier, and R.S. Rittmaster, *Insulin-like growth factor binding protein 5 is associated with involution of the ventral prostate in castrated and finasteride-treated rats.* Prostate., 1998. **35**(4): p. 273-8.

106. Thomas, L.N., A.S. Wright, C.B. Lazier, P. Cohen, and R.S. Rittmaster, *Prostatic involution in men taking finasteride is associated with elevated levels of insulin-like growth factor-binding proteins (IGFBPs)-2, -4, and -5.* Prostate, 2000. **42**(3): p. 203-10.
107. Miyake, H., C. Nelson, P.S. Rennie, and M.E. Gleave, *Overexpression of insulin-like growth factor binding protein-5 helps accelerate progression to androgen-independence in the human prostate LNCaP tumor model through activation of phosphatidylinositol 3'-kinase pathway.* Endocrinology., 2000. **141**(6): p. 2257-65.
108. Gleave, M.E. and H. Miyake, *Castration-induced upregulation of insulin-like growth factor binding protein-5 potentiates IGF-1 and accelerates androgen-independent progression in prostate cancer.* Prostate Cancer Prostatic Dis., 2000. **3**(S1): p. S16.
109. Miyake, H., M. Pollak, and M.E. Gleave, *Castration-induced up-regulation of insulin-like growth factor binding protein-5 potentiates insulin-like growth factor-I activity and accelerates progression to androgen independence in prostate cancer models.* Cancer Res., 2000. **60**(11): p. 3058-64.
110. Huynh, H., R.M. Seyam, and G.B. Brock, *Reduction of ventral prostate weight by finasteride is associated with suppression of insulin-like growth factor I (IGF-I) and IGF-I receptor genes and with an increase in IGF binding protein 3.* Cancer Res., 1998. **58**(2): p. 215-8.
111. Nickerson, T., H. Miyake, M.E. Gleave, and M. Pollak, *Castration-induced apoptosis of androgen-dependent shionogi carcinoma is associated with increased expression of genes encoding insulin-like growth factor-binding proteins.* Cancer Res., 1999. **59**(14): p. 3392-5.
112. Nickerson, T. and M. Pollak, *Bicalutamide (Casodex)-induced prostate regression involves increased expression of genes encoding insulin-like growth factor binding proteins.* Urology., 1999. **54**(6): p. 1120-5.
113. Huynh, H., M. Pollak, and J.C. Zhang, *Regulation of insulin-like growth factor (IGF) II and IGF binding protein 3 autocrine loop in human PC-3 prostate cancer cells by vitamin D metabolite 1,25(OH)2D3 and its analog EB1089.* Int J Oncol., 1998. **13**(1): p. 137-43.
114. Figueroa, J.A., S. De Raad, L. Tadlock, V.O. Speights, and J.J. Rinehart, *Differential expression of insulin-like growth factor binding proteins in high versus low Gleason score prostate cancer.* J Urol., 1998. **159**(4): p. 1379-83.
115. Nickerson, T., M. Pollak, and H. Huynh, *Castration-induced apoptosis in the rat ventral prostate is associated with increased expression of genes encoding insulin-like growth factor binding proteins 2,3,4 and 5.* Endocrinology., 1998. **139**(2): p. 807-10.
116. Baserga, R., F. Peruzzi, and K. Reiss, *The IGF-1 receptor in cancer biology.* Int J Cancer, 2003. **107**(6): p. 873-7.
117. Nickerson, T. and H. Huynh, *Vitamin D analogue EB1089-induced prostate regression is associated with increased gene expression of insulin-like growth factor binding proteins.* J Endocrinol., 1999. **160**(2): p. 223-9.
118. Kiyama, S., K. Morrison, T. Zellweger, M. Akbari, M. Cox, D. Yu, H. Miyake, and M.E. Gleave, *Castration-induced increases in insulin-like growth factor-binding protein 2 promotes proliferation of androgen-independent human prostate LNCaP tumors.* Cancer Res., 2003. **63**(13): p. 3575-84.
119. Koistinen, H., A. Paju, R. Koistinen, P. Finne, J. Lovgren, P. Wu, M. Seppala, and U.H. Stenman, *Prostate-specific antigen and other prostate-derived proteases cleave IGFBP-*

3, but prostate cancer is not associated with proteolytically cleaved circulating IGFBP-3. Prostate, 2002. **50**(2): p. 112-8.
120. Fielder, P.J., R.G. Rosenfeld, H.C. Graves, K. Grandbois, C.A. Maack, S. Sawamura, Y. Ogawa, A. Sommer, and P. Cohen, *Biochemical analysis of prostate specific antigen-proteolyzed insulin-like growth factor binding protein-3.* Growth Regul, 1994. **4**(4): p. 164-72.
121. Rajah, R., A. Bhala, S.E. Nunn, D.M. Peehl, and P. Cohen, *7S nerve growth factor is an insulin-like growth factor-binding protein protease.* Endocrinology, 1996. **137**(7): p. 2676-82.
122. Boes, M., B.L. Dake, B.A. Booth, N.E. Erondu, Y. Oh, V. Hwa, R. Rosenfeld, and R.S. Bar, *Connective tissue growth factor (IGFBP-rP2) expression and regulation in cultured bovine endothelial cells.* Endocrinology., 1999. **140**(4): p. 1575-80.
123. Zheng, B., J.B. Clarke, W.H. Busby, C. Duan, and D.R. Clemmons, *Insulin-like growth factor-binding protein-5 is cleaved by physiological concentrations of thrombin.* Endocrinology, 1998. **139**(4): p. 1708-14.
124. Fowlkes, J.L., J.J. Enghild, K. Suzuki, and H. Nagase, *Matrix metalloproteinases degrade insulin-like growth factor-binding protein-3 in dermal fibroblast cultures.* J Biol Chem, 1994. **269**(41): p. 25742-6.
125. Fowlkes, J.L., K. Suzuki, H. Nagase, and K.M. Thrailkill, *Proteolysis of insulin-like growth factor binding protein-3 during rat pregnancy: a role for matrix metalloproteinases.* Endocrinology, 1994. **135**(6): p. 2810-3.
126. Conover, C.A., J.E. Perry, and D.J. Tindall, *Endogenous cathepsin D-mediated hydrolysis of insulin-like growth factor-binding proteins in cultured human prostatic carcinoma cells.* J Clin Endocrinol Metab., 1995. **80**(3): p. 987-93.
127. Cohen, P., H.C. Graves, D.M. Peehl, M. Kamarei, L.C. Giudice, and R.G. Rosenfeld, *Prostate-specific antigen (PSA) is an insulin-like growth factor binding protein-3 protease found in seminal plasma.* J Clin Endocrinol Metab., 1992. **75**(4): p. 1046-53.
128. Cohen, P., D.M. Peehl, H.C. Graves, and R.G. Rosenfeld, *Biological effects of prostate specific antigen as an insulin-like growth factor binding protein-3 protease.* J Endocrinol., 1994. **142**(3): p. 407-15.
129. Cohen, P., H.C. Graves, D.M. Peehl, M. Kamarei, L.C. Giudice, and R.G. Rosenfeld, *Prostate-specific antigen (PSA) is an insulin-like growth factor binding protein-3 protease found in seminal plasma.* J Clin Endocrinol Metab, 1992. **75**(4): p. 1046-53.
130. Nunn, S.E., D.M. Peehl, and P. Cohen, *Acid-activated insulin-like growth factor binding protein protease activity of cathepsin D in normal and malignant prostatic epithelial cells and seminal plasma.* J Cell Physiol, 1997. **171**(2): p. 196-204.
131. Angelloz-Nicoud, P. and M. Binoux, *Autocrine regulation of cell proliferation by the insulin-like growth factor (IGF) and IGF binding protein-3 protease system in a human prostate carcinoma cell line (PC-3).* Endocrinology., 1995. **136**(12): p. 5485-92.
132. Kanety, H., Y. Madjar, Y. Dagan, J. Levi, M.Z. Papa, C. Pariente, B. Goldwasser, and A. Karasik, *Serum insulin-like growth factor-binding protein-2 (IGFBP-2) is increased and IGFBP-3 is decreased in patients with prostate cancer: correlation with serum prostate-specific antigen.* J Clin Endocrinol Metab, 1993. **77**(1): p. 229-33.
133. Ferry, R.J., Jr., R.W. Cerri, and P. Cohen, *Insulin-like growth factor binding proteins: new proteins, new functions.* Horm Res., 1999. **51**(2): p. 53-67.

134. Akaogi, K., J. Sato, Y. Okabe, Y. Sakamoto, H. Yasumitsu, and K. Miyazaki, *Synergistic growth stimulation of mouse fibroblasts by tumor-derived adhesion factor with insulin-like growth factors and insulin.* Cell Growth Differ, 1996. **7**(12): p. 1671-7.
135. Oh, Y., S.R. Nagalla, Y. Yamanaka, H.S. Kim, E. Wilson, and R.G. Rosenfeld, *Synthesis and characterization of insulin-like growth factor-binding protein (IGFBP)-7. Recombinant human mac25 protein specifically binds IGF-I and -II.* J Biol Chem, 1996. **271**(48): p. 30322-5.
136. Yang, D.H., H.S. Kim, E.M. Wilson, R.G. Rosenfeld, and Y. Oh, *Identification of glycosylated 38-kDa connective tissue growth factor (IGFBP-related protein 2) and proteolytic fragments in human biological fluids, and up-regulation of IGFBP-rP2 expression by TGF-beta in Hs578T human breast cancer cells.* J Clin Endocrinol Metab, 1998. **83**(7): p. 2593-6.
137. Kireeva, M.L., F.E. Mo, G.P. Yang, and L.F. Lau, *Cyr61, a product of a growth factor-inducible immediate-early gene, promotes cell proliferation, migration, and adhesion.* Mol Cell Biol, 1996. **16**(4): p. 1326-34.
138. Carmina, E., L. Wong, L. Chang, R.J. Paulson, M.V. Sauer, F.Z. Stanczyk, and R.A. Lobo, *Endocrine abnormalities in ovulatory women with polycystic ovaries on ultrasound.* Hum Reprod, 1997. **12**(5): p. 905-9.
139. Hwa, V., Y. Oh, and R.G. Rosenfeld, *The insulin-like growth factor-binding protein (IGFBP) superfamily.* Endocr Rev., 1999. **20**(6): p. 761-87.
140. Baxter, R.C., *Insulin-like growth factor (IGF)-binding proteins: interactions with IGFs and intrinsic bioactivities.* Am J Physiol Endocrinol Metab., 2000. **278**(6): p. E967-76.
141. Clemmons, D.R., *Role of insulin-like growth factor binding proteins in controlling IGF actions.* Mol Cell Endocrinol., 1998. **140**(1-2): p. 19-24.
142. Collett-Solberg, P.F. and P. Cohen, *Genetics, chemistry, and function of the IGF/IGFBP system.* Endocrine., 2000. **12**(2): p. 121-36.
143. Poretsky, L., N.A. Cataldo, Z. Rosenwaks, and L.C. Giudice, *The insulin-related ovarian regulatory system in health and disease.* Endocr Rev., 1999. **20**(4): p. 535-82.
144. Rechler, M.M., *Insulin-like growth factor binding proteins.* Vitam Horm., 1993. **47**: p. 1-114.
145. Gurumurthy, S., K.M. Vasudevan, and V.M. Rangnekar, *Regulation of apoptosis in prostate cancer.* Cancer Metastasis Rev, 2001. **20**(3-4): p. 225-43.
146. Gleave ME, H.J.-T., *Animal models in prostate cancer.* Principles and practice of genitourinary oncology., 1997. **Raghavan D, Scher HI, Leibel SA, Lange PH.** (eds. Philadelphia: Lippincott-Raven Publishers): p. 367-378.
147. Grossmann, M.E., H. Huang, and D.J. Tindall, *Androgen receptor signaling in androgen-refractory prostate cancer.* J Natl Cancer Inst, 2001. **93**(22): p. 1687-97.
148. Catalona, W.J., *Management of cancer of the prostate.* N Engl J Med, 1994. **331**(15): p. 996-1004.
149. Cohen, R.J., W.C. Chan, S.G. Edgar, E. Robinson, N. Dodd, S. Hoscek, and I.P. Mundy, *Prediction of pathological stage and clinical outcome in prostate cancer: an improved pre-operative model incorporating biopsy-determined intraductal carcinoma.* Br J Urol, 1998. **81**(3): p. 413-8.
150. Cifuentes, N. and J.W. Pickren, *Metastases from carcinoma of mammary gland: an autopsy study.* J Surg Oncol, 1979. **11**(3): p. 193-205.

151. Stephen, P., *The distribution of secondary growth in cancer of the breast.* Lancet., 1889. **1**: p. 571.
152. Kenny, P.A., G.Y. Lee, and M.J. Bissell, *Targeting the tumor microenvironment.* Front Biosci, 2007. **12**: p. 3468-74.
153. Langley, R.R. and I.J. Fidler, *Tumor cell-organ microenvironment interactions in the pathogenesis of cancer metastasis.* Endocr Rev, 2007. **28**(3): p. 297-321.
154. Mohla, S., *Tumor microenvironment.* J Cell Biochem, 2007.
155. Li, H., X. Fan, and J. Houghton, *Tumor microenvironment: The role of the tumor stroma in cancer.* J Cell Biochem, 2007.
156. Hanahan, D. and R.A. Weinberg, *The hallmarks of cancer.* Cell, 2000. **100**(1): p. 57-70.
157. Littlepage, L.E., M. Egeblad, and Z. Werb, *Coevolution of cancer and stromal cellular responses.* Cancer Cell, 2005. **7**(6): p. 499-500.
158. Kikugawa, T., Y. Kinugasa, K. Shiraishi, D. Nanba, K. Nakashiro, N. Tanji, M. Yokoyama, and S. Higashiyama, *PLZF regulates Pbx1 transcription and Pbx1-HoxC8 complex leads to androgen-independent prostate cancer proliferation.* Prostate, 2006. **66**(10): p. 1092-9.
159. Sahin, U., G. Weskamp, K. Kelly, H.M. Zhou, S. Higashiyama, J. Peschon, D. Hartmann, P. Saftig, and C.P. Blobel, *Distinct roles for ADAM10 and ADAM17 in ectodomain shedding of six EGFR ligands.* J Cell Biol, 2004. **164**(5): p. 769-79.
160. Kubo, H., T.A. Gardner, Y. Wada, K.S. Koeneman, A. Gotoh, L. Yang, C. Kao, S.D. Lim, M.B. Amin, H. Yang, M.E. Black, S. Matsubara, M. Nakagawa, J.Y. Gillenwater, H.E. Zhau, and L.W. Chung, *Phase I dose escalation clinical trial of adenovirus vector carrying osteocalcin promoter-driven herpes simplex virus thymidine kinase in localized and metastatic hormone-refractory prostate cancer.* Hum Gene Ther, 2003. **14**(3): p. 227-41.
161. Heiz, M., J. Grunberg, P.A. Schubiger, and I. Novak-Hofer, *Hepatocyte growth factor-induced ectodomain shedding of cell adhesion molecule L1: role of the L1 cytoplasmic domain.* J Biol Chem, 2004. **279**(30): p. 31149-56.
162. Smalley, D.M. and K. Ley, *L-selectin: mechanisms and physiological significance of ectodomain cleavage.* J Cell Mol Med, 2005. **9**(2): p. 255-66.
163. Ohnishi, H., H. Kobayashi, H. Okazawa, Y. Ohe, K. Tomizawa, R. Sato, and T. Matozaki, *Ectodomain shedding of SHPS-1 and its role in regulation of cell migration.* J Biol Chem, 2004. **279**(27): p. 27878-87.
164. Dolnik, O., V. Volchkova, W. Garten, C. Carbonnelle, S. Becker, J. Kahnt, U. Stroher, H.D. Klenk, and V. Volchkov, *Ectodomain shedding of the glycoprotein GP of Ebola virus.* Embo J, 2004. **23**(10): p. 2175-84.
165. Hiraga, T., P.J. Williams, G.R. Mundy, and T. Yoneda, *The bisphosphonate ibandronate promotes apoptosis in MDA-MB-231 human breast cancer cells in bone metastases.* Cancer Res, 2001. **61**(11): p. 4418-24.
166. Marcelli, M., S.J. Haidacher, S.R. Plymate, and R.S. Birnbaum, *Altered growth and insulin-like growth factor-binding protein-3 production in PC3 prostate carcinoma cells stably transfected with a constitutively active androgen receptor complementary deoxyribonucleic acid.* Endocrinology, 1995. **136**(3): p. 1040-8.
167. Unterman, T.G., A. Fareeduddin, M.A. Harris, R.G. Goswami, A. Porcella, R.H. Costa, and R.G. Lacson, *Hepatocyte nuclear factor-3 (HNF-3) binds to the insulin response*

sequence in the IGF binding protein-1 (IGFBP-1) promoter and enhances promoter function. Biochem Biophys Res Commun, 1994. **203**(3): p. 1835-41.
168. Tolcher, A.W., K. Chi, J. Kuhn, M. Gleave, A. Patnaik, C. Takimoto, G. Schwartz, I. Thompson, K. Berg, S. D'Aloisio, N. Murray, S.R. Frankel, E. Izbicka, and E. Rowinsky, *A phase II, pharmacokinetic, and biological correlative study of oblimersen sodium and docetaxel in patients with hormone-refractory prostate cancer.* Clin Cancer Res., 2005. **11**(10): p. 3854-61.
169. Dunstan, C.R., R. Boyce, B.F. Boyce, I.R. Garrett, E. Izbicka, W.H. Burgess, and G.R. Mundy, *Systemic administration of acidic fibroblast growth factor (FGF-1) prevents bone loss and increases new bone formation in ovariectomized rats.* J Bone Miner Res, 1999. **14**(6): p. 953-9.
170. Yi, B., P.J. Williams, M. Niewolna, Y. Wang, and T. Yoneda, *Tumor-derived platelet-derived growth factor-BB plays a critical role in osteosclerotic bone metastasis in an animal model of human breast cancer.* Cancer Res, 2002. **62**(3): p. 917-23.
171. Matuo, Y., N. Nishi, S. Matsui, A.A. Sandberg, J.T. Isaacs, and F. Wada, *Heparin binding affinity of rat prostatic growth factor in normal and cancerous prostates: partial purification and characterization of rat prostatic growth factor in the Dunning tumor.* Cancer Res, 1987. **47**(1): p. 188-92.
172. Mansson, P.E., P. Adams, M. Kan, and W.L. McKeehan, *Heparin-binding growth factor gene expression and receptor characteristics in normal rat prostate and two transplantable rat prostate tumors.* Cancer Res, 1989. **49**(9): p. 2485-94.
173. Pash, J.M., A.M. Delany, M.L. Adamo, C.T. Roberts, Jr., D. LeRoith, and E. Canalis, *Regulation of insulin-like growth factor I transcription by prostaglandin E2 in osteoblast cells.* Endocrinology, 1995. **136**(1): p. 33-8.
174. Cramer, S.D., D.M. Peehl, M.G. Edgar, S.T. Wong, L.J. Deftos, and D. Feldman, *Parathyroid hormone--related protein (PTHrP) is an epidermal growth factor-regulated secretory product of human prostatic epithelial cells.* Prostate, 1996. **29**(1): p. 20-9.
175. Arlen, P.M., J.L. Gulley, C. Parker, L. Skarupa, M. Pazdur, D. Panicali, P. Beetham, K.Y. Tsang, D.W. Grosenbach, J. Feldman, S.M. Steinberg, E. Jones, C. Chen, J. Marte, J. Schlom, and W. Dahut, *A randomized phase II study of concurrent docetaxel plus vaccine versus vaccine alone in metastatic androgen-independent prostate cancer.* Clin Cancer Res, 2006. **12**(4): p. 1260-9.
176. Achbarou, A., S. Kaiser, G. Tremblay, L.G. Ste-Marie, P. Brodt, D. Goltzman, and S.A. Rabbani, *Urokinase overproduction results in increased skeletal metastasis by prostate cancer cells in vivo.* Cancer Res, 1994. **54**(9): p. 2372-7.
177. Rabbani, S.A. and J. Gladu, *Urokinase receptor antibody can reduce tumor volume and detect the presence of occult tumor metastases in vivo.* Cancer Res., 2002. **62**(8): p. 2390-7.
178. Rabbani, S.A. and R.H. Xing, *Role of urokinase (uPA) and its receptor (uPAR) in invasion and metastasis of hormone-dependent malignancies.* Int J Oncol., 1998. **12**(4): p. 911-20.
179. Nelson, P.N. and T. Chambers, *Generation and characterization of putative monoclonal and polyclonal antibodies against tartrate-resistant acid phosphatase.* Hybridoma, 1995. **14**(1): p. 91-4.

180. Iwamura, M., J. Hellman, A.T. Cockett, H. Lilja, and S. Gershagen, *Alteration of the hormonal bioactivity of parathyroid hormone-related protein (PTHrP) as a result of limited proteolysis by prostate-specific antigen.* Urology, 1996. **48**(2): p. 317-25.
181. Dallas, S.L., K. Miyazono, T.M. Skerry, G.R. Mundy, and L.F. Bonewald, *Dual role for the latent transforming growth factor-beta binding protein in storage of latent TGF-beta in the extracellular matrix and as a structural matrix protein.* J Cell Biol, 1995. **131**(2): p. 539-49.
182. Dallas, S.L., S. Park-Snyder, K. Miyazono, D. Twardzik, G.R. Mundy, and L.F. Bonewald, *Characterization and autoregulation of latent transforming growth factor beta (TGF beta) complexes in osteoblast-like cell lines. Production of a latent complex lacking the latent TGF beta-binding protein.* J Biol Chem, 1994. **269**(9): p. 6815-21.
183. Guise, T.A., J.J. Yin, and K.S. Mohammad, *Role of endothelin-1 in osteoblastic bone metastases.* Cancer, 2003. **97**(3 Suppl): p. 779-84.
184. Ying Wang, J., F. Peruzzi, A. Lassak, L. Del Valle, S. Radhakrishnan, J. Rappaport, K. Khalili, S. Amini, and K. Reiss, *Neuroprotective effects of IGF-I against TNFalpha-induced neuronal damage in HIV-associated dementia.* Virology, 2003. **305**(1): p. 66-76.
185. Gori, F., L.C. Hofbauer, C.A. Conover, and S. Khosla, *Effects of androgens on the insulin-like growth factor system in an androgen-responsive human osteoblastic cell line.* Endocrinology, 1999. **140**(12): p. 5579-86.
186. Yonou, H., T. Yokose, T. Kamijo, N. Kanomata, T. Hasebe, K. Nagai, T. Hatano, Y. Ogawa, and A. Ochiai, *Establishment of a novel species- and tissue-specific metastasis model of human prostate cancer in humanized non-obese diabetic/severe combined immunodeficient mice engrafted with human adult lung and bone.* Cancer Res, 2001. **61**(5): p. 2177-82.
187. Goya, M., S. Miyamoto, K. Nagai, Y. Ohki, K. Nakamura, K. Shitara, H. Maeda, T. Sangai, K. Kodama, Y. Endoh, G. Ishii, T. Hasebe, H. Yonou, T. Hatano, Y. Ogawa, and A. Ochiai, *Growth inhibition of human prostate cancer cells in human adult bone implanted into nonobese diabetic/severe combined immunodeficient mice by a ligand-specific antibody to human insulin-like growth factors.* Cancer Res, 2004. **64**(17): p. 6252-8.
188. Logothetis, C.J. and S.H. Lin, *Osteoblasts in prostate cancer metastasis to bone.* Nat Rev Cancer, 2005. **5**(1): p. 21-8.
189. Ritchie, C.K., L.R. Andrews, K.G. Thomas, D.J. Tindall, and L.A. Fitzpatrick, *The effects of growth factors associated with osteoblasts on prostate carcinoma proliferation and chemotaxis: implications for the development of metastatic disease.* Endocrinology, 1997. **138**(3): p. 1145-50.
190. Gleave, M., J.T. Hsieh, C.A. Gao, A.C. von Eschenbach, and L.W. Chung, *Acceleration of human prostate cancer growth in vivo by factors produced by prostate and bone fibroblasts.* Cancer Res, 1991. **51**(14): p. 3753-61.
191. Gleave, M.E., J.T. Hsieh, A.C. von Eschenbach, and L.W. Chung, *Prostate and bone fibroblasts induce human prostate cancer growth in vivo: implications for bidirectional tumor-stromal cell interaction in prostate carcinoma growth and metastasis.* J Urol, 1992. **147**(4): p. 1151-9.
192. Cunha, G.R., P.S. Cooke, and T. Kurita, *Role of stromal-epithelial interactions in hormonal responses.* Arch Histol Cytol, 2004. **67**(5): p. 417-34.

193. Figueroa, J.A., S. De Raad, L. Tadlock, V.O. Speights, and J.J. Rinehart, *Differential expression of insulin-like growth factor binding proteins in high versus low Gleason score prostate cancer.* J Urol, 1998. **159**(4): p. 1379-83.
194. Nam, T.J., W.H. Busby, Jr., C. Rees, and D.R. Clemmons, *Thrombospondin and osteopontin bind to insulin-like growth factor (IGF)-binding protein-5 leading to an alteration in IGF-I-stimulated cell growth.* Endocrinology., 2000. **141**(3): p. 1100-6.
195. Bichell, D.P., P. Rotwein, and T.L. McCarthy, *Prostaglandin E2 rapidly stimulates insulin-like growth factor-I gene expression in primary rat osteoblast cultures: evidence for transcriptional control.* Endocrinology, 1993. **133**(3): p. 1020-8.
196. Jones, J.I., A. Gockerman, W.H. Busby, Jr., C. Camacho-Hubner, and D.R. Clemmons, *Extracellular matrix contains insulin-like growth factor binding protein-5: potentiation of the effects of IGF-I.* J Cell Biol, 1993. **121**(3): p. 679-87.
197. Minesita, T. and K. Yamaguchi, *An androgen-dependent mouse mammary tumor.* Cancer Res., 1965. **25**(7): p. 1168-75.
198. Andress, D.L. and R.S. Birnbaum, *Human osteoblast-derived insulin-like growth factor (IGF) binding protein-5 stimulates osteoblast mitogenesis and potentiates IGF action.* J Biol Chem., 1992. **267**(31): p. 22467-72.
199. Arai, T., J. Clarke, A. Parker, W. Busby, Jr., T. Nam, and D.R. Clemmons, *Substitution of specific amino acids in insulin-like growth factor (IGF) binding protein 5 alters heparin binding and its change in affinity for IGF-I response to heparin.* J Biol Chem., 1996. **271**(11): p. 6099-106.
200. Huynh, H., X. Yang, and M. Pollak, *Estradiol and antiestrogens regulate a growth inhibitory insulin-like growth factor binding protein 3 autocrine loop in human breast cancer cells.* J Biol Chem., 1996. **271**(2): p. 1016-21.
201. Andress, D.L., S.M. Loop, J. Zapf, and M.C. Kiefer, *Carboxy-truncated insulin-like growth factor binding protein-5 stimulates mitogenesis in osteoblast-like cells.* Biochem Biophys Res Commun., 1993. **195**(1): p. 25-30.
202. Conover, C.A., L.K. Bale, J.T. Clarkson, and O. Torring, *Regulation of insulin-like growth factor binding protein-5 messenger ribonucleic acid expression and protein availability in rat osteoblast-like cells.* Endocrinology., 1993. **132**(6): p. 2525-30.
203. Gleave, M., J.T. Hsieh, C.A. Gao, A.C. von Eschenbach, and L.W. Chung, *Acceleration of human prostate cancer growth in vivo by factors produced by prostate and bone fibroblasts.* Cancer Res., 1991. **51**(14): p. 3753-61.
204. Lim, D.J., X.L. Liu, D.M. Sutkowski, E.J. Braun, C. Lee, and J.M. Kozlowski, *Growth of an androgen-sensitive human prostate cancer cell line, LNCaP, in nude mice.* Prostate, 1993. **22**(2): p. 109-18.
205. Corporation, S.B., *GEArray Q Series Mouse Androgen Signaling and Prostate Cancer Gene Array: MM-031.*
206. Meeting, P.A.N., 2004.
207. Gleave, M.E., J.T. Hsieh, A.C. von Eschenbach, and L.W. Chung, *Prostate and bone fibroblasts induce human prostate cancer growth in vivo: implications for bidirectional tumor-stromal cell interaction in prostate carcinoma growth and metastasis.* J Urol., 1992. **147**(4): p. 1151-9.
208. Gleave, M.E., J.T. Hsieh, H.C. Wu, A.C. von Eschenbach, and L.W. Chung, *Serum prostate specific antigen levels in mice bearing human prostate LNCaP tumors are*

determined by tumor volume and endocrine and growth factors. Cancer Res, 1992. **52**(6): p. 1598-605.
209. Pautke, C., M. Schieker, T. Tischer, A. Kolk, P. Neth, W. Mutschler, and S. Milz, *Characterization of osteosarcoma cell lines MG-63, Saos-2 and U-2 OS in comparison to human osteoblasts.* Anticancer Res, 2004. **24**(6): p. 3743-8.
210. Conover, C.A. and D.R. Powell, *Insulin-like growth factor (IGF)-binding protein-3 blocks IGF-I-induced receptor down-regulation and cell desensitization in cultured bovine fibroblasts.* Endocrinology, 1991. **129**(2): p. 710-6.